# Course of Geodynamics

Dr. Magdala Tesauro

Course Outline:

1. Thermo-physical structure of the continental and oceanic crust
2. **Thermo-physical structure of the continental lithosphere**
3. Thermo-physical structure of the oceanic lithosphere and oceanic ridges
4. Rheology and mechanics of the lithosphere
5. Plate tectonics and boundary forces
6. Hot spots, plumes, and convection
7. Subduction zones systems
8. Orogens formation and evolution
9. Sedimentary basins formation and evolution

The current paradigm of plate dynamics is based on the "LAB hypothesis"

- The kinematic entities we call plates (lithosphere) are decoupled from deeper mantle flow by a weak zone of lateral shearing (asthenosphere) within the uppermost mantle

- *The lithosphere-asthenosphere boundary (LAB) marks the base of the tectonic plates*
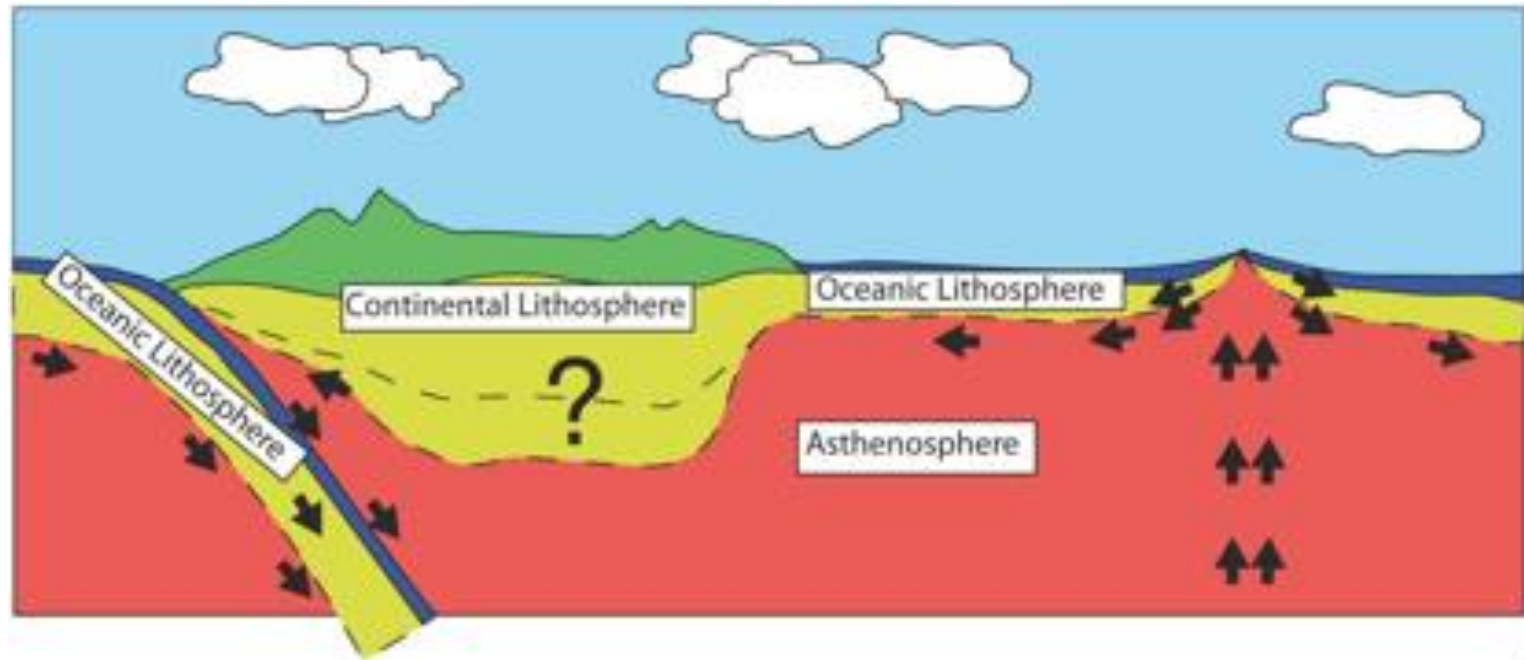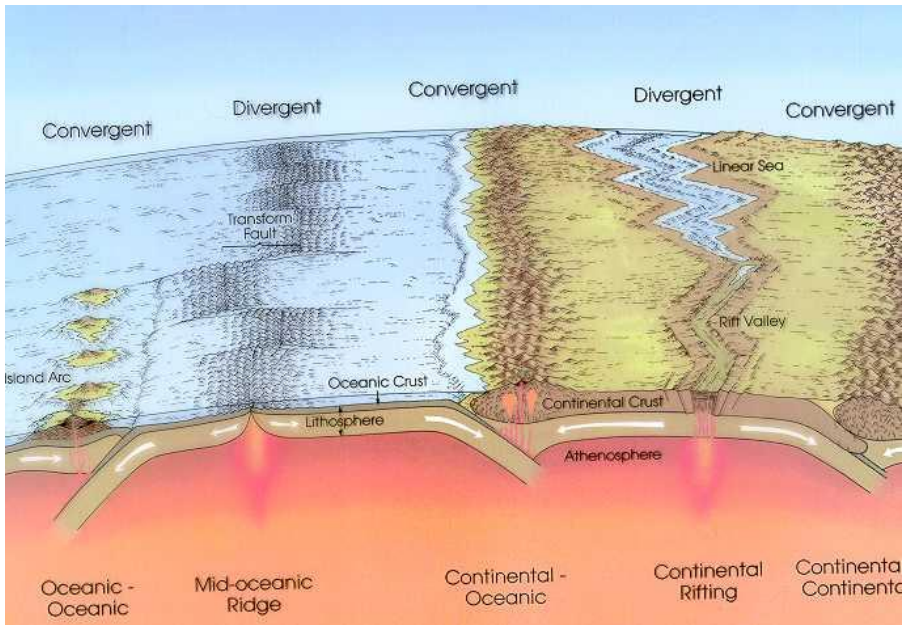
Oceanic and continental lithosphere

Oceanic lithosphere

- Thin
    - Crust: approximately constant (7-8 km)
    - Lithospheric thickness increases with age (max 100-125 km)
- Young: less than 200 million years
- Heavy: ultimately always subduction
- Enriched in FeO and MgO
- Hardly any heat production

Continental lithosphere

- Thick
    - Crust: 20 – 60 km
    - Lithosphere: 25 – 250 km
- Old: More than 4 billion years
- Light: virtually never subduction
- Enriched in SiO_2
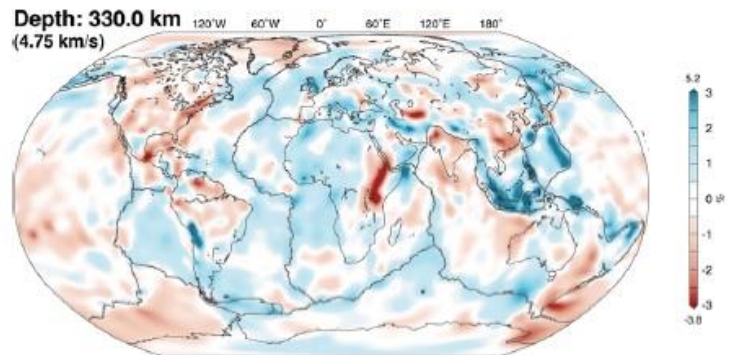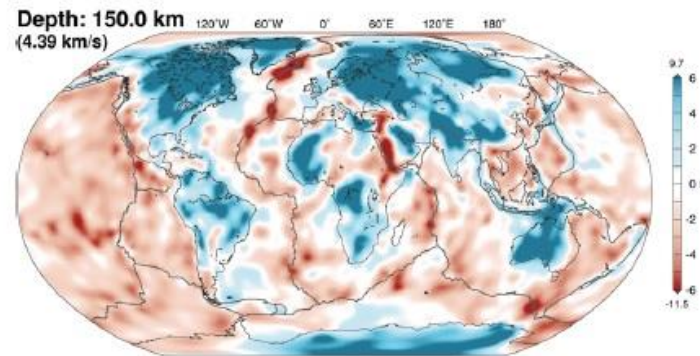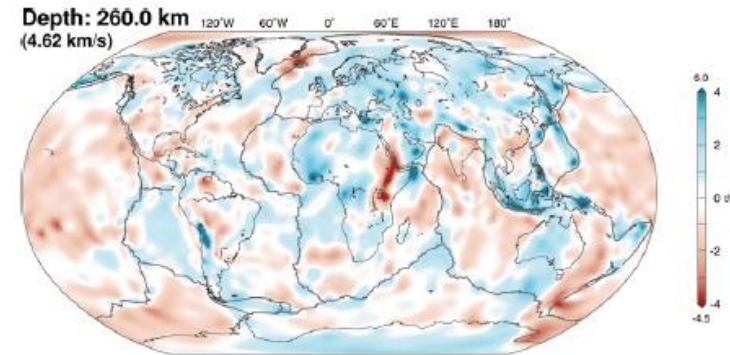- Substantial heat production
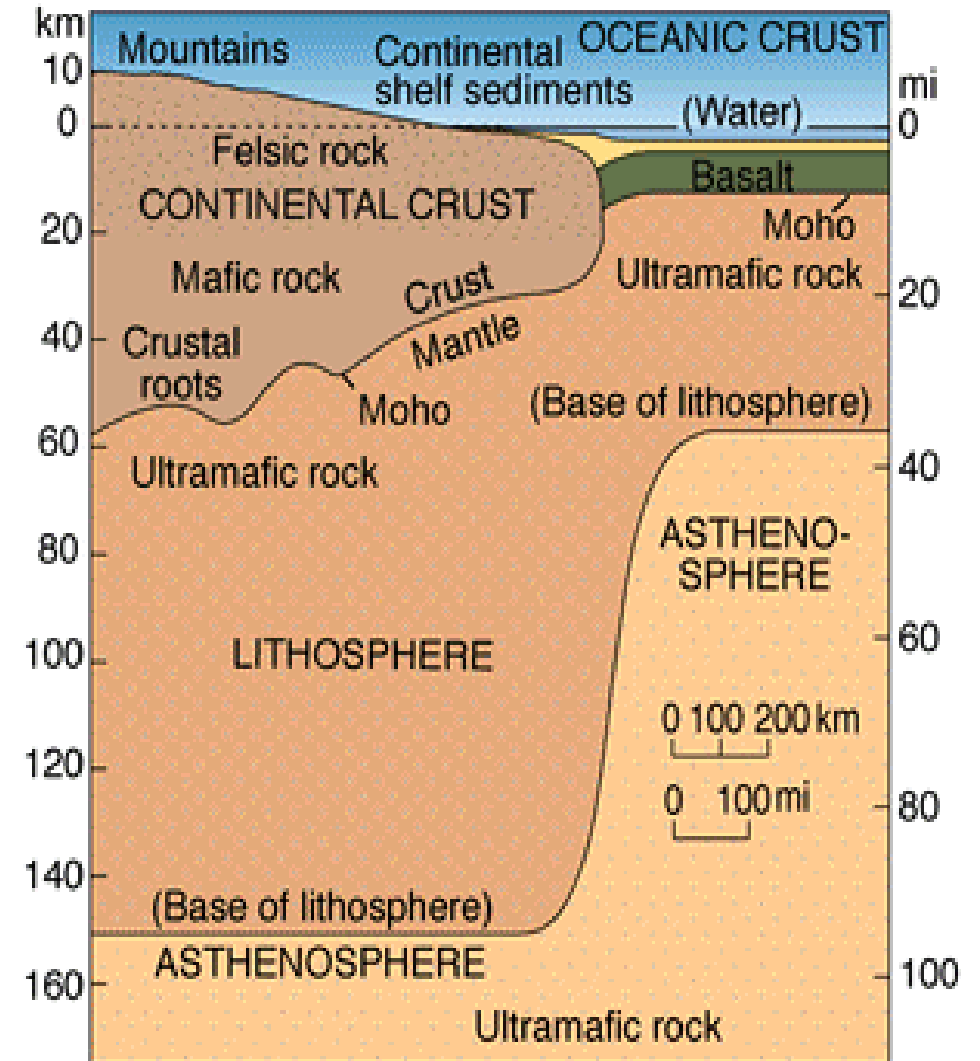
Upper mantle heterogenity detected from seismic tomography

Seismic wave velocity is a function of temperature:
Warm → slower
Cold → faster

Shear waves anomalies   Scaheffer and Lebedev, 2013, Geophys. J. Int., 194
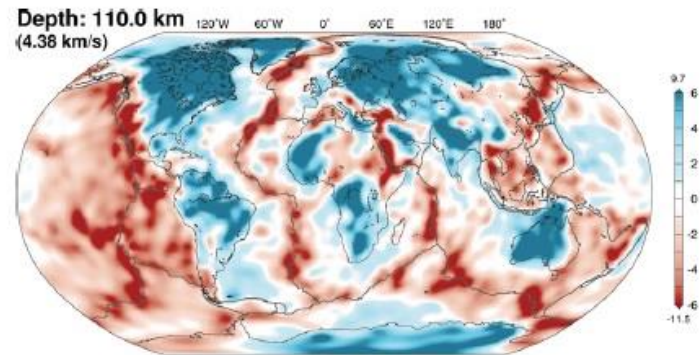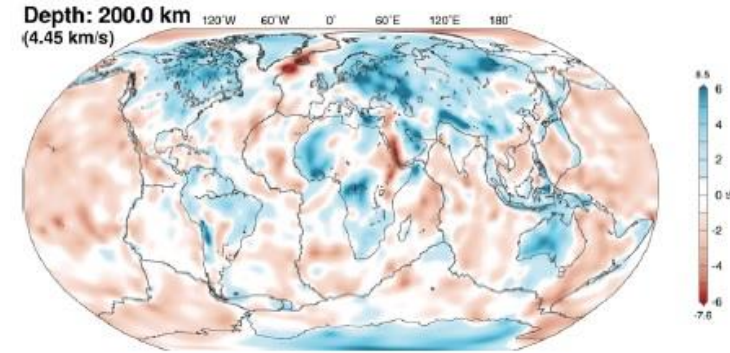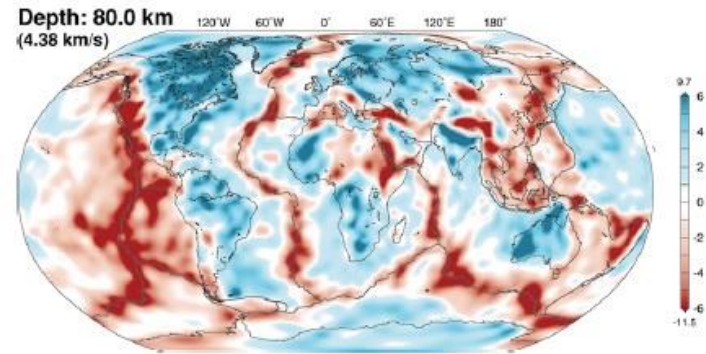
Dependance of seismic velocities on volatiles
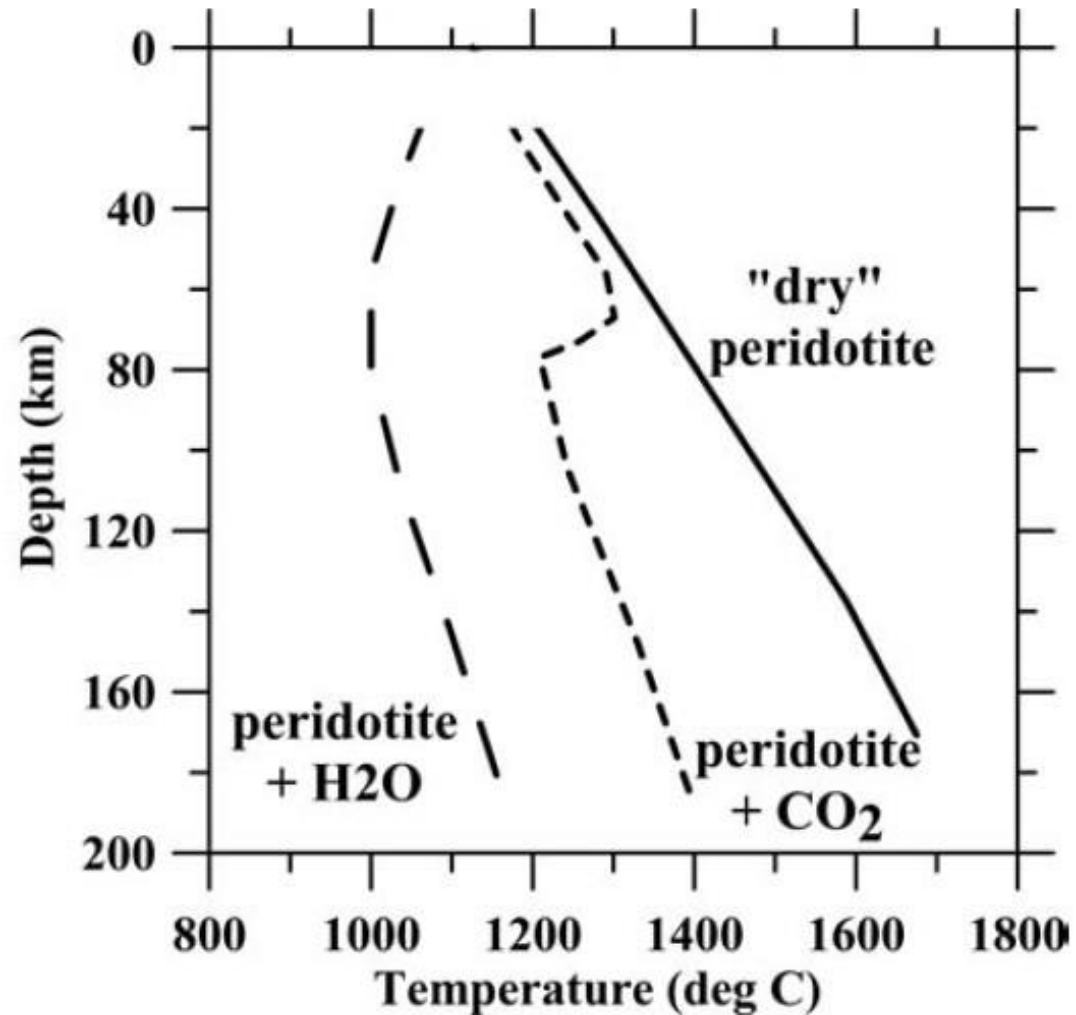
- At a depth > 80 km at high temperatures, the presence of even small volumes of volatiles (water and carbon dioxide) in the upper mantle indirectly reduces seismic velocities by lowering mantle melting temperature.

Global Tectonic Regionalization
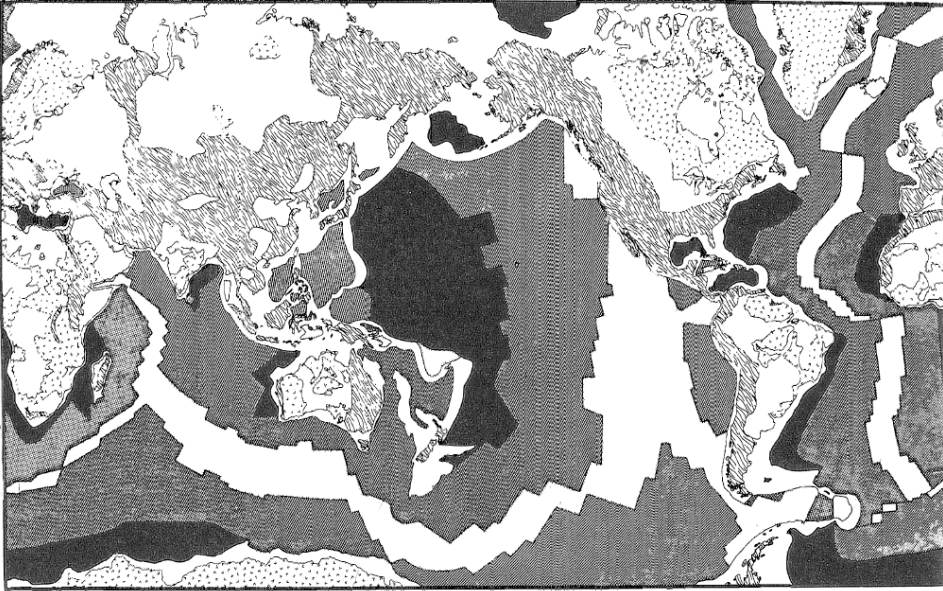
GRT1 (Jordan, 1981)

- Three oceanic regions A, B, C
    - based on lithospheric age

- Three continental regions Q, P, S
    - based on generalized tectonic behavior during the Phanerozoic
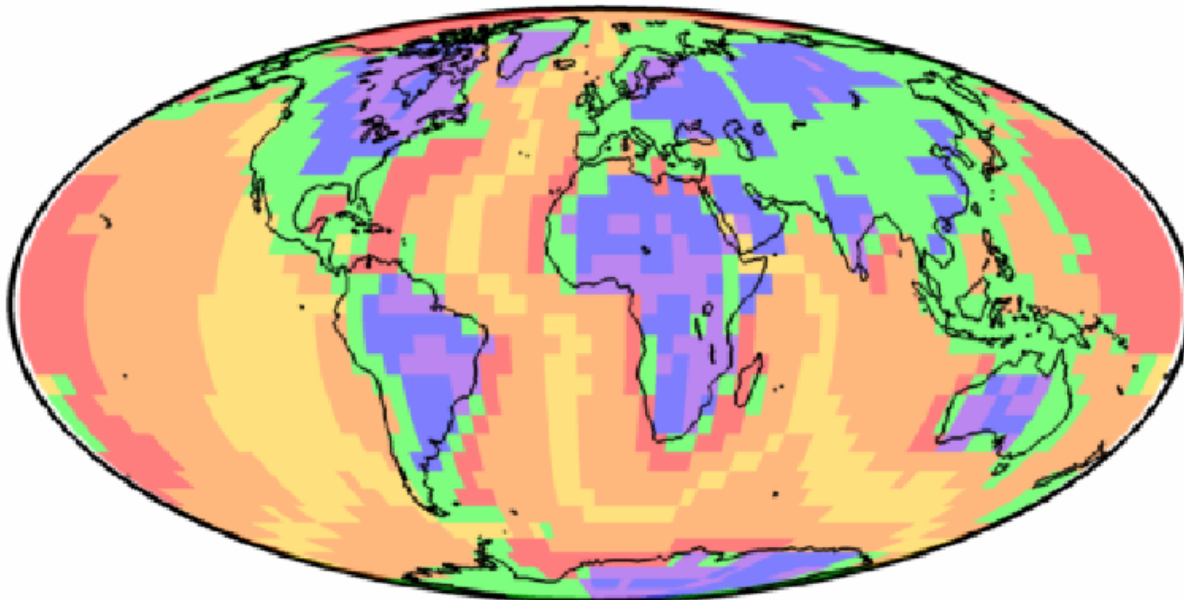
A- Young Oceans
B- Intermediate Oceans
C- Old Oceans
Q- Phanerozoic Orogenic Zones and Magmatic Belts
P- Precambrian Platform
S- Precambrian Shield

Global Tectonic Regionalization

Values from averaging a spherical map over GTR1 regions

150 km depth

Depth (km)

410 km

660 km

A
B
C
Q
P
S

$\Delta v_S / v_S$ (percent)
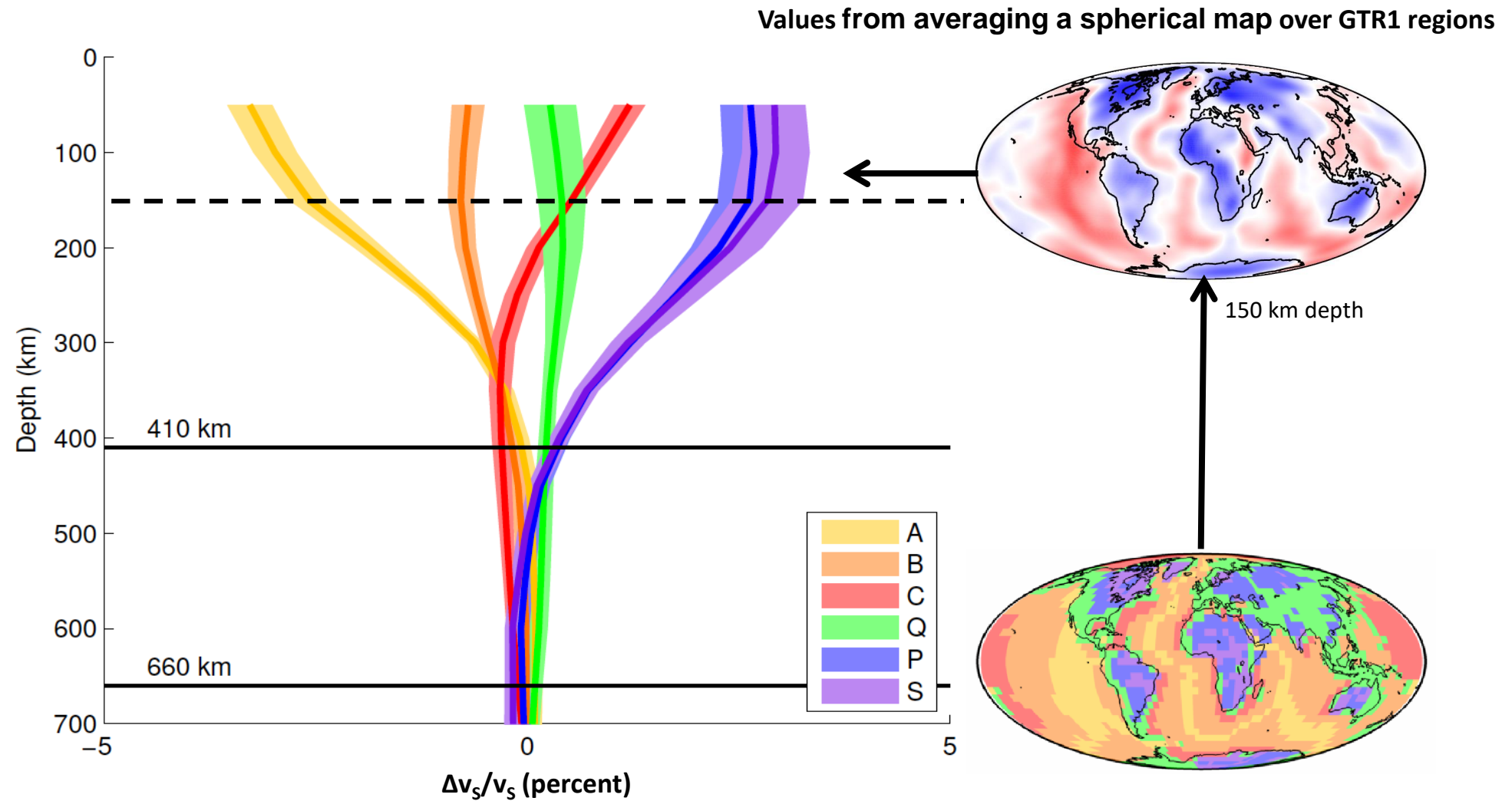
Model TX2008 (Simmons et al., 2009 *Geophys. J. Int.*, 177)

Global Tectonic Regionalization
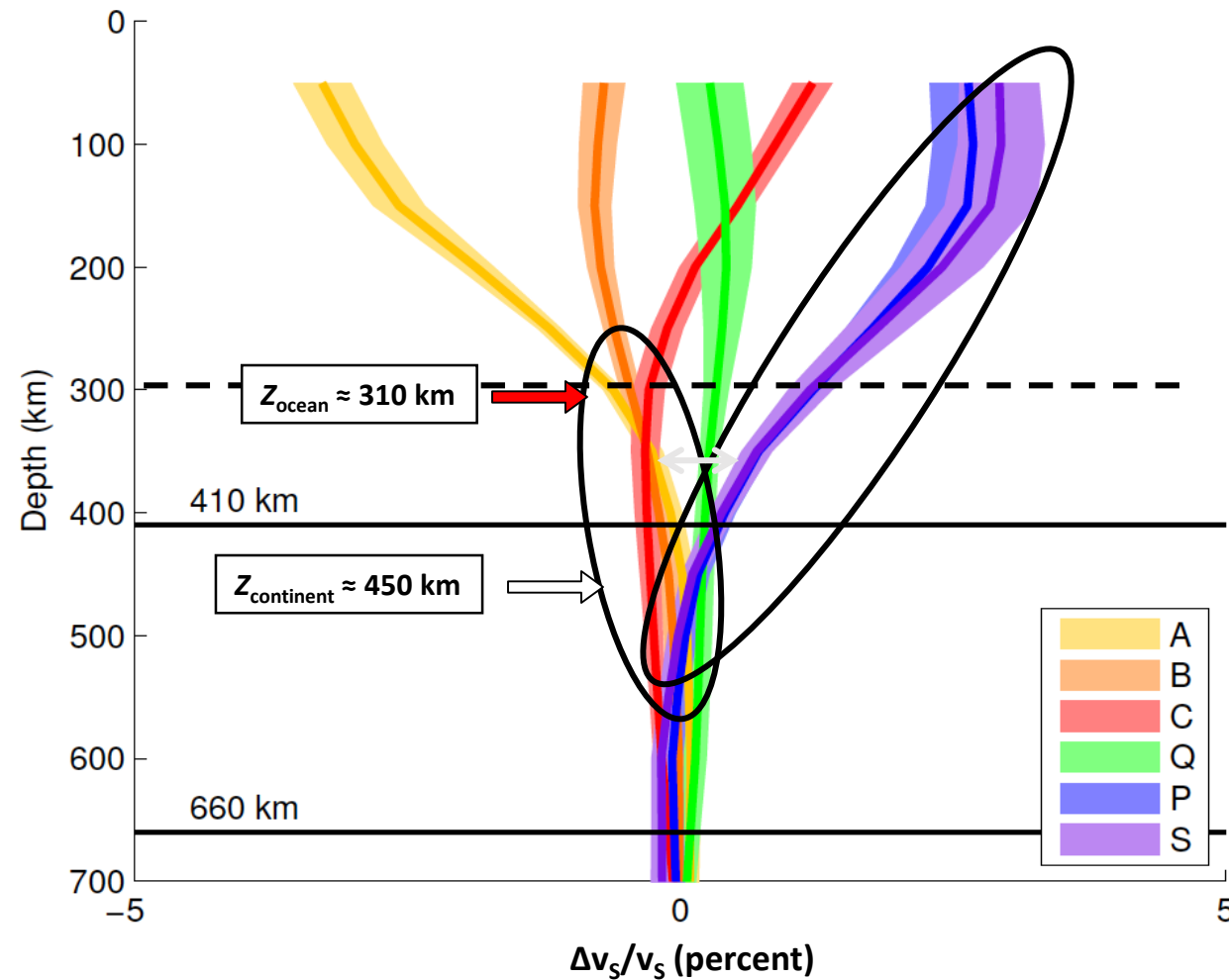
Common Features:

1. Platform and shield regions (P, S) show similar variations at all mantle depths

2. Ocean regions (A, B, C) show similar variations below 250-300 km

3. Differences between stable continents and oceans persist below 300 km

Model TX2008 (Simmons et al., 2009 *Geophys. J. Int.,* 177)

Upper mantle composition

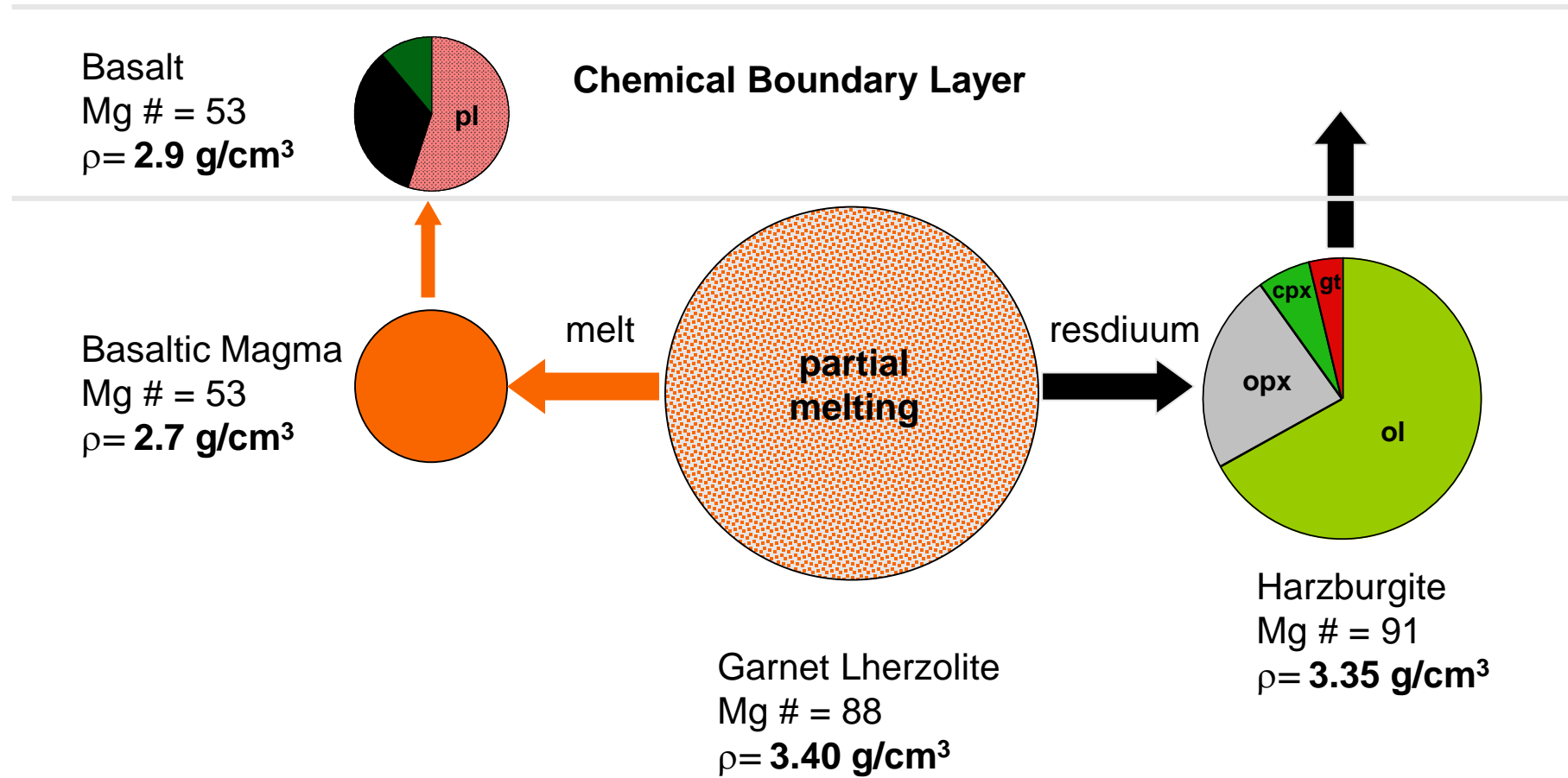|	Archons (mean garnet SCLM)	Protons (mean garnet SCLM + massifs + xenoliths)	Tectons (mean garnet SCLM)	Tectons (mean Spinel peridotite)	Primitive Mantle, McDonough and Sun (1995)
SiO_2	45.7	44.6	44.5	44.4	45.0
TiO_2	0.04	0.07	0.14	0.09	0.20
Al_2O_3	0.99	1.9	3.5	2.6	4.5
Cr_2O_3	0.28	0.40	0.40	0.40	0.38
FeO	6.4	7.9	8.0	8.2	8.1
MnO	0.11	0.12	0.13	0.13	0.14
MgO	45.5	42.6	39.8	41.1	37.8
CaO	0.59	1.70	3.1	2.5	3.6
Na_2O	0.07	0.12	0.24	0.18	0.36
NiO	0.30	0.26	0.26	0.27	0.25
Zn	34	52	55	53	55
V	20	48	70	59	82
Co	93	107	110	110	105
Sc	7	10	14	12	16
Mg#	92.7	90.6	89.9	89.9	89.3
Mg/Si	1.49	1.43	1.33	1.38	1.25
Ca/Al	0.55	0.80	0.82	0.85	0.73
Cr/Cr+Al	0.16	0.12	0.07	0.09	0.05
Fe/Al	4.66	3.02	1.66	2.23	1.30
Olivine/orthopyroxene/ clinopyroxene/garnet	69/25/2/4	70/17/6/7	60/17/11/12	66/17/9/8	57/13/12/18
Density, g/cc	3.31	3.34	3.37	3.36	3.39
Vp, km/s (room temperature)	8.34	8.32	8.30	8.30	8.33
Vp, 100 km, 700 °C	8.18	8.05	7.85	7.85	
Vs, Km/s (room temperature)	4.88	4.84	4.82	4.82	4.81
Vs, 100 km, 700 °C	4.71	4.6	4.48	4.48	

Griffin et al., 2003, Precambrian Research 127   SCLM=Sublithospheric Continental Mantle

Chemical Boundary Layer
Partial Melting of Mantle Lherzolites

Chemical Boundary Layer

Basalt
Mg # = 53
ρ= **2.9 g/cm³**

pl

Basaltic Magma
Mg # = 53
ρ= **2.7 g/cm³**

melt

partial melting

resdiuum

cpx gt
opx
ol

Harzburgite
Mg # = 91
ρ= **3.35 g/cm³**

Garnet Lherzolite
Mg # = 88
ρ= **3.40 g/cm³**

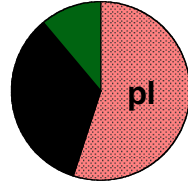**O' Hara (1975), Boyd & McCallister (1976), Jordan (1976, 1979)**

Chemical Boundary Layer
Partial Melting of Mantle Lherzolites

Chemical Boundary Layer

Basalt
Mg # = 53
ρ= **2.9 g/cm^3**

Eclogite
Mg # = 53
ρ= **3.60 g/cm^3**
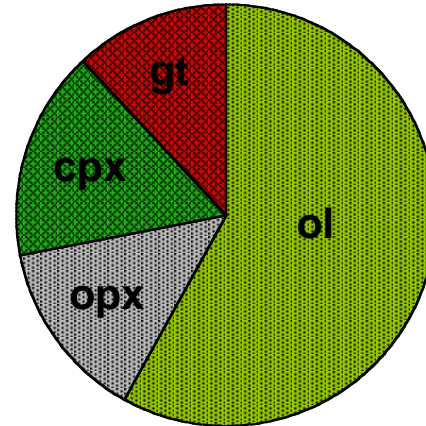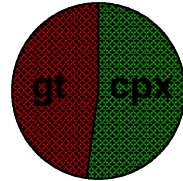
Garnet Lherzolite
Mg # = 88
ρ= **3.40 g/cm^3**

Harzburgite
Mg # = 91
ρ= **3.35 g/cm^3**

O'Hara (1975), Boyd & McCallister (1976), Jordan (1976, 1979)
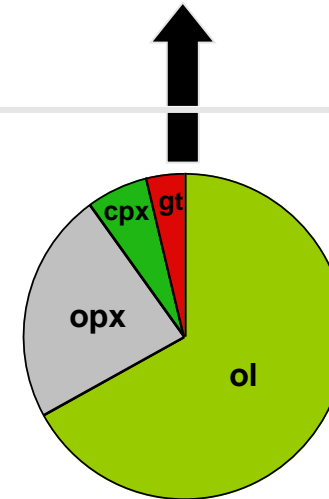
Compositional lithospheric variations in terms of Mg# ((Mg/Mg+Fe)x 100)

Lee, 2003, JGR, 108
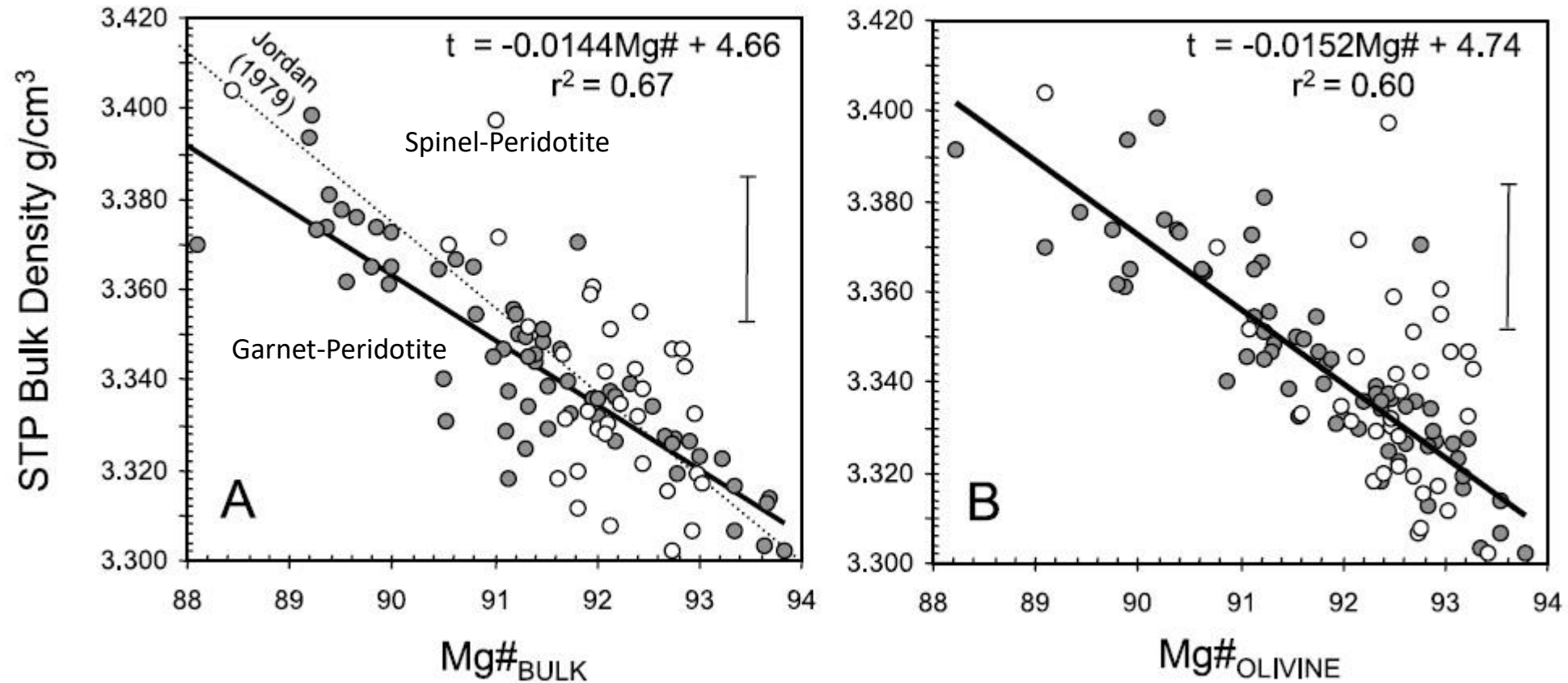
Lithosphere-Asthenosphere Boundary (LAB)

The lithosphere-asthenosphere boundary (LAB) is a transtion zone over which a gradual change in physical and chemical characteristics occurs. It reflects the processes related to both global evolution and plate tectonics

Definition of the LAB depth depends on:
- Physical parameter variation with depth (e.g., temperature, seismic velocity, mechanical strength)
- Geophysical method used (e.g., seismic tomography, receiver functions, magnetotelluric)

Seismic lithosphere: It is the seismic high-velocity layer above the low-velocity zone (LVZ) caused by partial melting or by the effect of temperature (decrease of seismic velocity) prevailing on that of pressure (increase of seismic velocities).
- Large-scale tomography models (sensitive to velocity anomalies associated to convective mantle) identify the LAB depth as the top of a large-scale mantle convection (where the positive velocity anomaly is redueced to 1%).
- The depth at which the axis of anisotropy changes orientation from fossil, frozen-in anisotropy (lithosheric mantle) to the present plate motions and mantle flow (asthenosphere).

Thermal lithosphere: It extends up to the depth of a costant isotherm (1250-1350 °C).
Lithospheric geotherms are costrained by: surface heat flow, from conversion of seismic velocities into temperatures, from pressure-temperature equilibrium conditions of mantle mineral phases constrained by xenoliths.

Electrical lithosphere: It is the highly resistive upper layer above the higly conductive athenospehre. Its base corresponds to a sharp change in mantle conductivity, explained by the presence of 1-3% of melt fraction.

Elastic Lithosphere: It is the rheologically strong layer providing the isostatic response of the plate to topographic and/or subsurface loads, overlying a viscous mantle. It mechanically supports the elastic stresses induced by lithospheric bending (shallower than the other boundaries).

Seismic Lithospheric Thickness

Conrad & Lithgow–Bertelloni [2006]
Model for Lithosphere Thickness

Lithosphere Thickness (km)

0   30   50   70   90   110   140   170   200   230   260   300   350
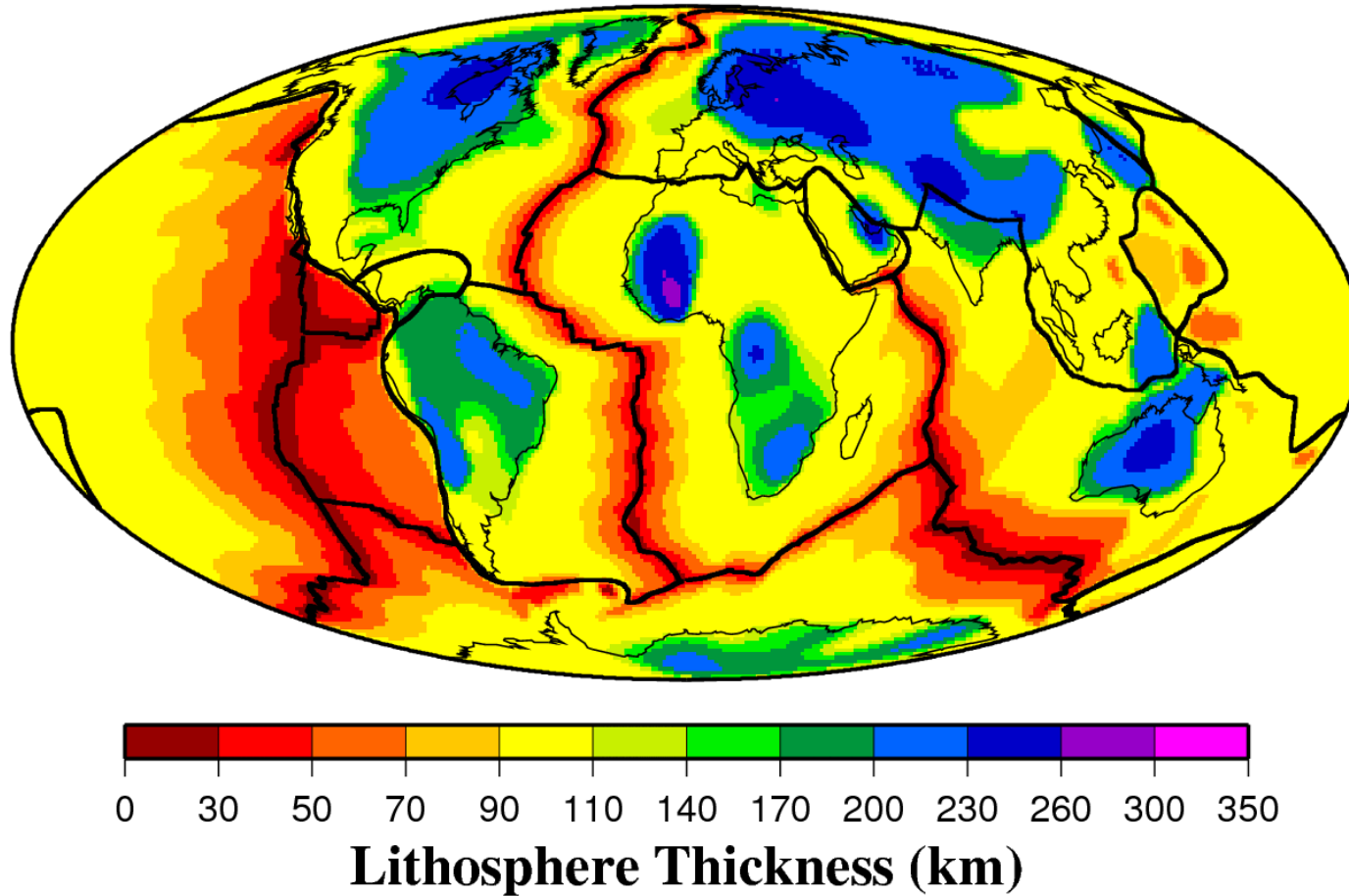
Estimated thickness of the lithosphere, determined using lithospheric age for oceanic areas and the thickness of positive seismic velocity anomalies for continental areas

Seismic Lithospheric Thickness
(Reciever Functions)
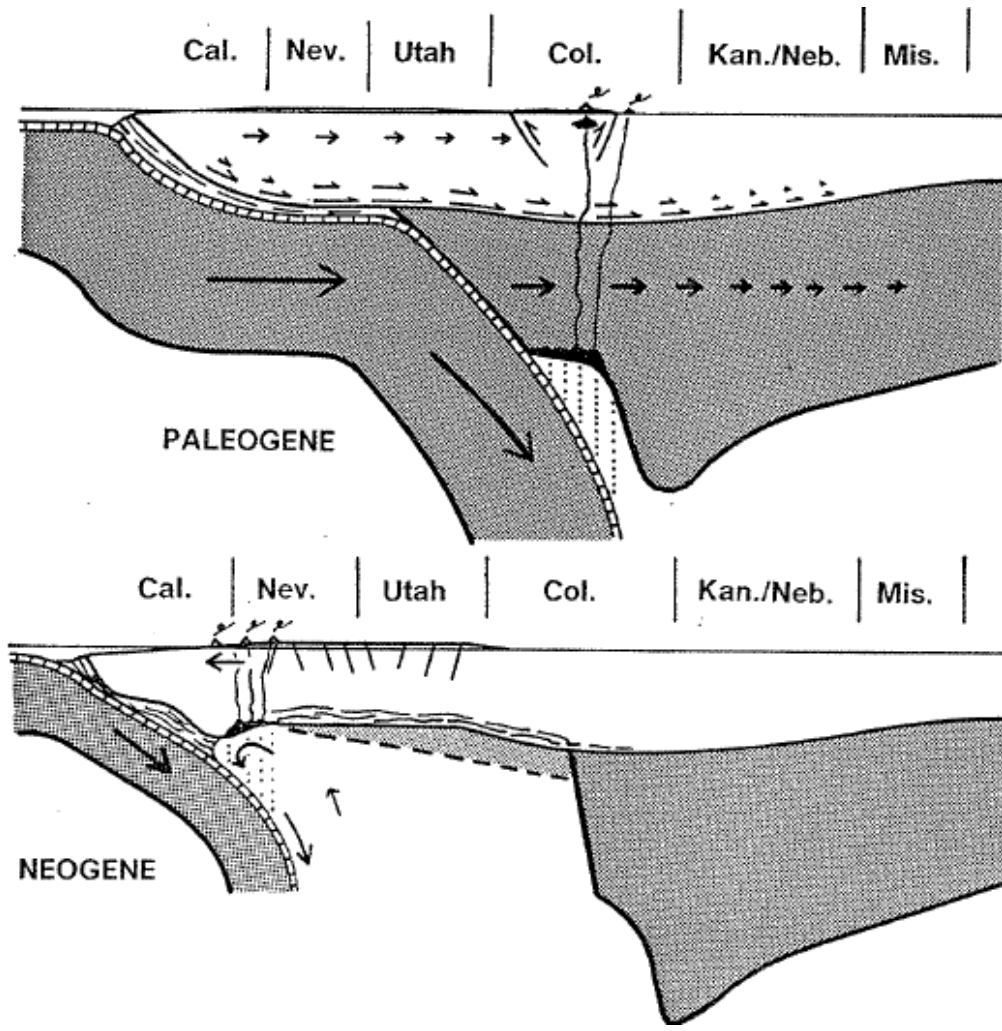
Bird, 1992
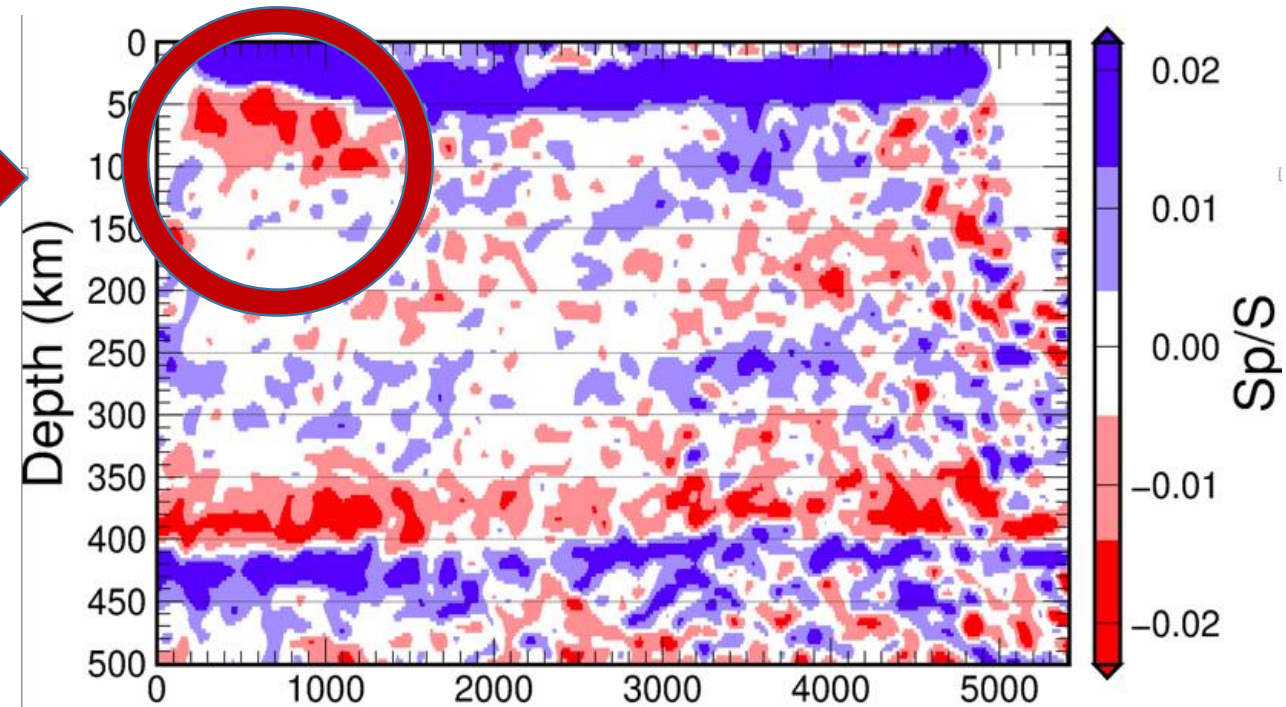
Old seismic boundaries from reciever functions

Moho

Precambrian Plate Tectonics

Archean   Proterozoic

ARCHEAN SUPERIOR
PROVIANCE

PROTEROZOIC
CONTINENT

LABc

LM
ARCHEAN SUPERIOR
PROVIANCE

PROTEROZOIC
CONTINENT

Old seismic boundaries and paleogeography

Archean

Proterozoic

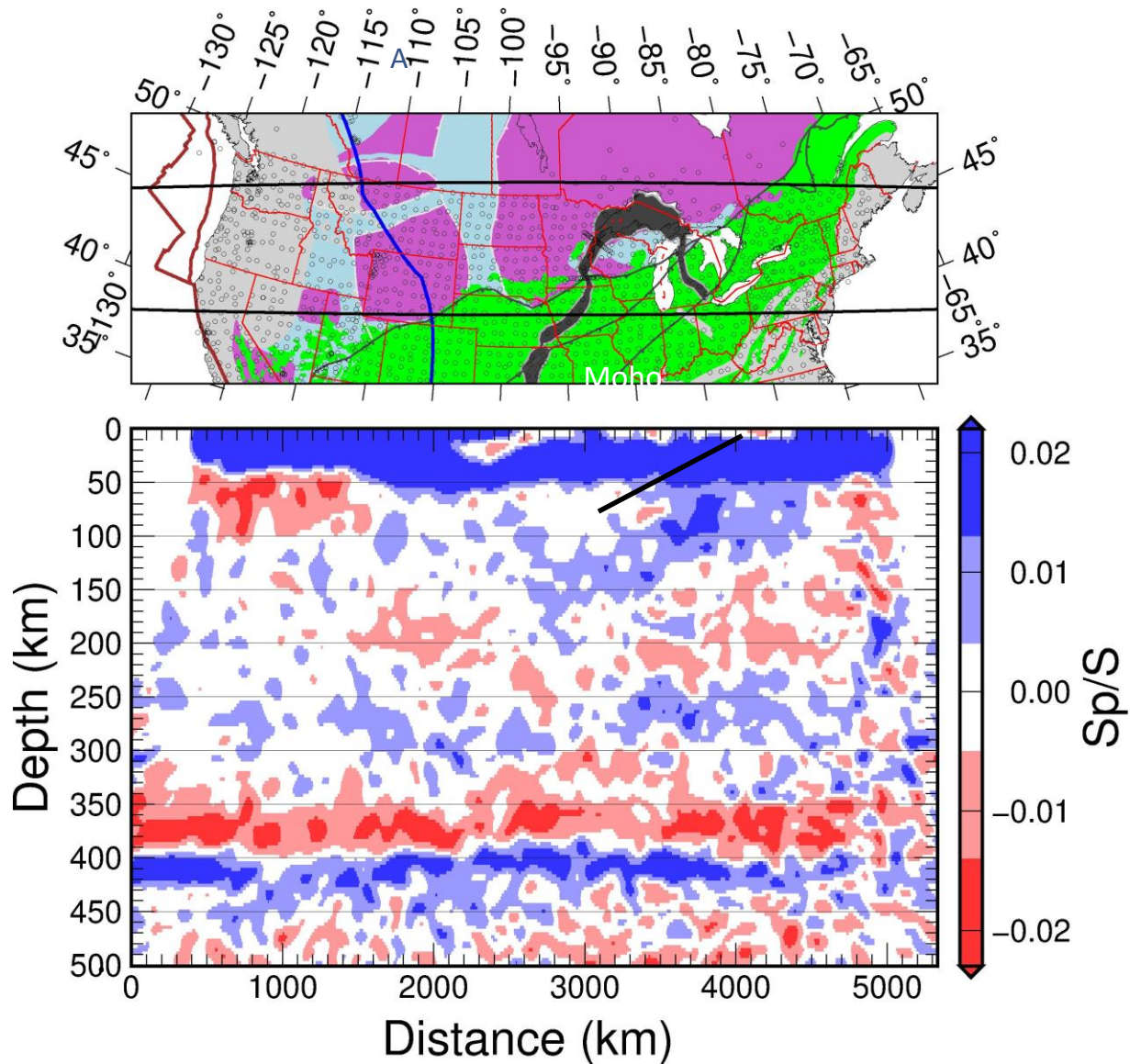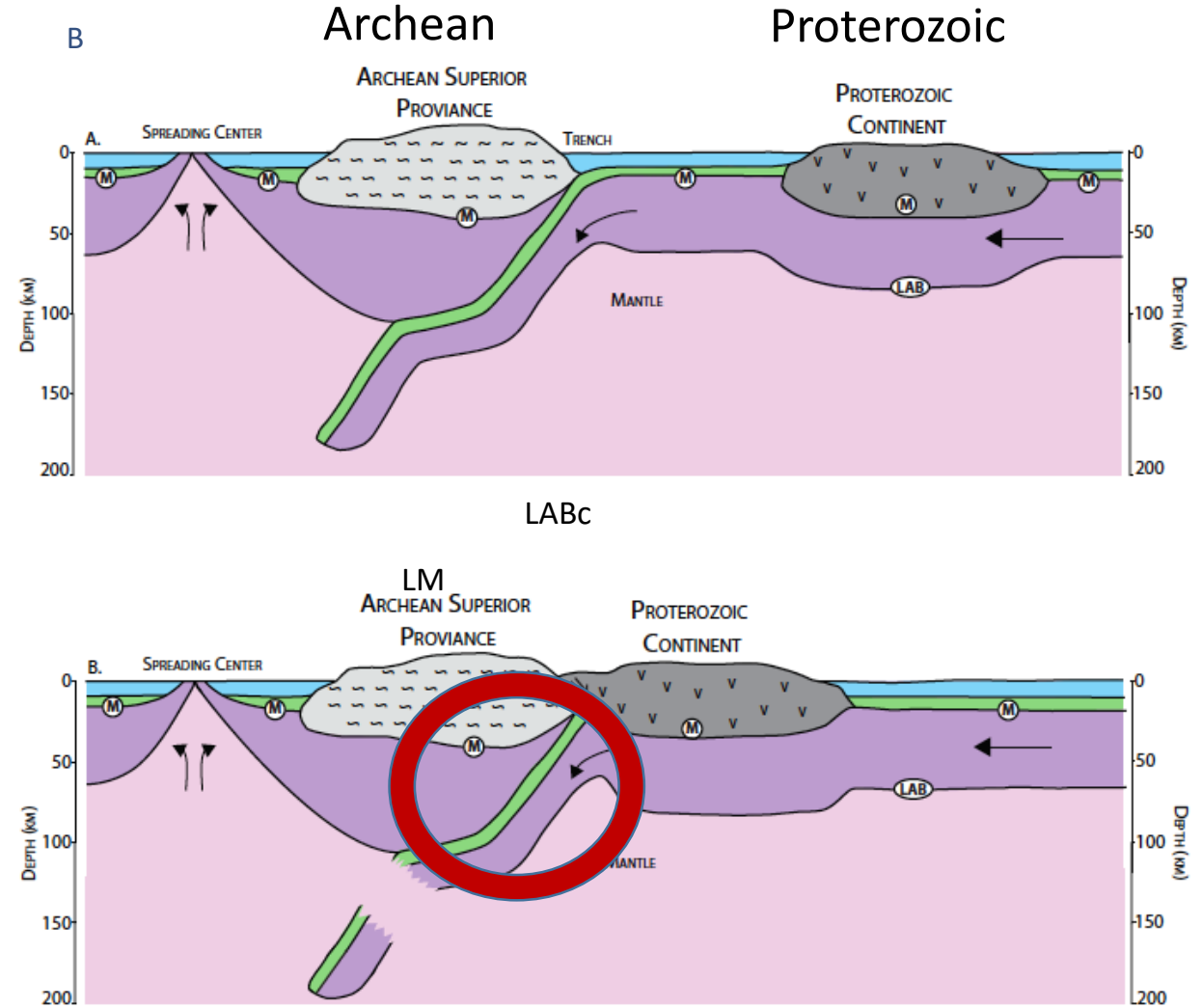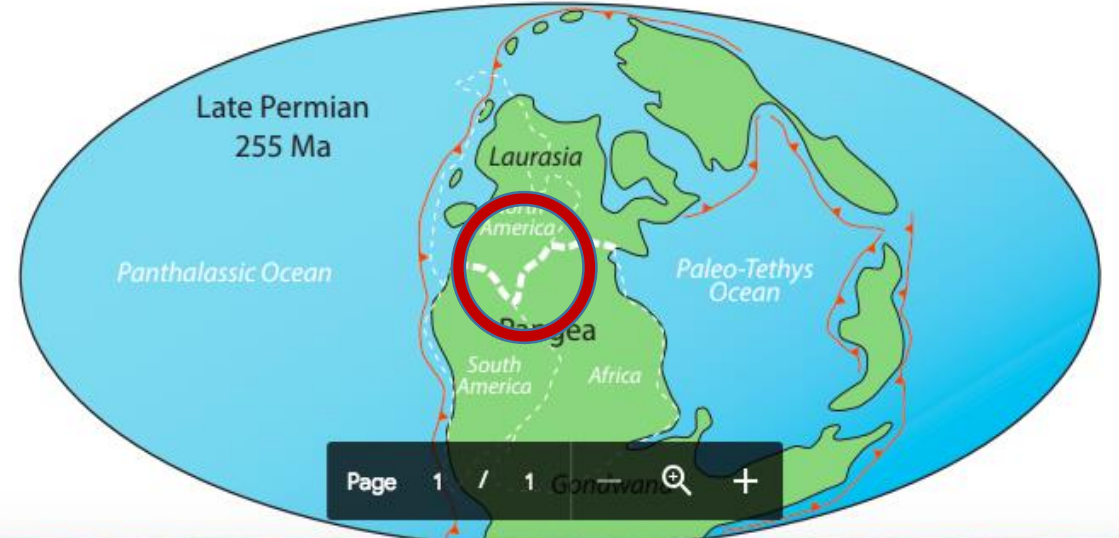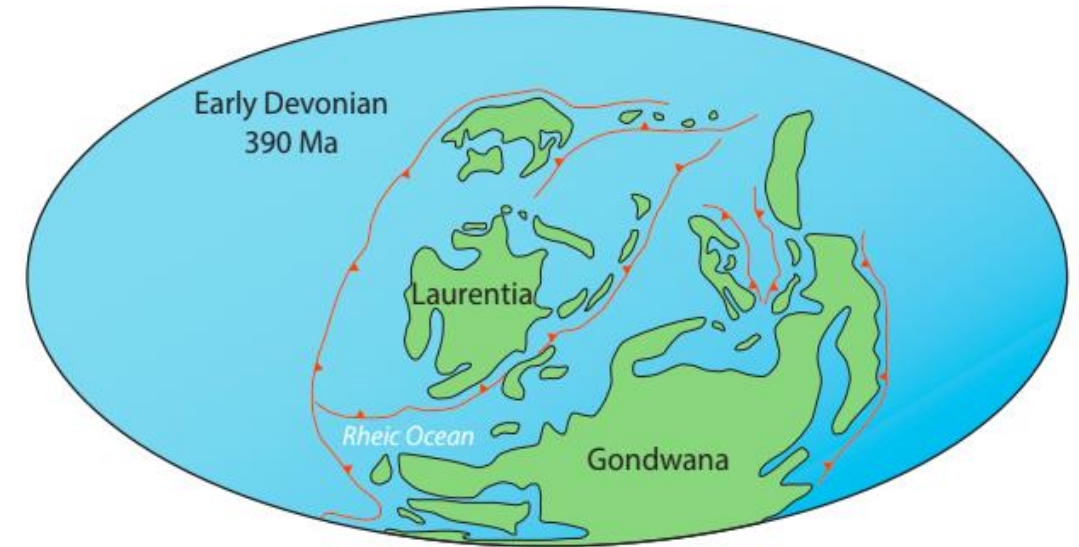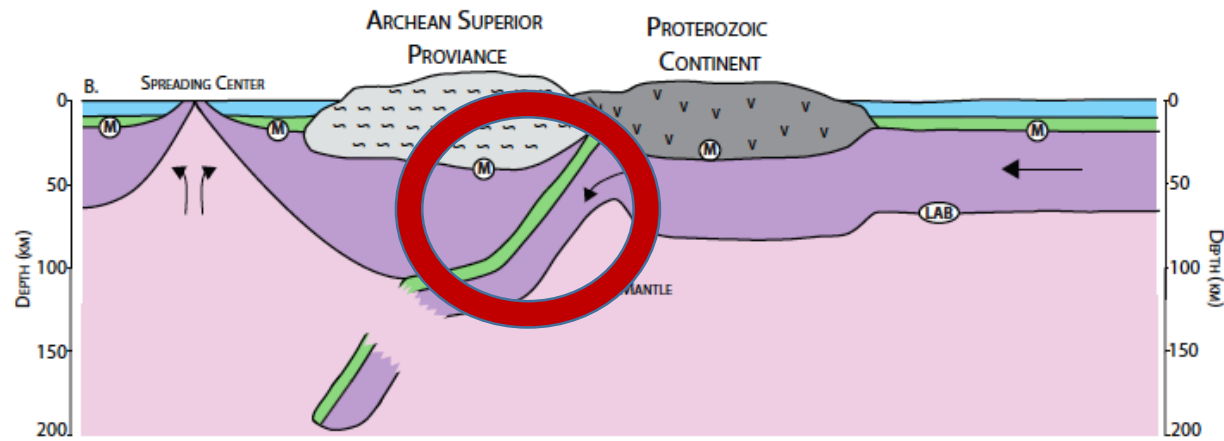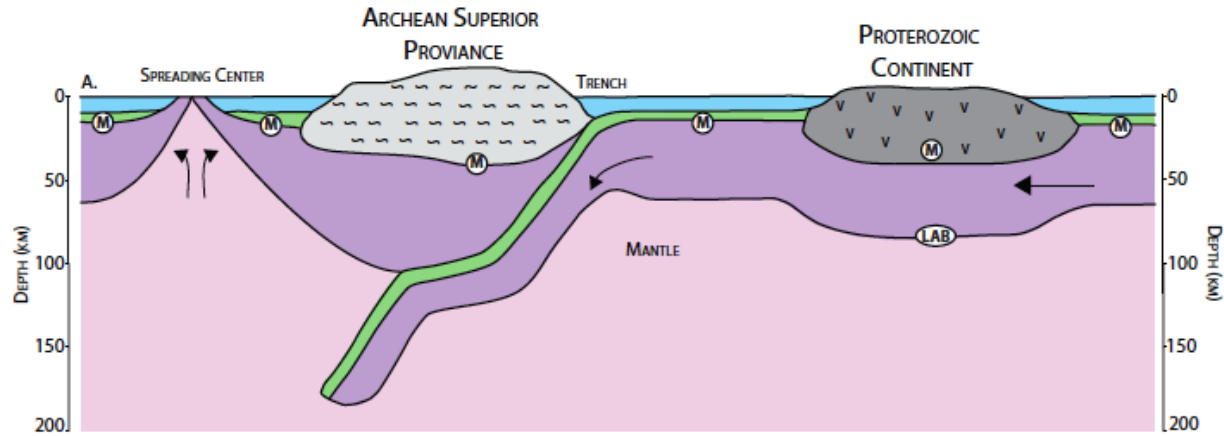# Cratonic roots from seismic anisotropy

- Seismic anisotropy can be produced at the *crystal scale* by **lattice-preferred orientation (LPO)** due to alignment of anisotropic crystals such as olivine and OPX, at the *rock scale* by **rock fabric**, at the *crustal scale*, caused by **rock foliation and layering**, and at *large scale in the mantle*, by a **temperature difference between upgoing and downgoing flow in mantle convective cells**.
- **Three major types of anisotropy include intrinsic, azimuthal, and polarization (or radial) anisotropy:**
1. Intrinsic anisotropy refers to the material itself and depends on the difference between the maximum and minimum velocities in a medium.
2. Azimuthal anisotropy is the variation of wavespeed for a certain type of wave as a function of the azimuth of the propagation direction.
3. Polarization (or radial) anisotropy is the variation of wavespeed of phases with different polarization that travel along the same direction (e.g., Love and Rayleigh surface waves, since horizontally polarized Love waves travel faster than vertically polarized Rayleigh waves).
- Anisotropy in the upper mantle is most probably caused by lattice preferred orientation of anisotropic crystals and holds clues to dynamical processes responsible for past and present deformation.
- The top layer is thick (at ~150 km) under the Archaean core corresponds to the highly depleted iron layer inferred from thermo-barometric analysis of xenoliths. The LAB is relatively flat (from 180 to 240 km in depth), in agreement with the presence of a thermal conductive root that subsequently formed around the depleted chemical layer.
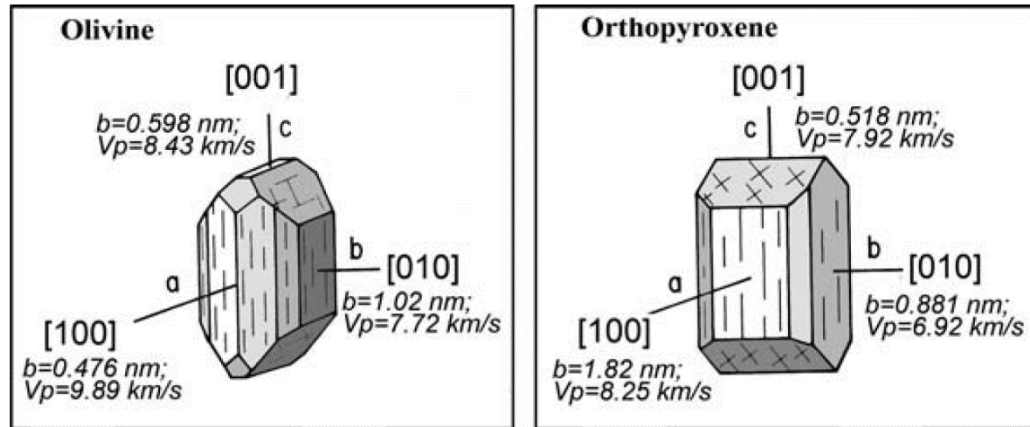
Lithospheric stratification of NA continent
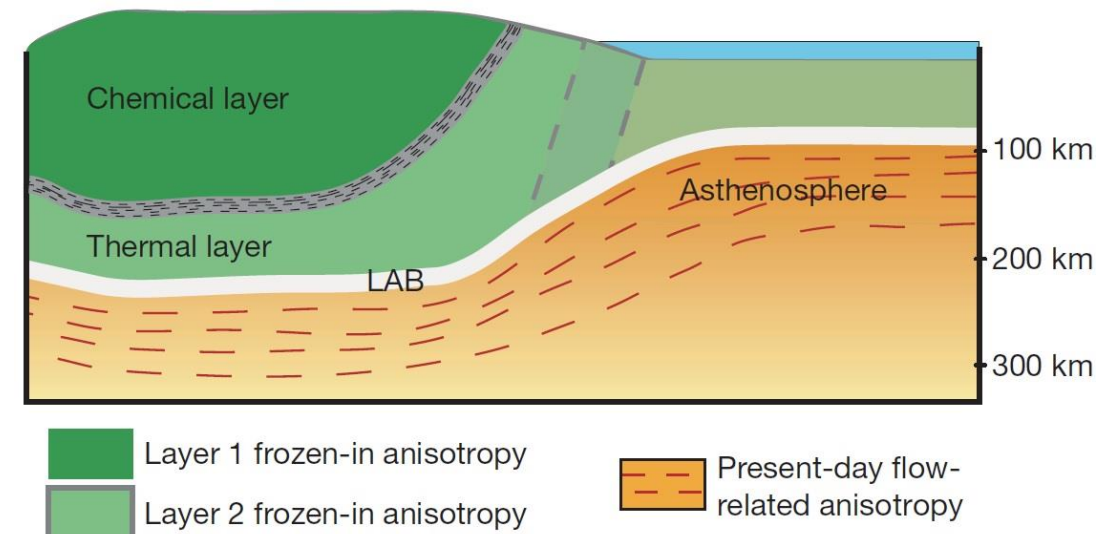
- The slip direction is characterized by the Burgers vector, which specifies the magnitude and direction of the lattice distortion in dislocations in a crystal lattice.
- The slip direction with the shortest Burgers vector is favored because of the lower strain energy associated with formation or motion of lattice dislocations.

Yuan and Romanowicz, 2010, Nature, 466

Cratonic roots from seismic anisotropy
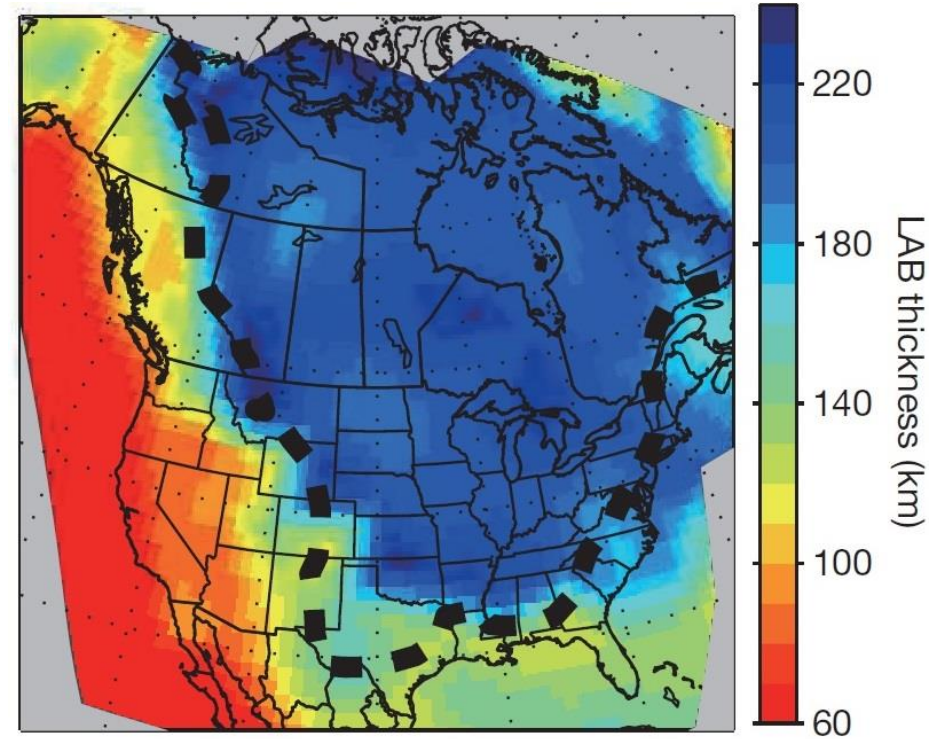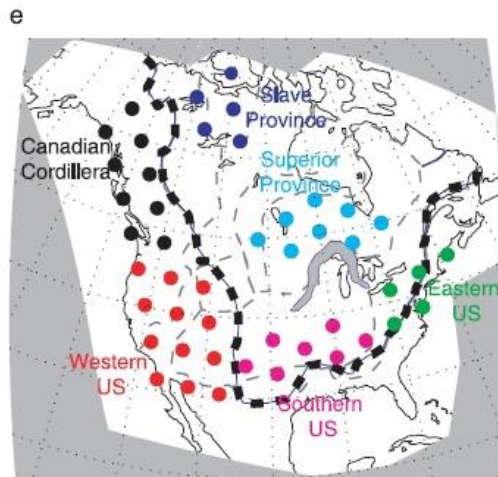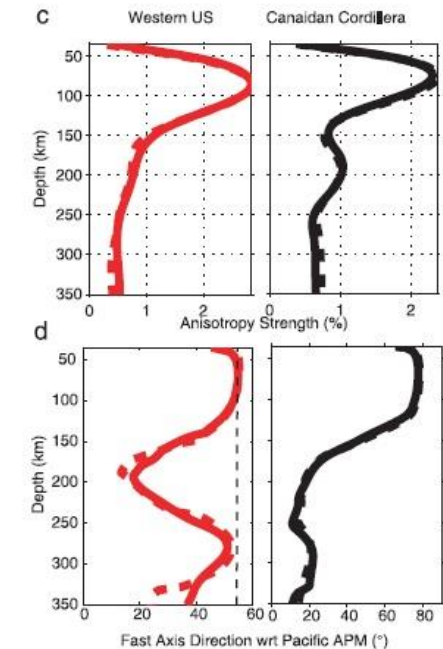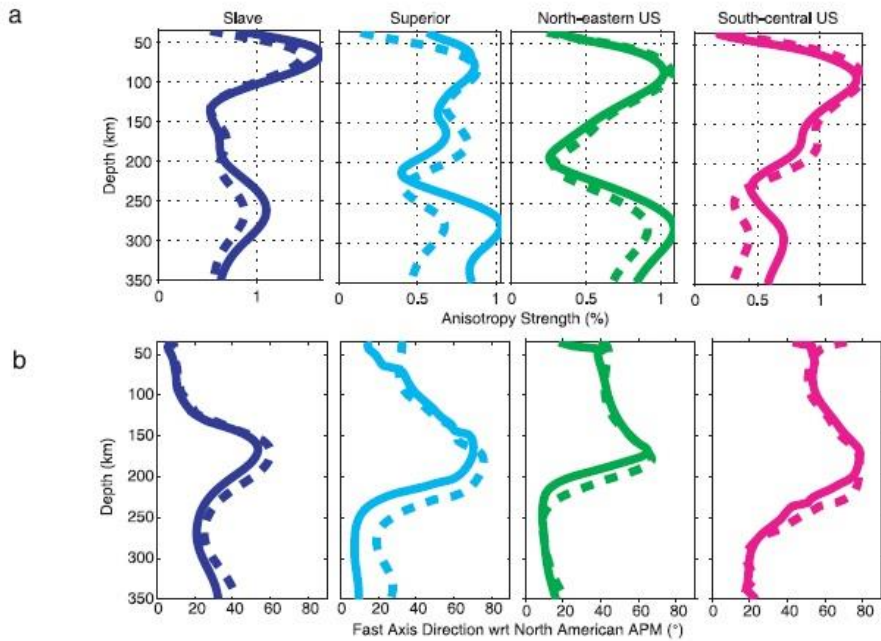
Yuan and Romanowicz, 2010, Nature, 466

Average depth profiles of anisotropy strength (a and c) and fast axis direction (b and d) for six subregions of the North American continent:

- In (a) and (b) the anisotropy direction becomes subparallel to the North American Absolute Plate Motion (APM) below 200 km, with a maximum amplitude around 270 km.
- Large anisotropy strength is observed at 80–100 km depth in the western US (WUS) and the Canadian Cordillera, which corresponds to sublithospheric depths. Subasthenospheric mantle is moving to the east with a velocity of ~5cm yr⁻¹.

Yuan et al., 2011, *Geophys. J. Int., 184*

European LAB depth
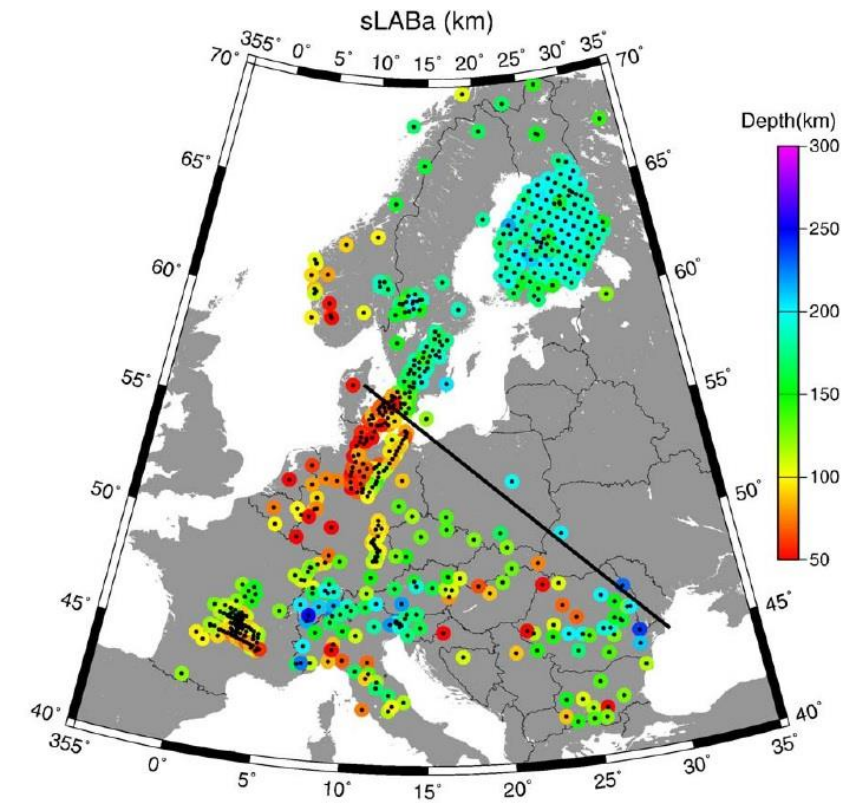
Seismic LAB (Anisotropy)
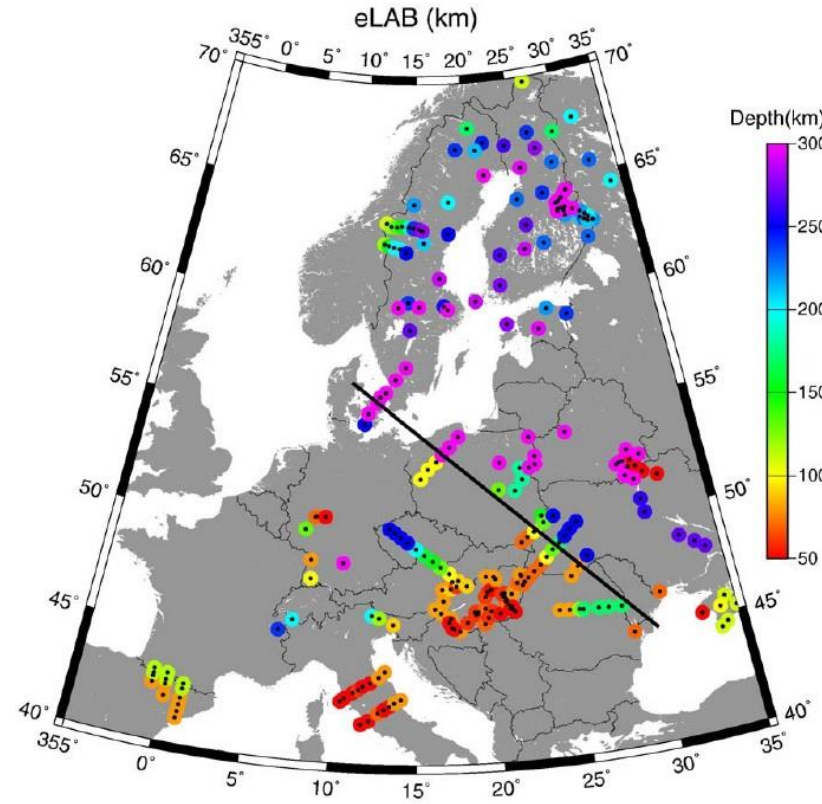
Electrical LAB
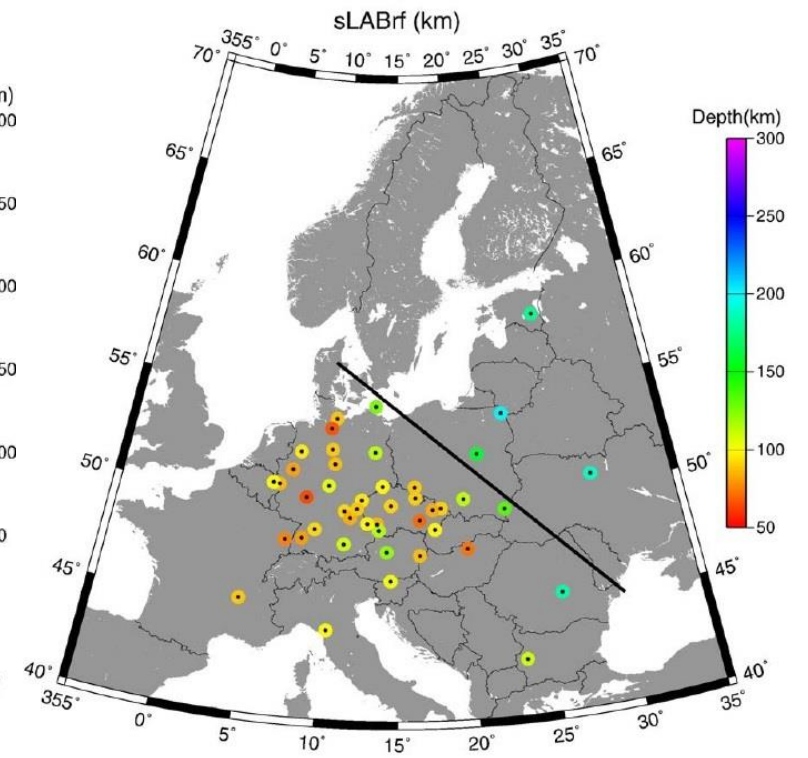
Seismic LAB (receiver functions)

Jones et al., 2010, Lithos, 120

European LAB depth
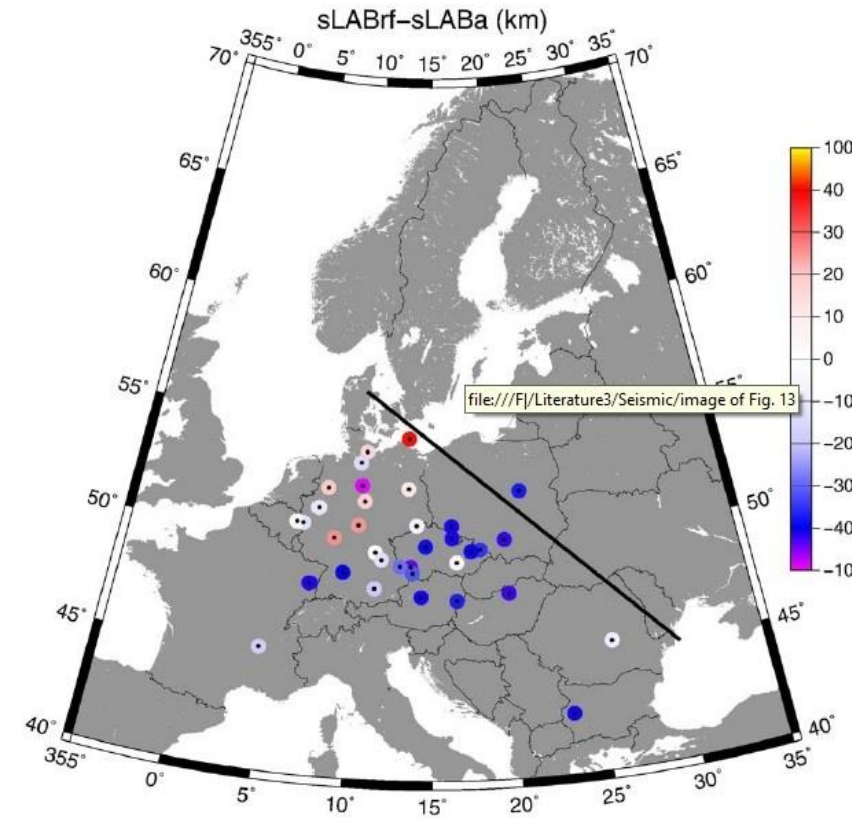
Jones et al., 2010, Lithos, 120
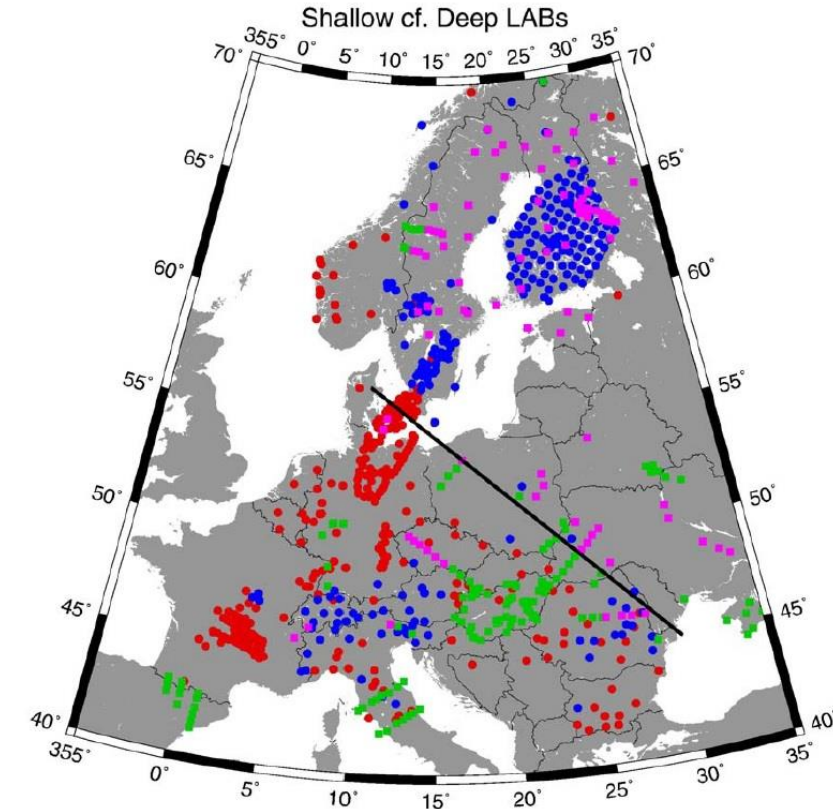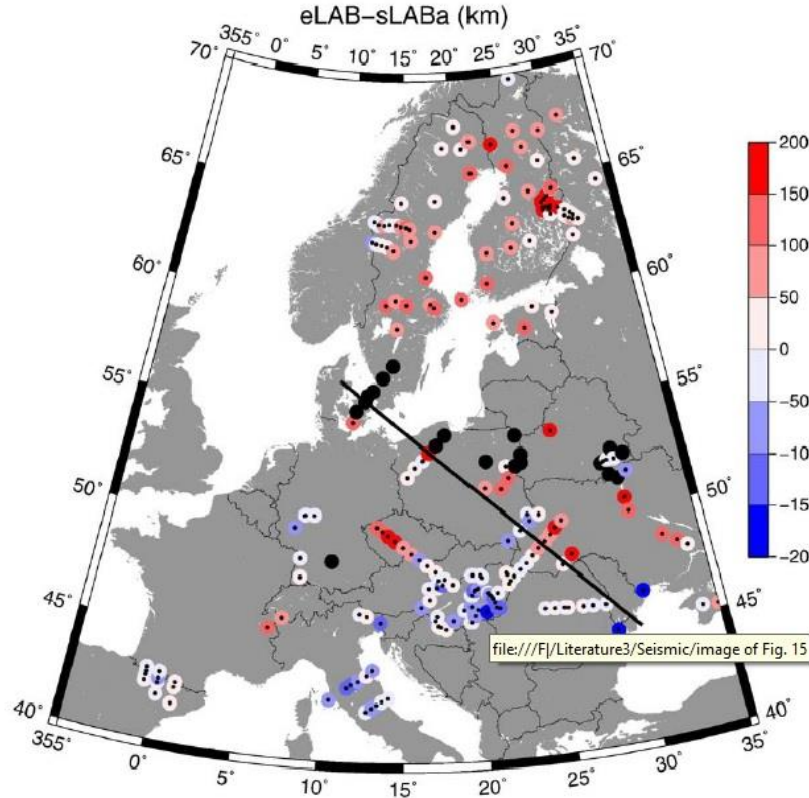
Shallow sLABa estimates (<150 km) dots in red, deep sLABa estimates (>150 km) in blue. Shallow eLAB estimates (<150 km) squares in green, deep eLAB estimates (>150 km) in purple.

The quantitative differences between the three types of LAB estimates reflect some aspect(s) of the physical transition from the lithosphere to the asthenosphere, which need not be the same for different parameters and for the different age of the provinces.

European LAB depth
(Statistics)

Statistical estimates of the depth to the lithosphere–asthenosphere boundary from the different techniques and subsets.

	sLABa [km]	sLABrf [km]	eLAB [km]
All	137 ± 48	106 ± 34	170 ± 112
Within 95% of mean	138 ± 46	96 ± 18	153 ± 95
LABs<150 km	100 ± 27		78 ± 28
LABs>150 km	183 ± 19		250 ± 51
Phanerozoic[a]	118 ± 45	96 ± 17	98 ± 56
–Median smoothed[b]	133 ± 49		89 ± 49
Precambrian	169 ± 35	172 ± 26	237 ± 66
–Median smoothed	182 ± 13		253 ± 29

[a] Alps excluded.
[b] Northern Germany excluded.

Jones et al., 2010, Lithos, 120
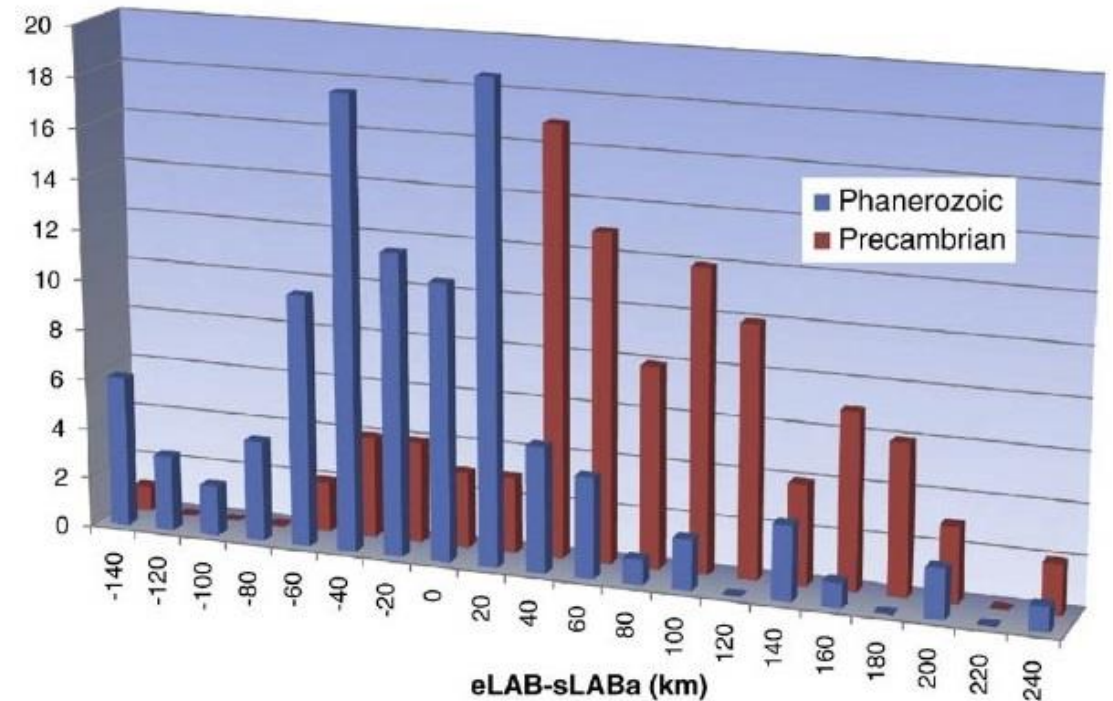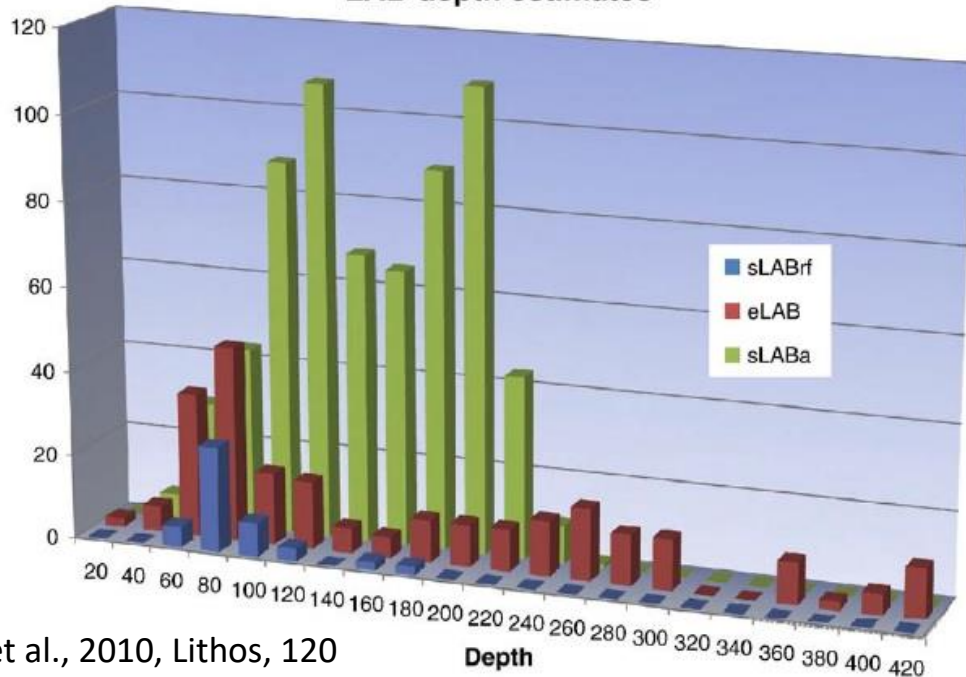
Cratons

The cratons have usually a lithospheric roots of ~200–250 km and are characterized by high seismic velocities, low electrical conductivities and low surface heat flow.
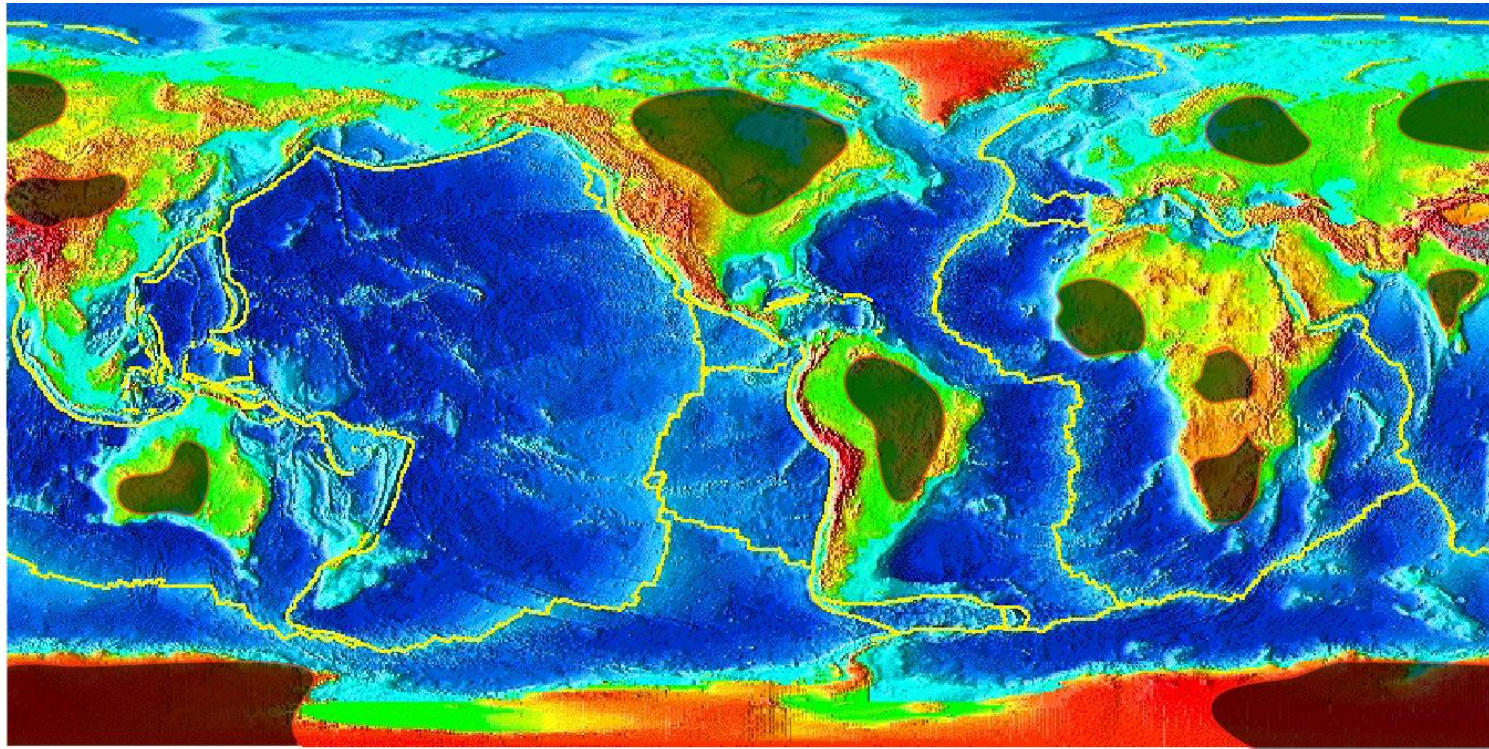
Why the cratonic lithosphere is so thick and stable? Isopycnic hypothesis:

The effect of composition and temperature on density cancel in cratonic roots making them neutrally buoyant

Higher densities due to lower temperatures are almost exactly balanced by lower densities due to lower ratios of Fe/Mg and Al/Mg (basalt depletion hypothesis)

Cratonic roots identified by seismic tomography

Average 110–150 km depth dVs (%) - ref: 4.38 km/s

Yellow Diamonds: Hot spots location
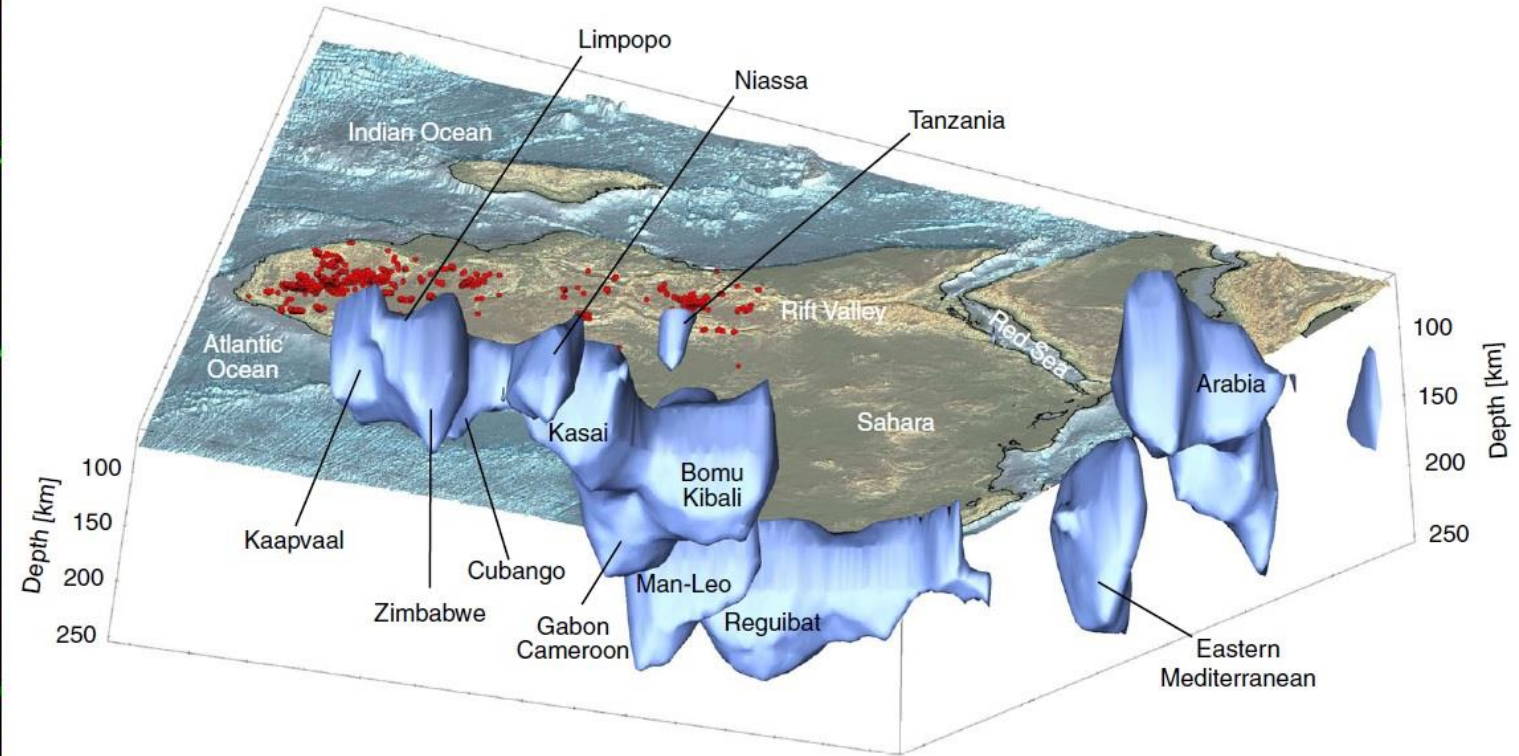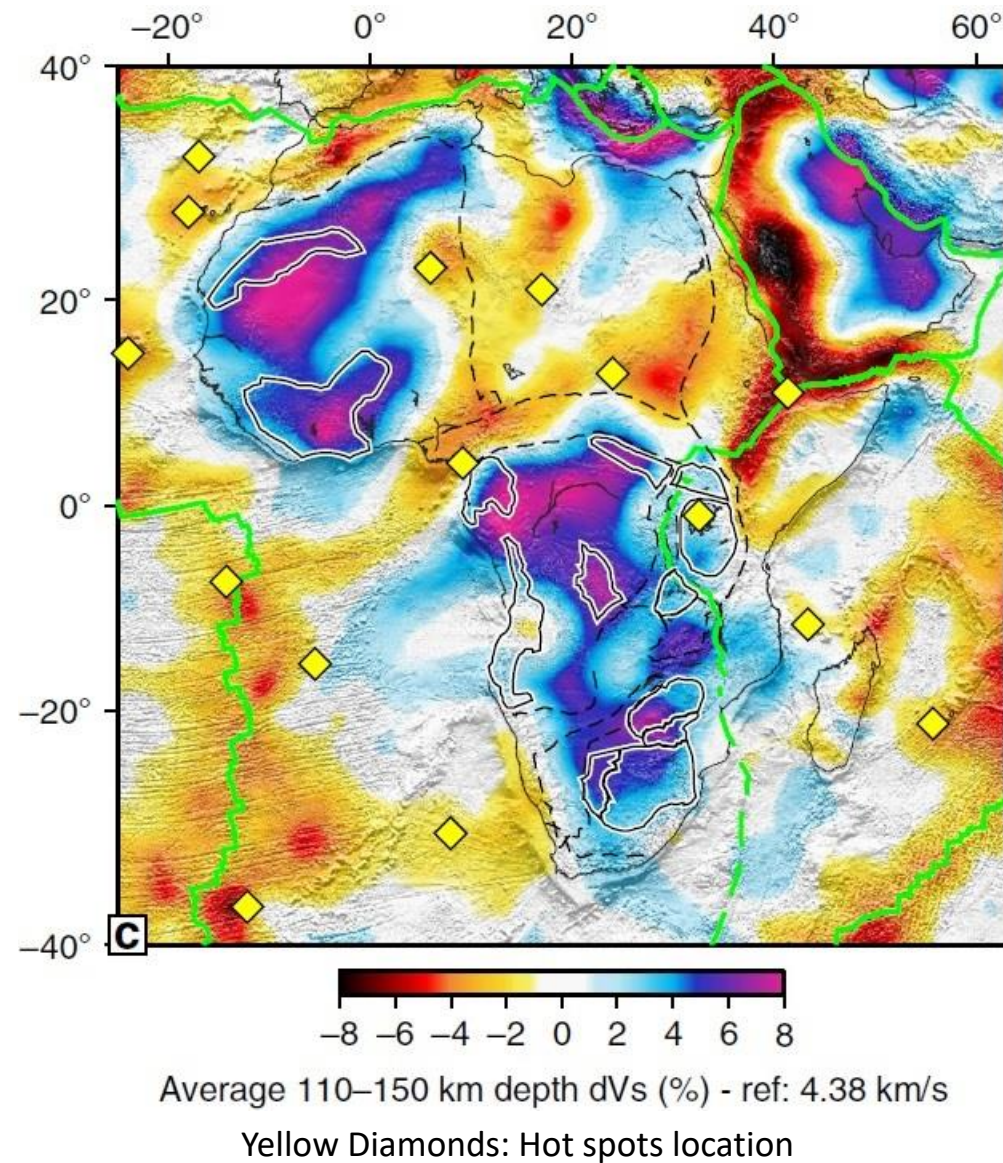
Celli et al., 2020, Nature Communications

- **Cratons have been eroded and fragmented during geological time**

Models of cratonic roots formation

Mantle Plume — Plume origin — $F = 50\%$, $F = 0\%$

Slab Stacking — Oceanic lithosphere underthrusting and imbrication
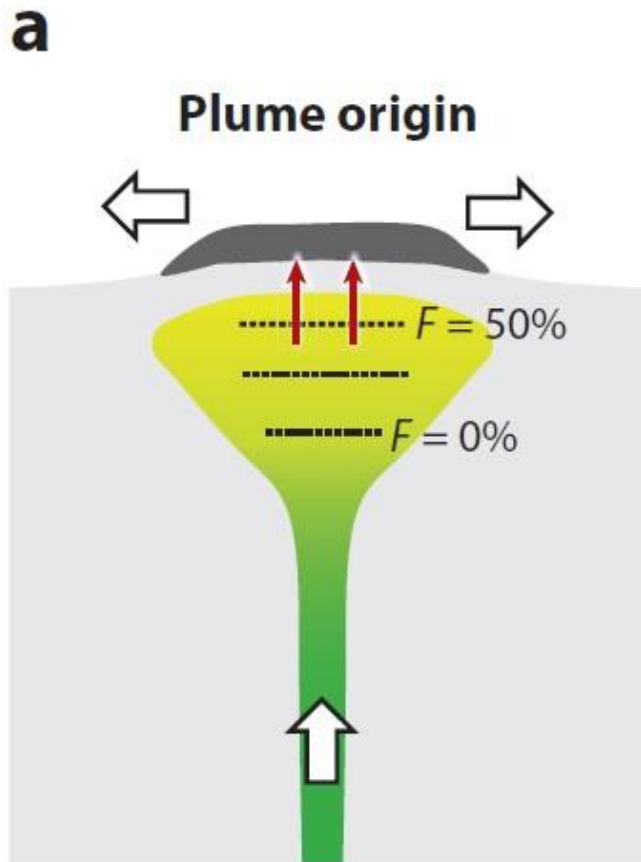
Advective Thickening — Arc thickening/accretion
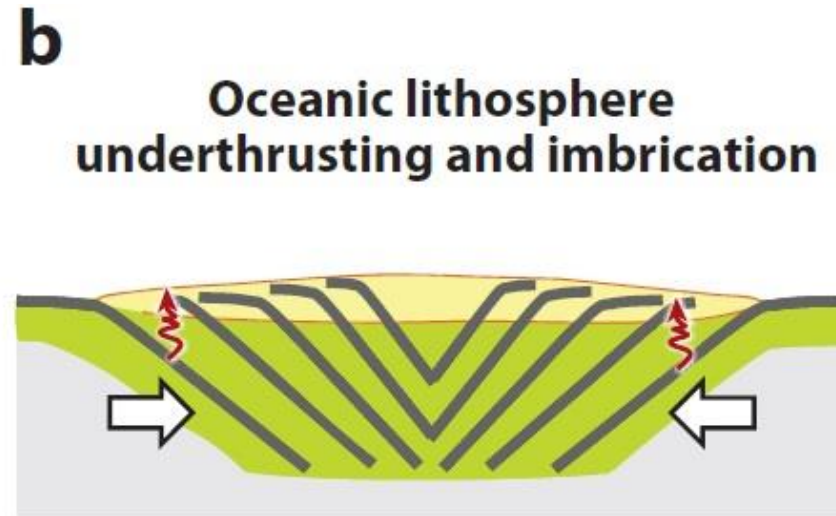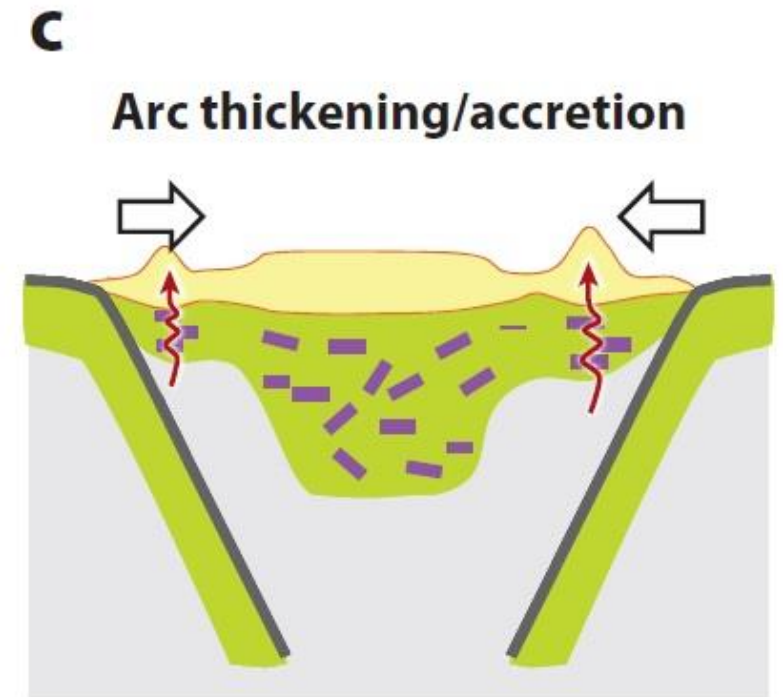
Legend:
- Basalt or komatiite
- Depleted peridotite
- Felsic crust
- Arc pyroxenites
- Ambient mantle

Lee et al., 2011, Annu. Rev. Earth Planet. Sci., 39

Models of cratonic roots formation

Three processes could have resulted in the mechanical segregation and accumulation of a layer of buoyant, viscous mantle during the Archean time:

(a) Model 1: Segregation of residue from an upwelling mantle plume

Komatiite lavas

Primitive crust or lithosphere

Residue of high-degree melting

Residue of low-degree melting
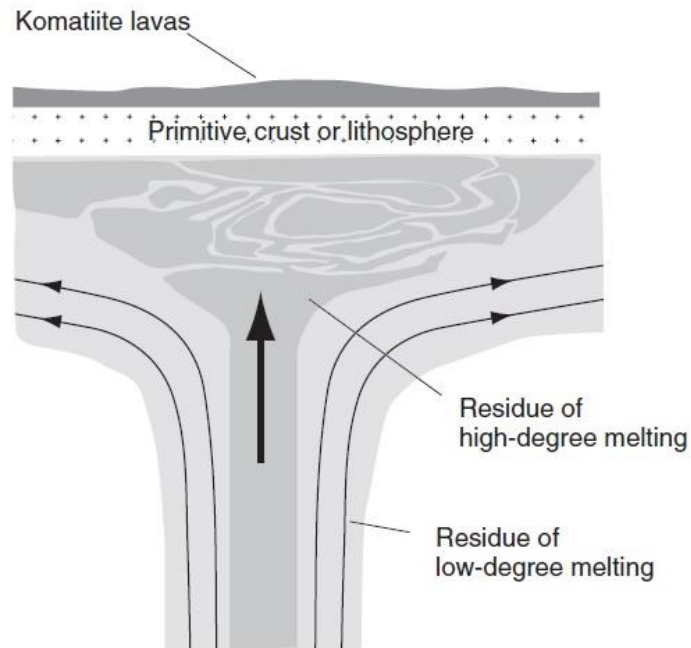
(b) Model 2: Segregation of recycled refractory residue

Oceanic plateau

Extraction and accumulation of recycled refractory residue
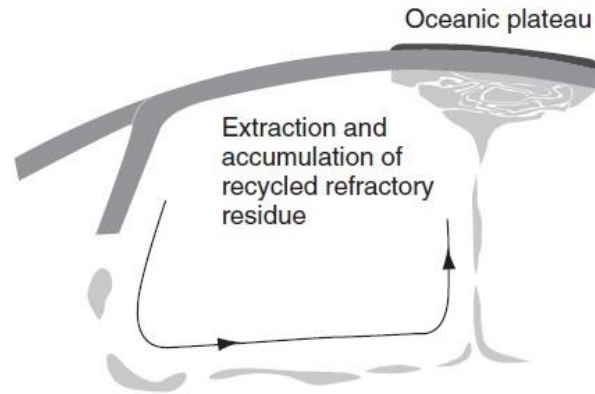
(c) Model 3: Preservation of remnants of the crust of a magma ocean

Crust

Flotation and/or in-situ crystallization of ol + opx

Liquid interior of magma ocean
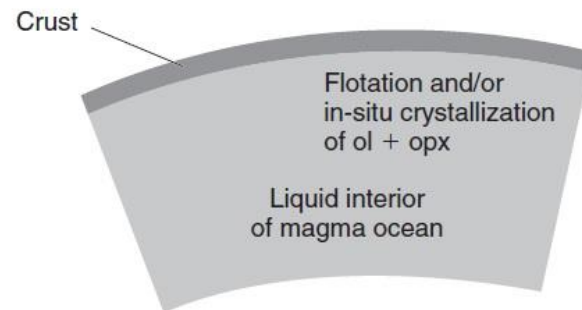
1. Upwelling buoyant residue in the core of a mantle plume could have separated from the cooler, denser exterior and accumulated during ascent.
2. Buoyant residue could have segregated slowly as material was transported down subduction zones and recycled through the mantle in convection cells.
3. Some subcontinental lithosphere could be the remnants of an initial crust that crystallized in an Archean magma ocean that formed during the final stages of Earth accretion.

Archean mantle roots probably resulted from more than one tectonic environment (no single setting is applicable)

Models of cratonic roots formation

1. **Plume Origin**: A highly melt-depleted, dehydrated, and low-density chemical boundary layer is an immediate product of very hot plume (> 1650 °C) melting, resulting in the formation of a craton from the outset.

   - The plume model predicts a gradual stratification from highly melt-depleted (high Mg#) peridotite at shallow depths to fertile peridotites (low Mg#) at the base of the thermal boundary layer, but such stratification is not a general feature of cratons.
   - This model predicts high-degree melting at a depth of ~200 km, but the 1700°C temperatures of melting recorded by cratonic peridotites are not high enough to generate extensive melting at these depths.

2. **Underthrusting or imbrication of oceanic lithosphere (favored in the mid-Archean to the early Proterozoic):**

   - It can explain the low-P and low-T components of cratonic peridotites, the general lack of systematic compositional stratification with depth, and the presence of sub-horizontal and dipping discontinuities within the continental mantle.
   - Partial melting of underthrusting oceanic crust could generate felsic magmas such that formation of evolved continental crust and thick continental mantle would be tectonically linked.
   - This process is thought to be unlikely because negatively buoyant oceanic lithosphere should subduct instead of subcrete. In addition, the predicted amount of eclogite exceeds the present amount in the continents.
   - However, during the Archean the oceanic lithosphere could have been buoyant, on account of the thick basaltic crust. This condition would not be permanent if a significant portion of the basaltic crust transforms to eclogite once at depth.

3. **Accretion and Orogenic Thickening of Arcs:**
   - Young arcs are typically under extension, but as subduction zones mature, arcs often evolve into a compressional state as exemplified by the Cretaceous North American Cordilleran.
   - Lithological similarities make this hypothesis attractive, but further data are needed.
   - This hypothesis would be problematic, considering that mafic cumulates are the complementary residue to the more felsic or intermediate buoyant crust.

Models of cratonic roots formation

Burial / reworking

Cooper et al., 2021, Tectonophysics, 695

Delamination
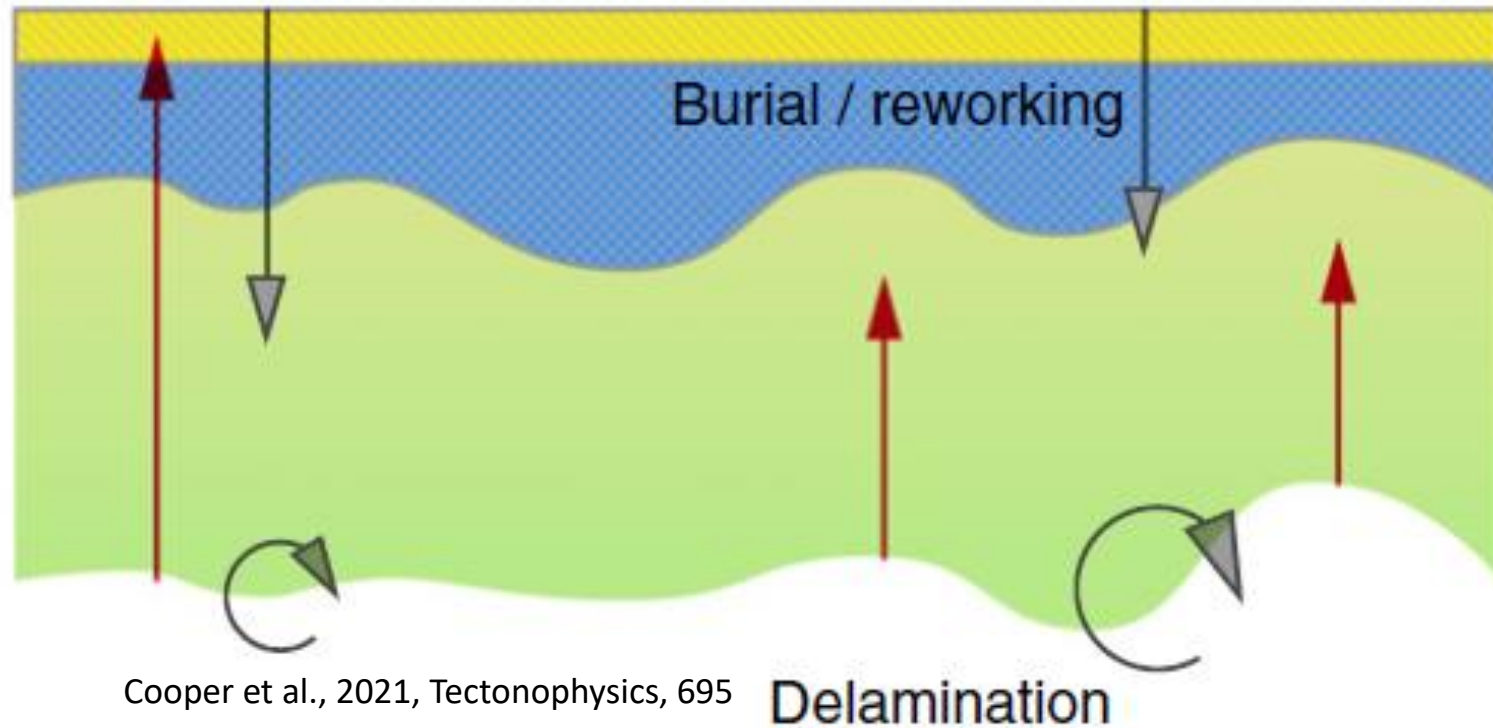
- The authors propose that variations in the thickness of the early lithosphere could have driven horizontal gravitational forces sufficient to cause yielding of the adjacent thinner oceanic lithosphere simultaneously initiating subduction and collapse within the continental lithosphere.
- The gravitational collapse initiates decompression melting at the base of the continental lithosphere. This melting event introduces depleted residue at the base of the thinned continental lithosphere.
- In this model, the lithosphere continues to thicken and strengthen via cooling.

Models of Komatiite generation

Influence of lithospheric thickness on the melting depth
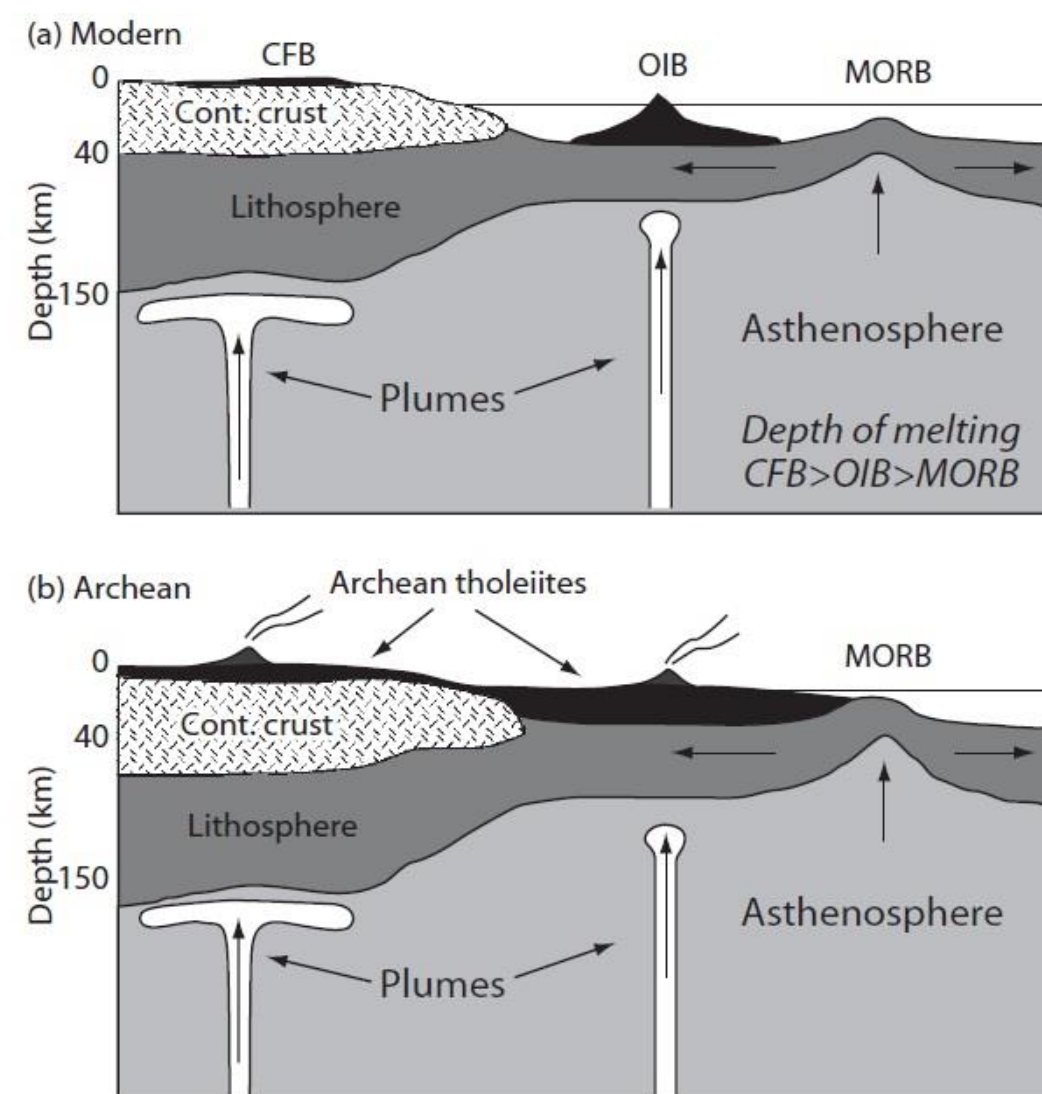
- If the source rocks of komatiites were dry then high ambient T in the Archean mantle would have caused melting to begin at larger depths, which would have produced large volumes of basalt (LIPs) and oceanic crust that was much thicker (20–40 km) than it is today.
- Source of the melting producing komatiites has important consequences for both the tectonic setting and the Earth's thermal evolution.

Mantle melt generation temperatures
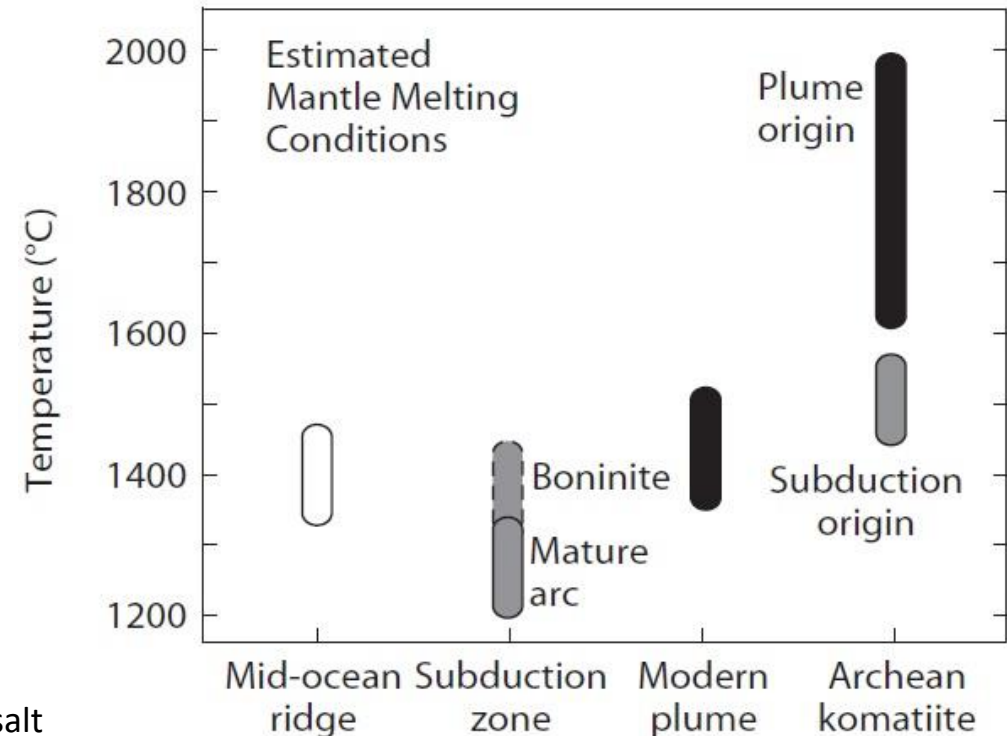
CFB=Continental Flood Basalt, OIB=Oceanic Island Basalt, MORB=mid-ocean ridge basalt

Models of Komatiite generation

(a) Subduction initiation
Komatiitic crust
continent

(b) Mature subduction zone
Calc-alkaline arc magmas
continent

(c) Subduction termination – continent collision
continent
continent

(obduction of komatiite)

▨ Highly depleted mantle lithosphere
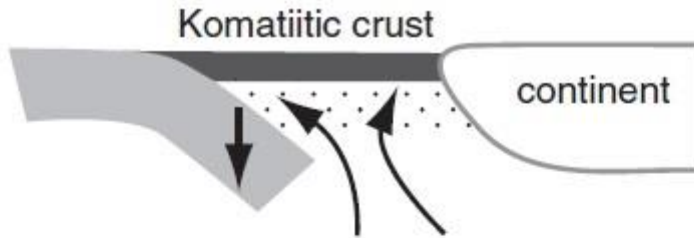
High magnesium contents and high degrees of melting associated with the formation of komatiites reflect melting T (1400–1600°C) that are higher than those of modern basaltic magmas.
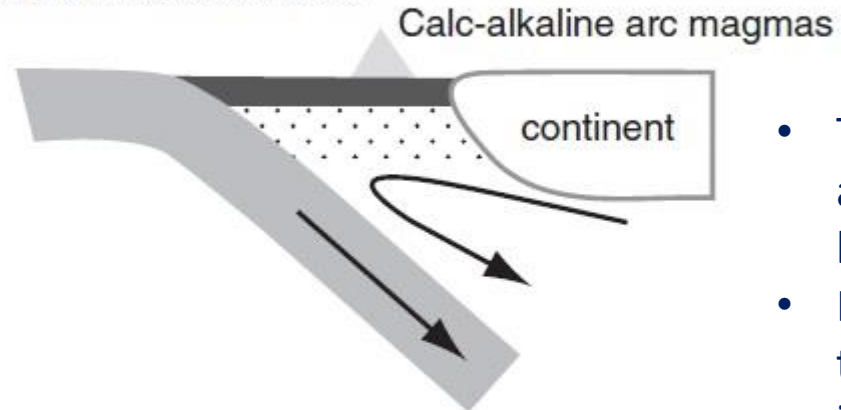
- The komatiite may be the result of the melting of hydrous mantle in anomalously hot forearc regions above young subduction zones, like the boninites (high-Mg andesites) of in the Izu-Bonin-Marianna island arc.
- In this case, shallow melting and subduction result in the formation and thickening of highly depleted mantle lithosphere that some time later is incorporated into the cratonic mantle below a continent.

Evolution of the cratonic lithosphere

- In most of cratons, isotopic ages from mantle xenoliths and various crustal assemblages indicate that chemical depletion in the mantle lithosphere was coupled to accretionary processes in the overlying crust.

- This is a strong evidence that the crust and the underlying lithospheric mantle formed more or less contemporaneously and have remained mechanically coupled since at least the Late Archean.
- A progressive decrease in the degree of depletion in the lithospheric mantle since the Archean indicates that the Archean–Proterozoic boundary represents a major shift in the nature of lithosphere-forming processes, with more gradual changes occurring during the Phanerozoic.
- The main driving mechanism of this change is the secular cooling of the Earth and subsequently processes related to subduction, collision, terrane accretion, and magma addition.
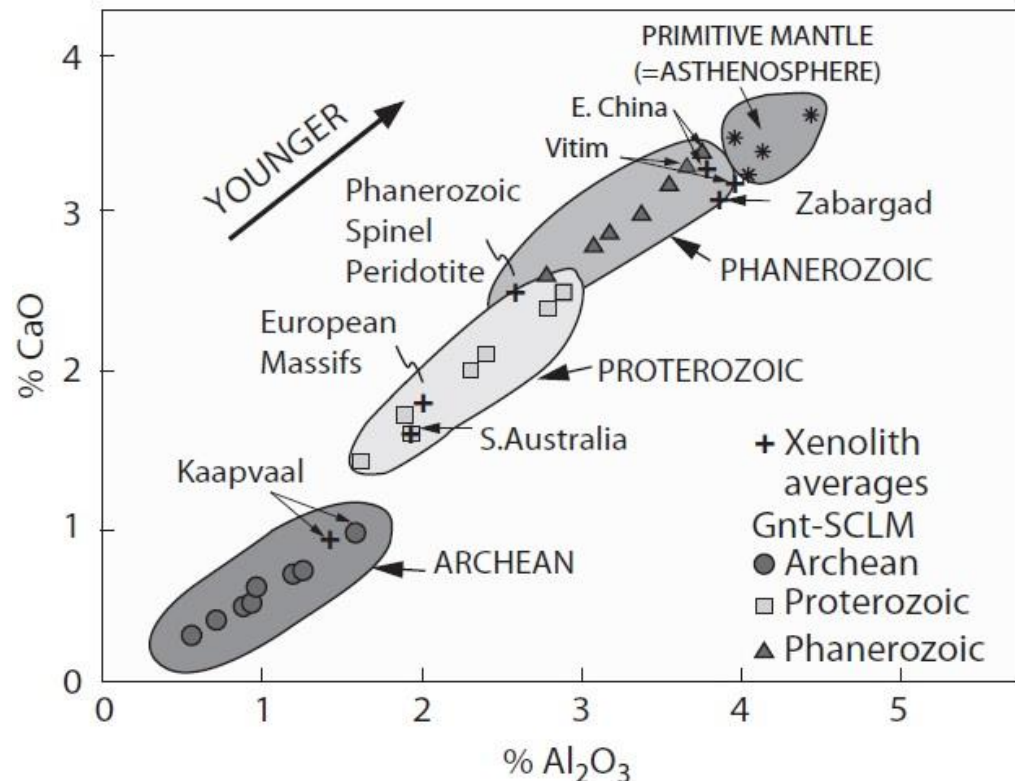
o *Range of subcontinental lithospheric mantle (SCLM) compositions for selected cratons that have been matched with ages of the youngest tectonothermal events in the overlying crust.*
o *Newly formed subcontinental lithospheric mantle has become progressively less depleted in Al and Ca contents from Archean through Proterozoic and Phanerozoic time.*

Precambrian Geodynamics

- Major of the lithosphere was formed (or preserved) at 3.2–2.8 Gyr. Archean geodynamics was dominated by plume tectonics and the development of hot accretionary orogens with low topography.
- Due to the hot mantle temperature, slab break-off was more frequent in the Precambrian time and limited occurrence of ultrahigh-pressure (UHP) rocks. Mantle downwellings and slab break-off processes are likely to have played a key role in assembling and stabilizing the hot orogens.
- Both oceanic and continental lithospheres were rheologically weak due to the high temperatures.
- Numerical models suggest that the long-term stability of cratons sustaining multiple supercontinent cycles can be achieved if their viscosity and yield strength are sufficiently high and weak mobile belts are present along the boundaries of the cratons.
- Stable cratons facilitate subduction initiation of very young seafloor during continental growth and dispersal.
- Wide spread development of modern-style (cold) collision on Earth started during Neoproterozoic at 600–800 Myr. Cold collision created favorable conditions for the generation of UHP metamorphic complexes, which become widespread in Phanerozoic orogens.

Gerya, 2014, Gondwana Research, 25
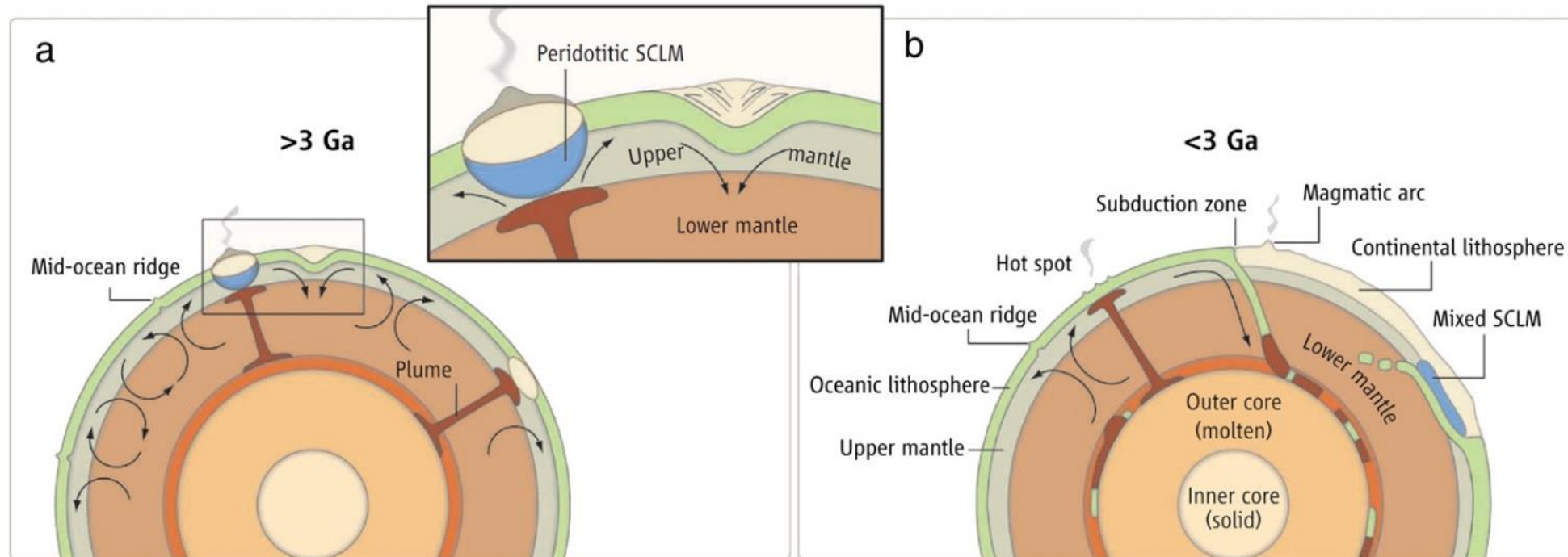
Precambrian Geodynamics

Pre-Archaean 4.0–4.5 Ga

Labels: Lithosphere, Unstable cold boundary layer, Hot plume, Cold drips, Core, Depleted mantle

Post-Archaean 0–2.0 Ga

Labels: Subducted slab, Spreading center, Upper mantle, Lower mantle, Lithosphere, Hot plume, Core, Enriched mantle
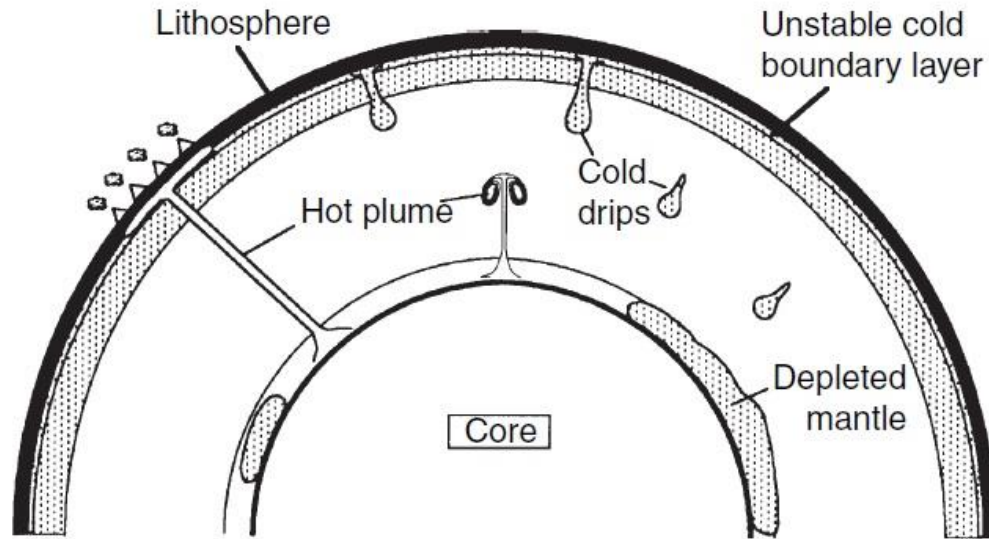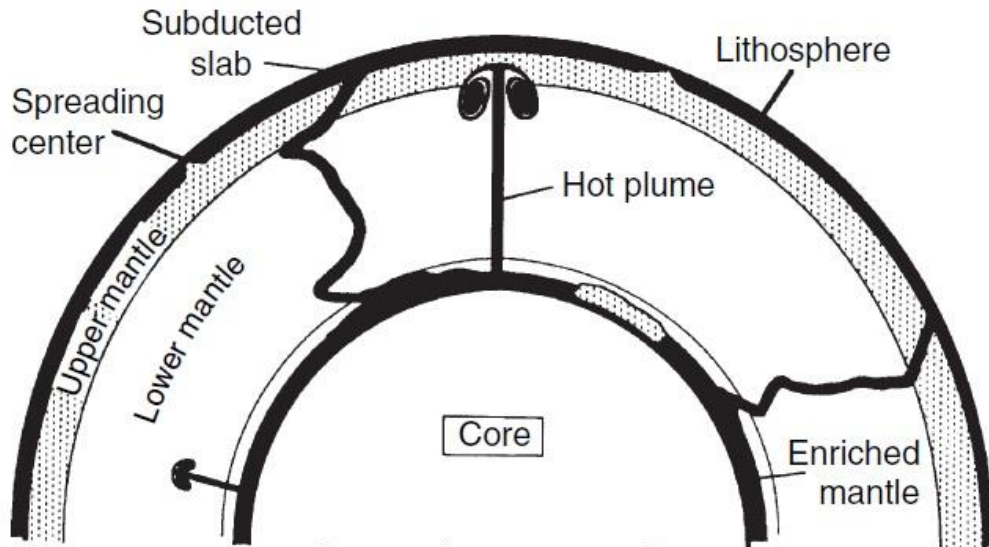
- During the pre-Archean or Hadean (4.5–4 Ga), the mafic crust was too buoyant to founder, and only the underlying mantle part of the thermal boundary layer (already cold) foundered.
- The post-Archean change in chemistry is attributed to the replacement of the early depleted D″ layer by enriched subducted mafic crust.
- The higher temperatures of the plume during the Archean, may be due to the fact that the earlier phase the D″ layer covered only part of the core, leaving hot core directly in contact with mantle elsewhere and thus generating very hot plumes.

Davies, 2007, Treatise of geophysics, vol. 9

Precambrian Geodynamics
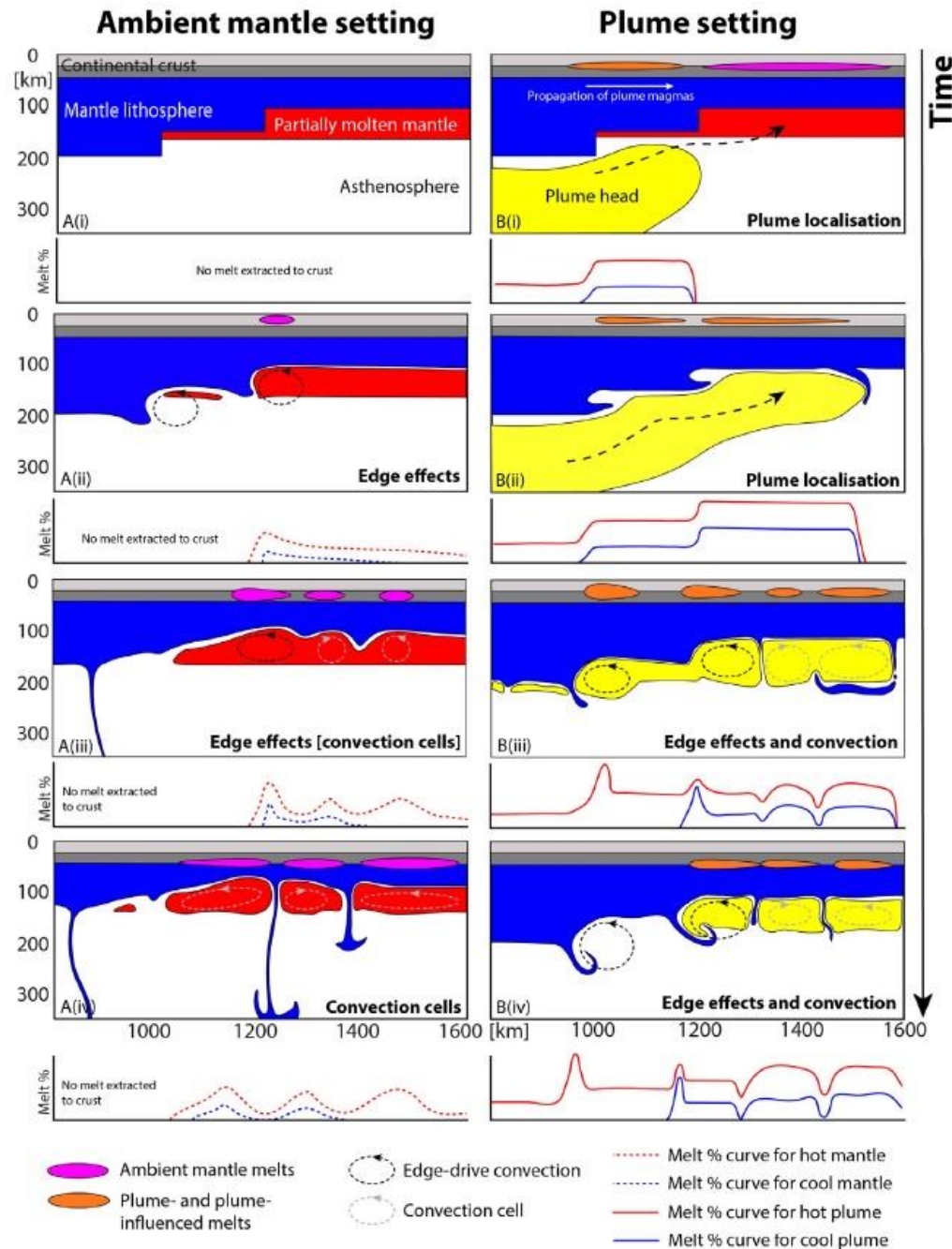
Lithospheric architecture controls the volume and location of continental magmatism throughout Earth history:

- In ambient mantle only Archean and Paleoproterozoic T_p (1600-1550°C) values yield significant sub-lithospheric melt volumes, resulting in 'passive' geodynamic emplacement of basaltic magmatic provinces, while no melts are extracted at 100 km for Meso-Neoproterozoic and Phanerozoic T_p (1500-1400°C).

- Thermal erosion of the lithosphere is much greater in a hotter mantle and would have led to significant convective removal of lithosphere in both in plume and ambient mantle settings.

- The decrease in production of sub-lithospheric melts in the early Proterozoic and the observation of the first eclogites and at around 2.0 Ga suggest an empirical link between the disappearance of deep ambient mantle melting and the onset of subduction: melt percolation into the overrding plate weakens it and allows internal deformation, precluding one-sided modern-style subduction.

Gorczyk et al., 2018, Tectonophysics, 746

Cratonic Roots: How did they form?

- Cratonization process could occur through shortening and thickening of depleted mantle, but how do the cratons evolve to their stable roots without under-going collapse?
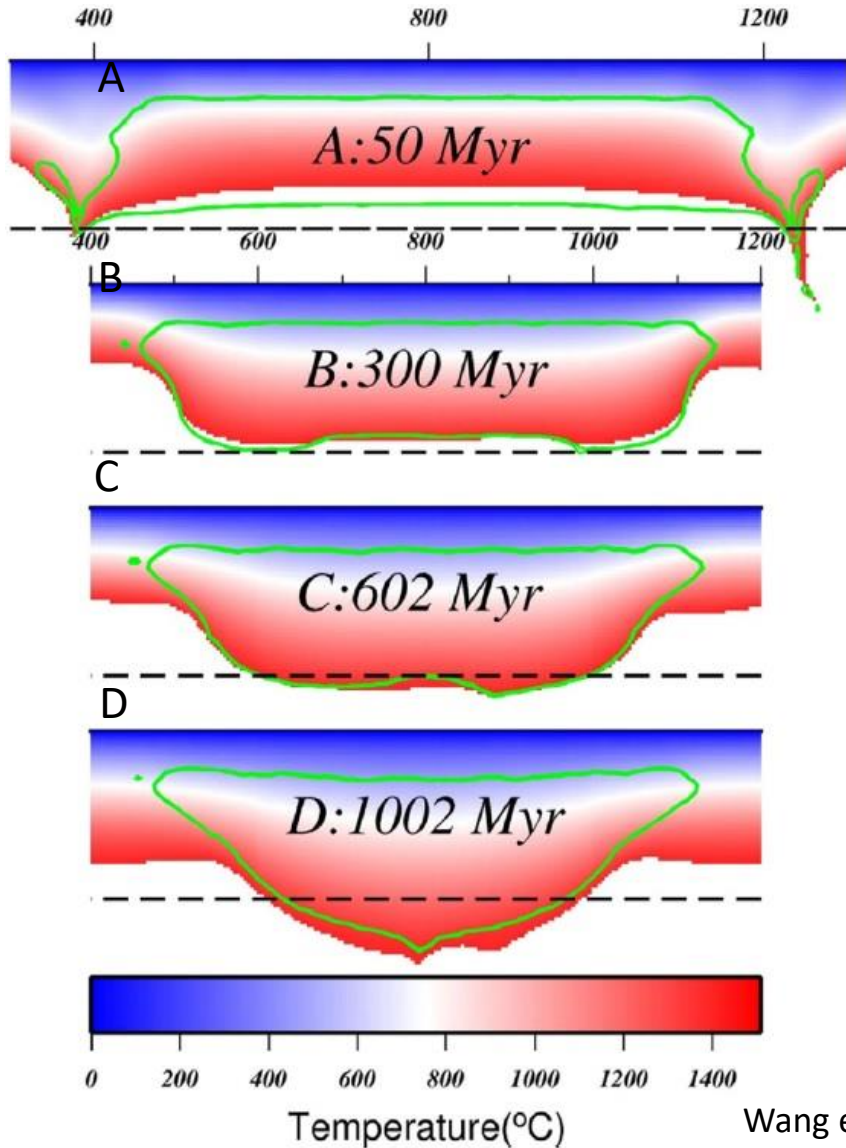
Thickening process

1. A first stage (A) of tectonic shortening, resulting in more thickening at the edge of the cratons than at its interior. Indeed, the depleted mantle material, compositionally buoyant and more viscous resists this thickening process.
2. When the thickened root cools and becomes denser, its negative thermal buoyancy starts to exceed the inherent chemical buoyancy and results in further thickening (stage B-D).
3. Significant initial thickening and shortening of depleted lithospheric mantle material is essential for the development of subsequent late-stage gravitational thickening of the cratonic root (Stage D).

Wang et al., 2018, Tectonophysics, 746

Cratonic Roots: How did they form?
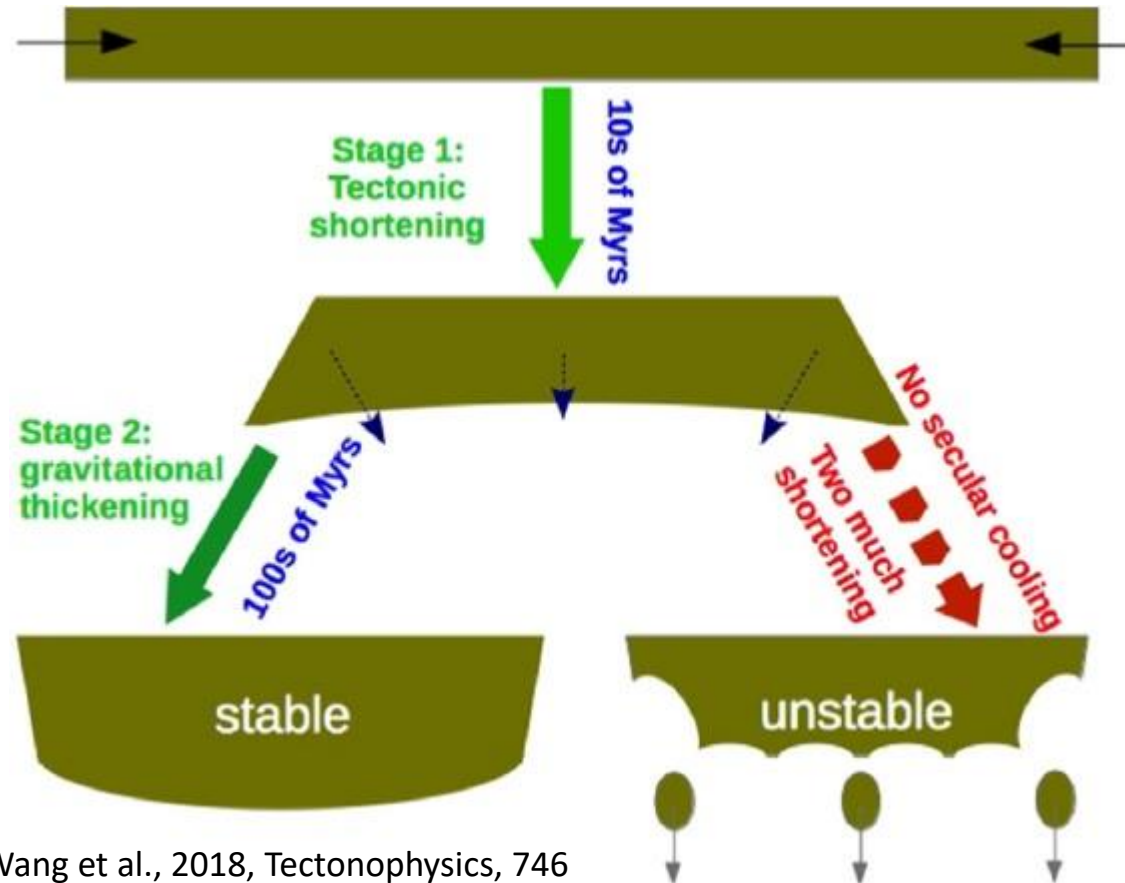
Wang et al., 2018, Tectonophysics, 746

1. Rapid compressive shortening of a depleted mantle lithosphere alone may not form a stable thermo-chemical structure.
2. A slow self-driven thickening (gravitational thickening stage is driven by the diffusive cooling of the root) and adjustment processes, as a result of thermal equilibration is required to stabilize the newly formed cratonic root.
3. Thickening cratonic lithosphere may be formed by processes analogous to modern tectonics, involving subduction accretion, lithospheric underplating, or continental collision (all of which require localized deformation).
4. **Craton formation requires lithosphere to gradually develop strength and a balance between compositional and thermal buoyancies such that deformable lithosphere can grow into virtually indestructible cratons.**

Crustal Structure of South African Craton
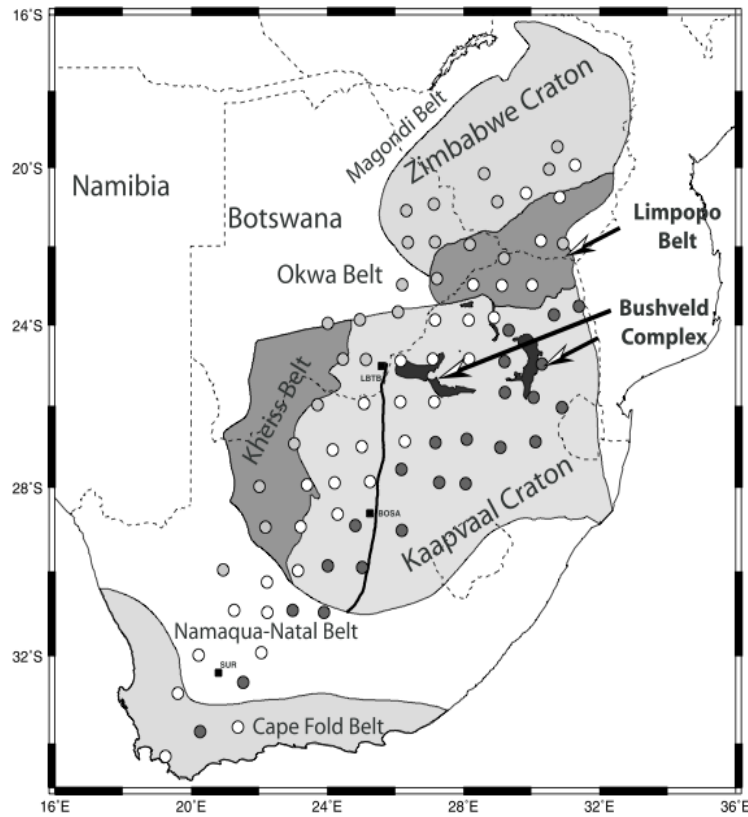
James et al, 2004, G3, 5
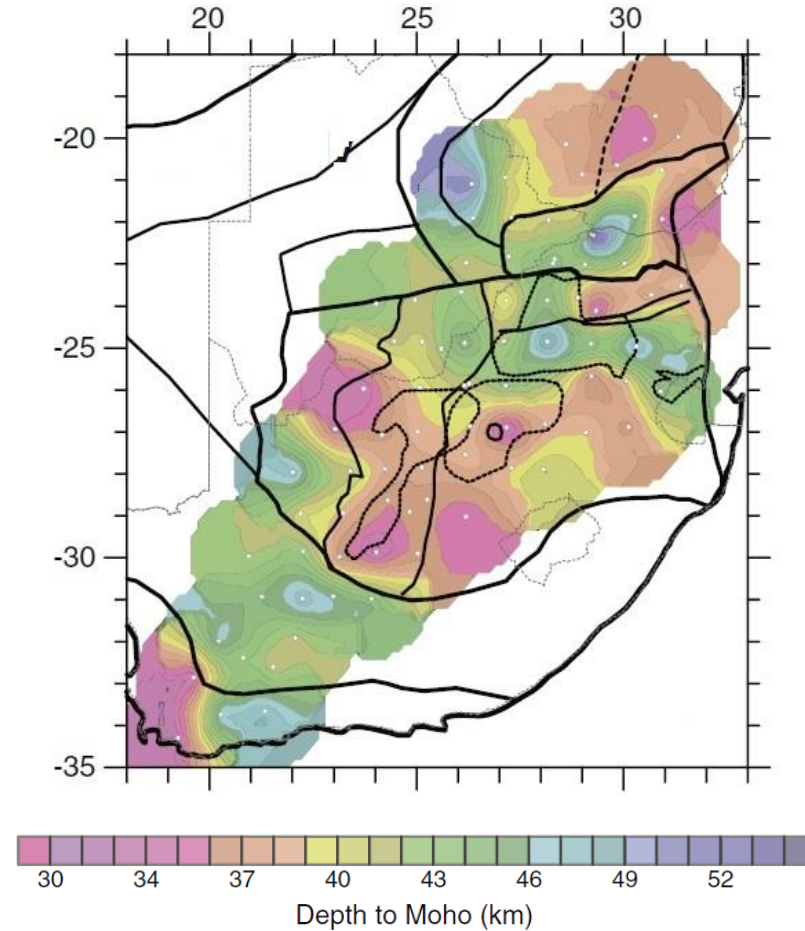
Youssof et al., 2013, Tectonophysics, 209
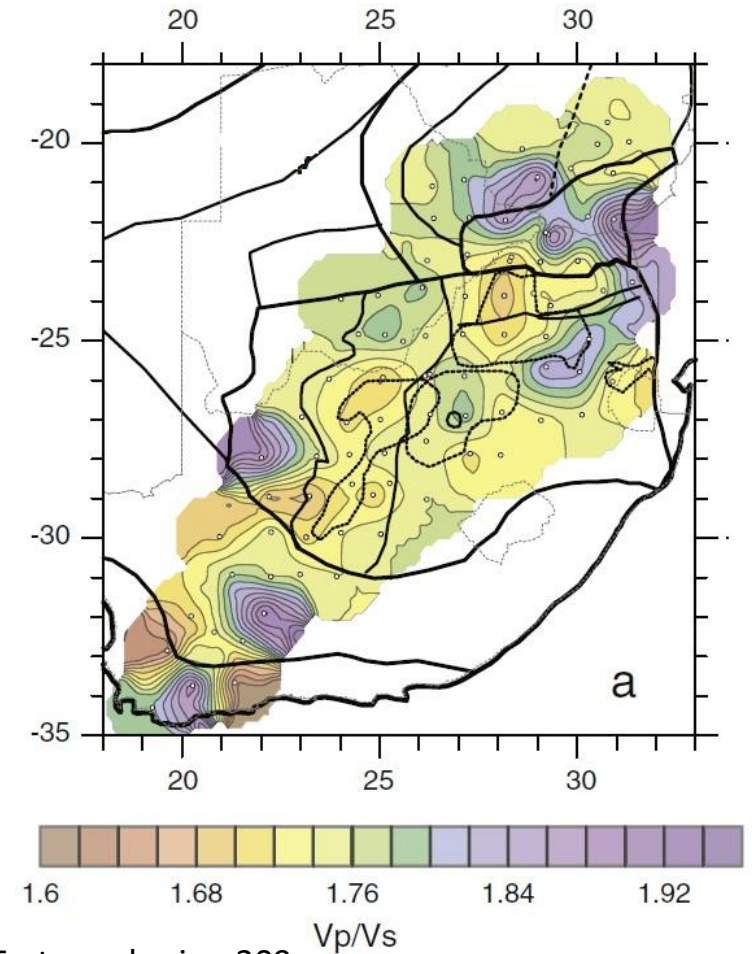
- Most of the Kaapvaal craton and Zimbawe craton have thin (35–40 km) crust and Vp/Vs ~1.74, which may indicate delamination of pre-existing lower crust, also supported by a very sharp Moho transition.
- Extreme values of Vp/Vs 1.90–1.94 at the dyke swarms in eastern Limpopo, and 1.84 in the easternmost Bushveld Intrusion Complex (BIC) indicate voluminous magmatic intrusions in the whole crust.
- Highly heterogeneous crust, both in thickness and Vp/Vs-ratio is typical of the Namaqua–Natal and Cape Fold Belts.

Cratonic roots from Regional Tomography
South African Craton

Southern Africa Seismic Experiment

depth = 150 km

P-wave velocity anomaly (%)

James et al. (2003)

P-wave velocity anomaly (%)

Kaapvaal craton Bushveld

Old ocean

approximate thickness of lithosphere?
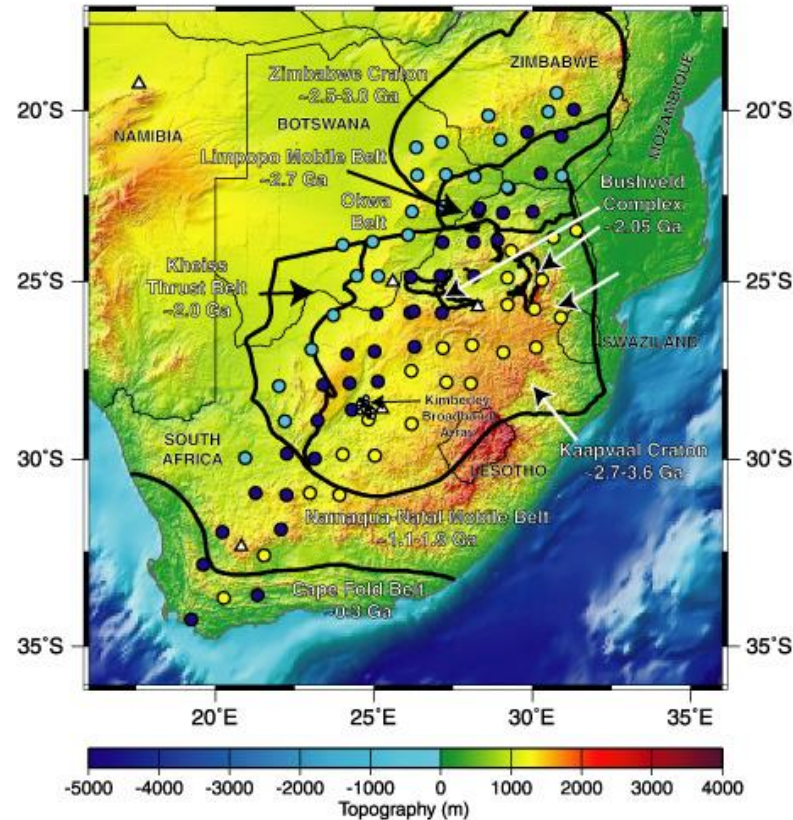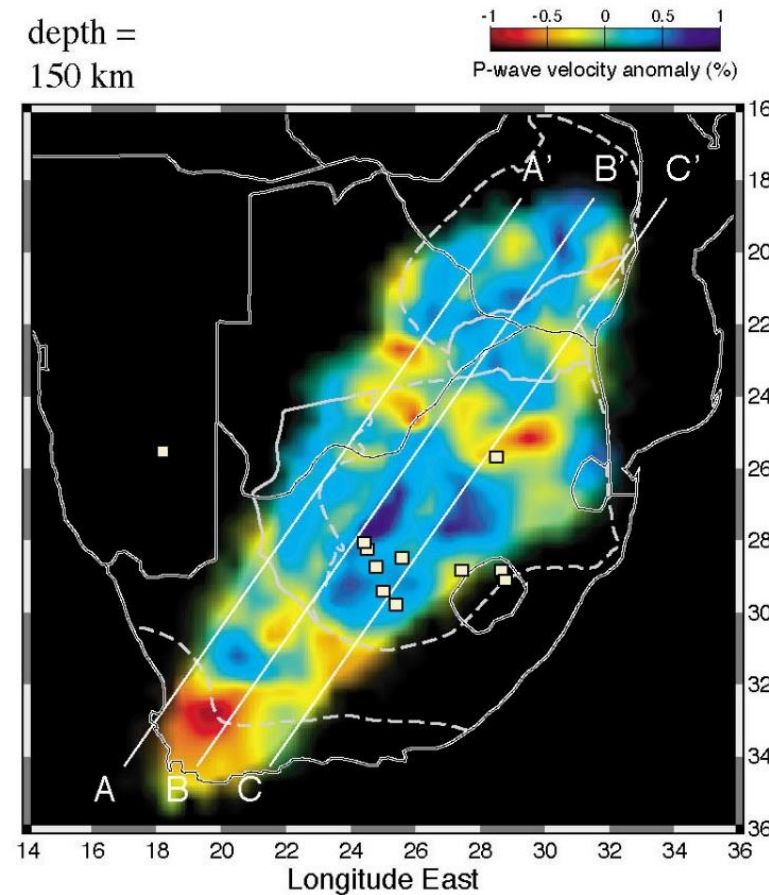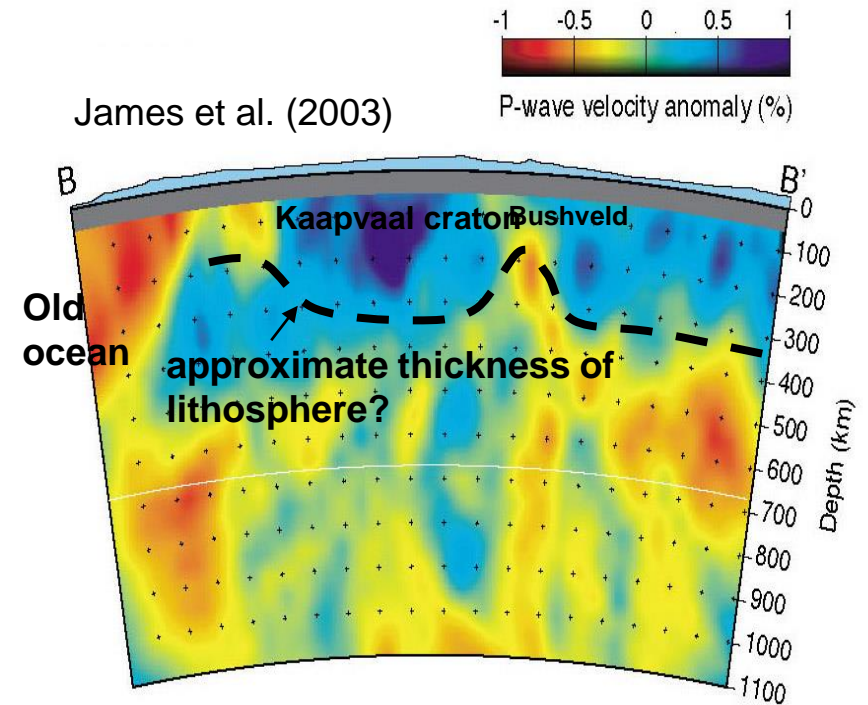
James et al, 2001, GRL, 28   James et al, 2004, G3, 5

- Cratonic root structures are irregular, reaching depths of at least 250-300 km in the southern part of the Kaapvaal craton and in regions of the Zimbabwe craton.
- The mantle beneath the Bushveld province exhibits anomalously low velocities suggesting refertilization of the cratonic mantle during the Bushveld magmatic event.
- There is a jump to low velocities at Cape Fold belt, intermediate beneath Proterozoic Namaqua-Natal belt.

Magamatic Activity after the cratonic roots stabilitation
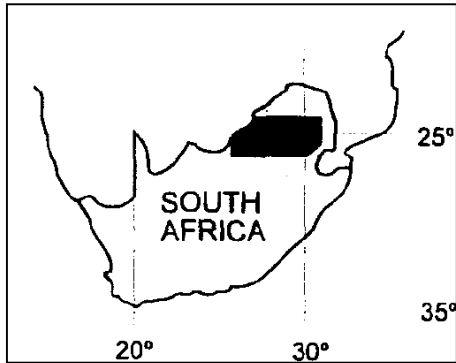
Bushveld Complex

Largest intrusion of layered mafic rocks

Rustenberg Layered Suite

Largest accumulation of siliceous volcanism

Rooiberg Group

Largest granite plutonism

Lebowa Granite Suite

What does explain the persistent magmatic activity after cratonic stabilization?

Proposed mechanisms:

Exogenous

Bolide impact

Deep mantle plume

Endogenous

Lithospheric instability (eclogite bodies formation)

Higher mantle T at the base of the lithosphere
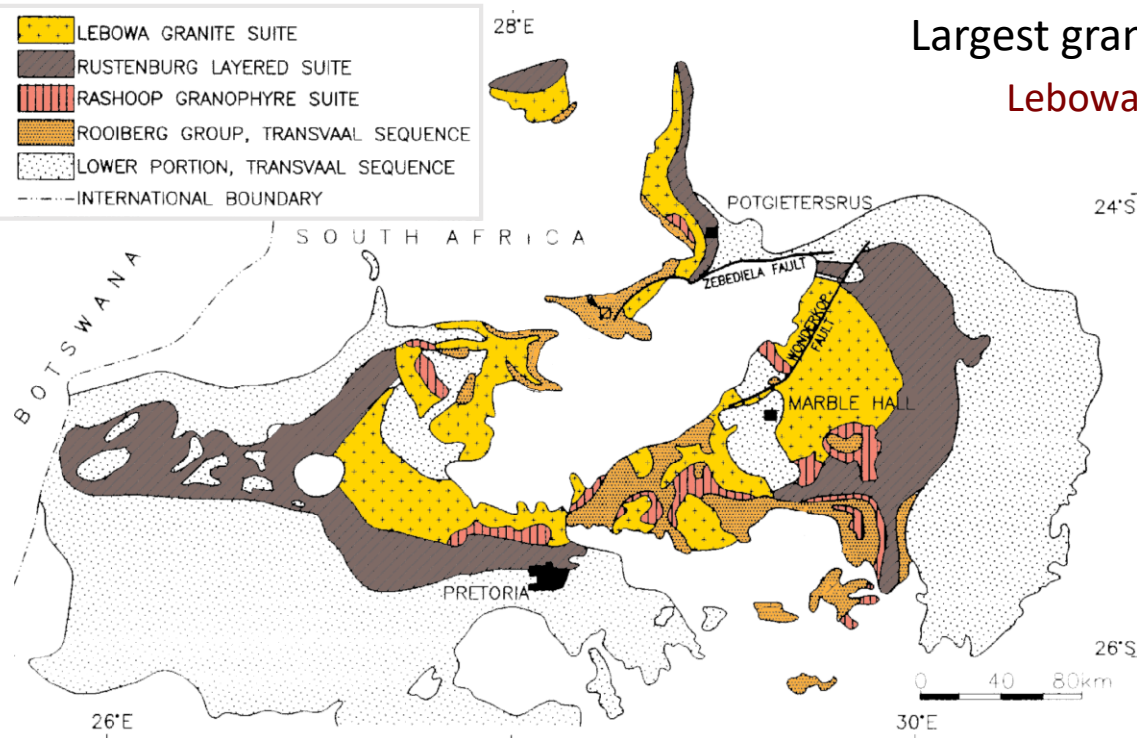
- **Thick continental lithosphere has a thermal blanketing effect on the mantle below which result in higher mantle T up to the point that the geotherm could cross the solidus of fertile peridotite, while at the same time leaving the refractory depleted lithosphere intact.**

Lithosphere Deformation Mapped in Southern Africa by S-Wave Splitting

Orientations of shear wave splitting fast polarization directions
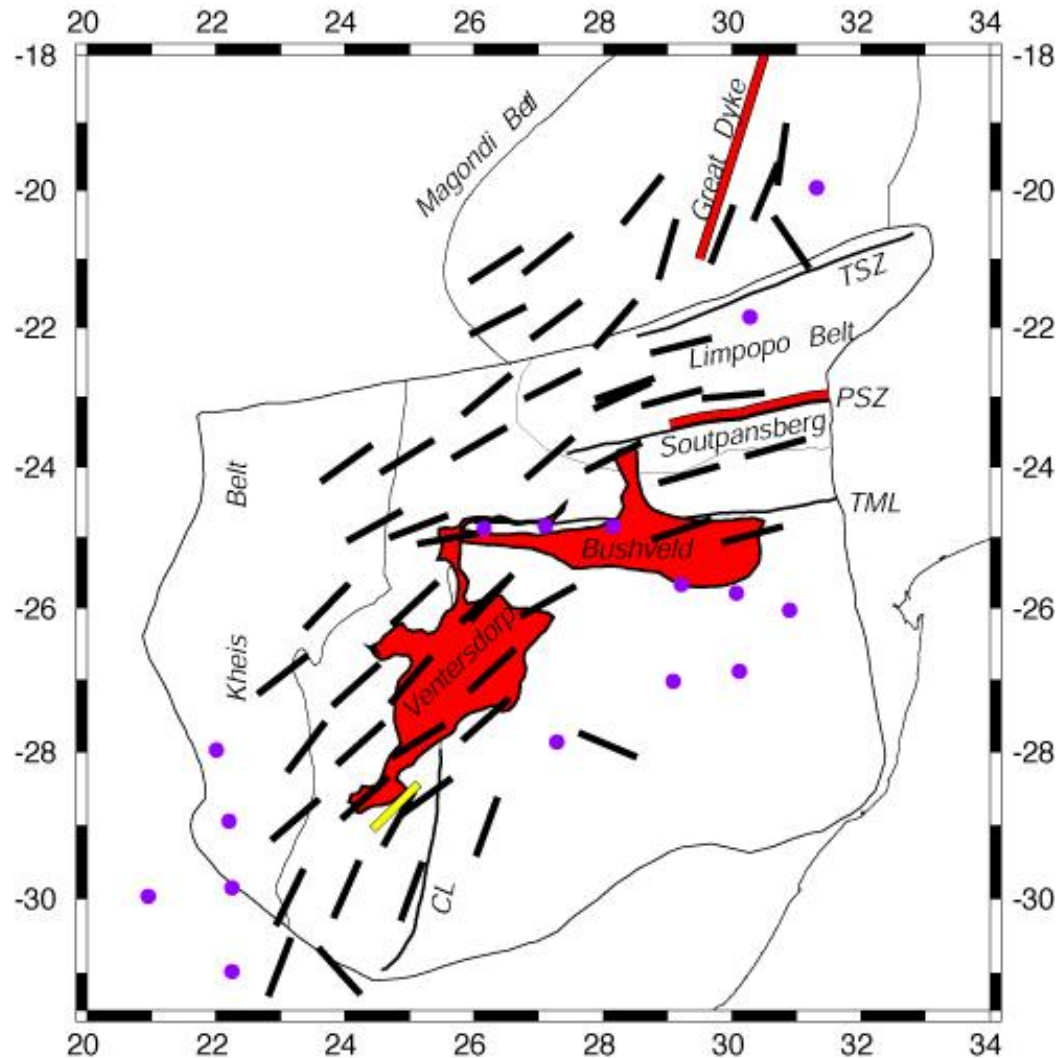
The values of lineation direction exhibit systematic spatial variations:

- In the southwestern Kaapvaal they are roughly north-northeast to south-southwest, rotate to northeast-southwest further north, and to nearly east-west in the northeastern part of the craton, including the Limpopo belt. Just north of the Limpopo, in the vicinity of the Great Dyke the values oriented north-northeast to south-southwest.

- Mantle anisotropy was produced by Archean deformation within the lithosphere, rather than present-day processes in the sublithospheric mantle

- Neo-Archean collisional orogenesis imparted a mechanical anisotropy to the lithosphere that controlled the subsequent magmatic history of cratonic southern Africa.

Silver et al., 2004, S. Afr. J. Geol., 107

Purple dots represent measurements with zero or near-zero splitting delay times. TML: Thabazimbi Murchison Lineament, CL: Colesberg Lineament, KGB: Kraaipan Greenstone Belts, SZ, shear zone

Interpretation of anisotropic structure of the mantle of cratonic Southern Africa

Tectonic stabilization by ~2.8 Gyr and subsequent magmatic history

Silver et al., 2004, S. Afr. J. Geol., 107
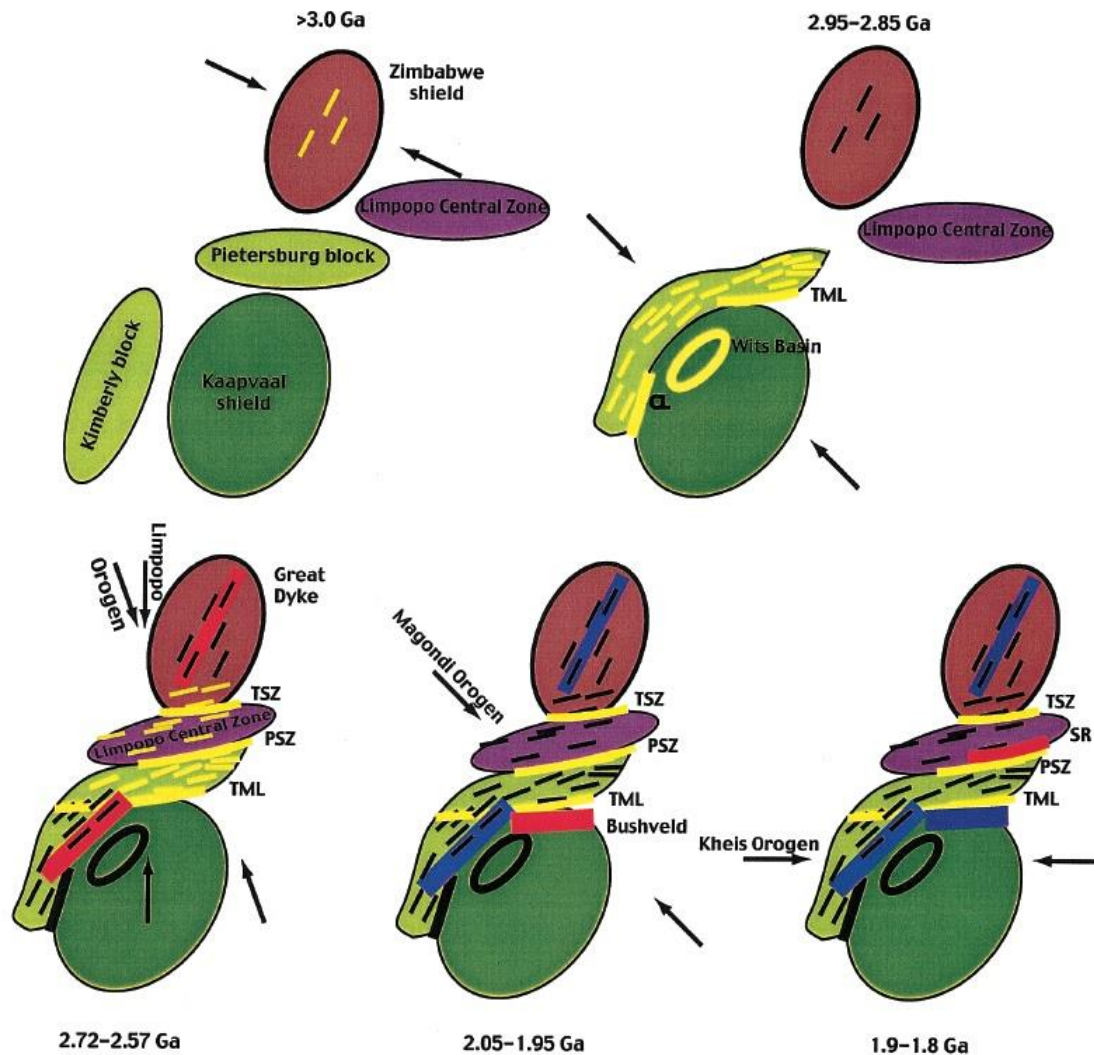
Five major deformational phases control the history of the South African Craton:

i.   An unknown pre-2.9 Gyr orogen that imparts a mantle fabric to the Zimbabwe craton;

ii.   A collision at ~2.9 Gyr along the western and northern boundaries of the Kaapvaal Shield, imparting mantle fabric to the Kimberly and Pietersburg terranes;

iii. The Limpopo orogen, at ~2.6 to ~2.7 Ga, which imparts mantle fabric to the three Limpopo zones, and which produces collisional rifts to the north and south, namely the Great Dyke and Ventersdorp;

iv.   The ~2.0 Ga Magondi orogen, both reactivating shear zones in the Limpopo and producing the Bushveld as another collisional rift;

v.   The ~1.8 to 1.9 Gyr Kheis orogen, which produces the final collisional rift, namely the Soutpansberg trough.

In all of these cases, the rifts formed at an orientation that is parallel to preexisting mantle fabric, as inferred from mantle anisotropy.

Collisional Rifts form where the stress field associated with collision produces extension and rifting for orientations at a small angle to the direction of the collision.

Chemical Limitations on Cratonic Growth

Why do older continental cratons have thicker lithosphere than younger continents?

Observations:

- Isopycnicity implies thick lithosphere stabilized by depleted peridotites

- Highly depleted, low-density peridotites (Mg # > 92) observed in the subcratonic mantle are primarily of Archean age

- Subsequent Proterozoic and Phanerozoic magmatism has not generated large volumes of such rocks

Implication:

- Proterozoic transition from thick to relatively thin lithosphere can plausibly be explained by the exhaustion of Archean mantle peridotitites with Mg # > 92

Can be the cratonic lithosphere destroyed?

- A number of processes can erode or destroy cratonic lithosphere and, by lowering the viscosity and density contrast between cratonic root and convecting mantle, compromise its stability: Heating by impinging plumes, addition of water by dehydration of slabs beneath cratons, injection of wet melts at the LAB, or addition of *Fe*-rich melts during metasomatism.
- The consequences are: (1) partial melt of the litospheric roots (2) compositional changes (e.g., *Fe* enrichment) of the litospheric roots with densifications and rheological weakening of the lithosphere due to melt infiltration.

Example: North China Craton

Liu et al., GCA, 2011
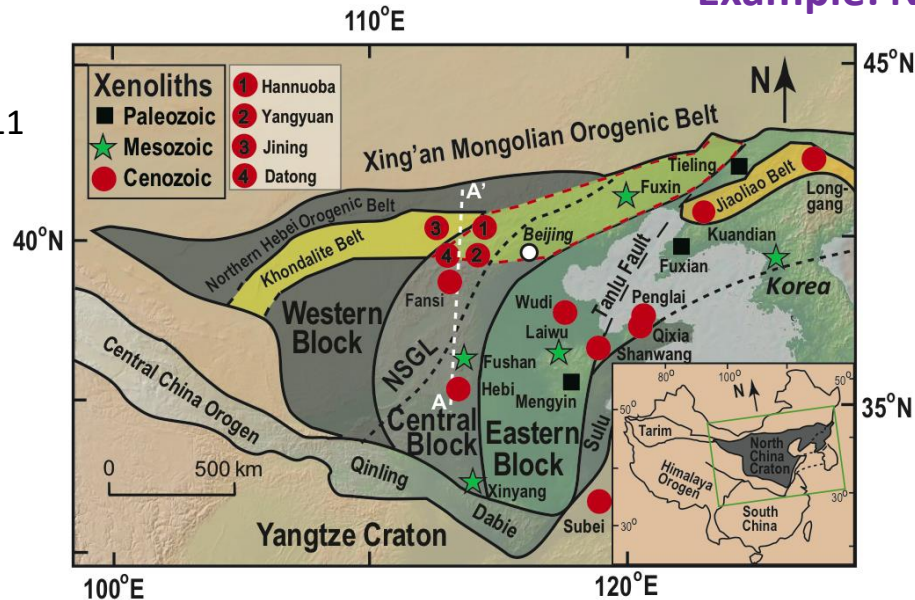
Obrebski et al., 2012, JGR, 117
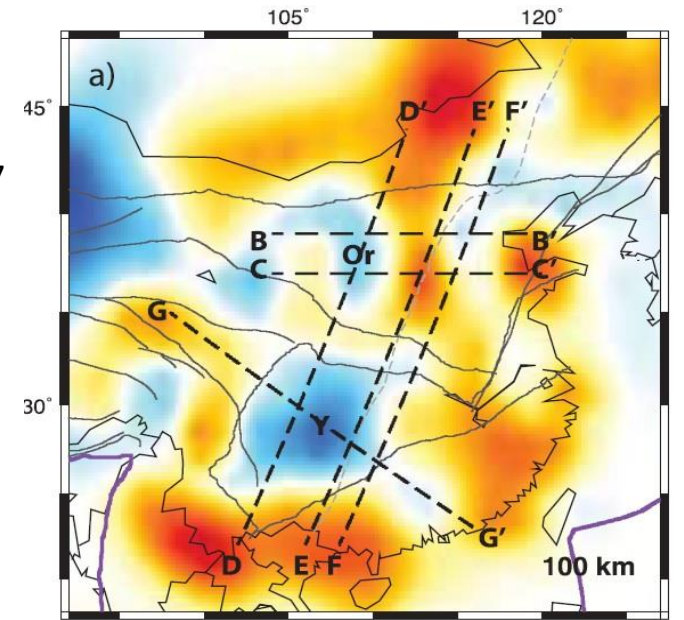
Ordos block (Or), Yangtze Craton (Y)
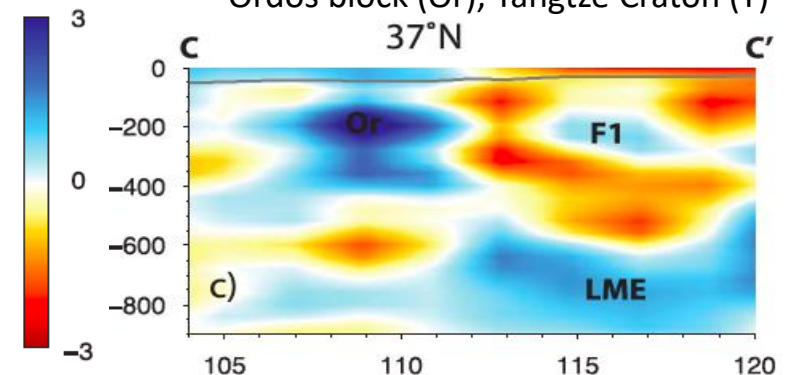
- High velocities only beneath western block, slower to the east beneath an area where the crust is still Archean, but the lithospheric mantle is Proterozoic to modern.
- Loss of the lithospheric root beneath the NCC is shown by the composition of mantle xenoliths present in early Palaeozoic and Mesozoic to Tertiary volcanic rocks.
- The subduction of the Pacific Plate started during the Mesozoic has extensively hydro-weakened the upper mantle beneath the NCC, causing its destabilization, thinning, and replacement.
- The tectonics of much of Asia changed from contractional to extensional at c. 130–120 Myr, at the same time of the subcontinental mantle root loss beneath the NCC.

Evolution of the North China Craton

3.5–2.7 Ga
exotic block   future Eastern block

2.7 Ga
rifts off proto Eastern block   passive margin

2.5 Ga
COB
WB   EB

1.8 Ga
older COB is overprinted by 1.8 Ga events
IMNHO
WB NCC EB
1.85 Ga collision in north causes granulite facies metamorphism in much of craton

Palaeozoic
NCC

Mesozoic
Solonker   Dabie-Sulu
NCC

Cenozoic
NCC   NCC

Kusky et al., 2018, Geol. Soc., London, 280
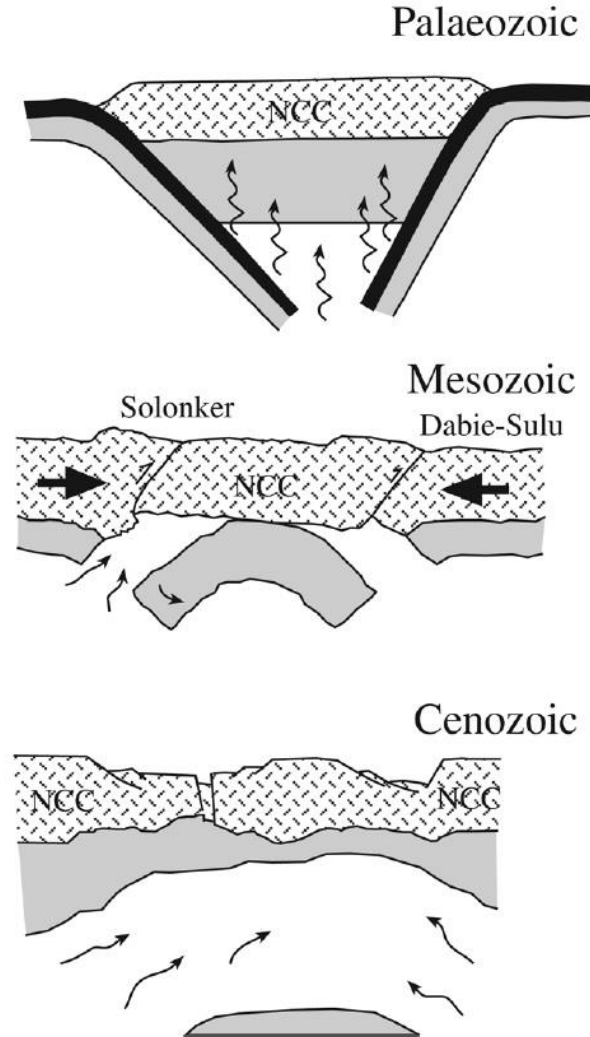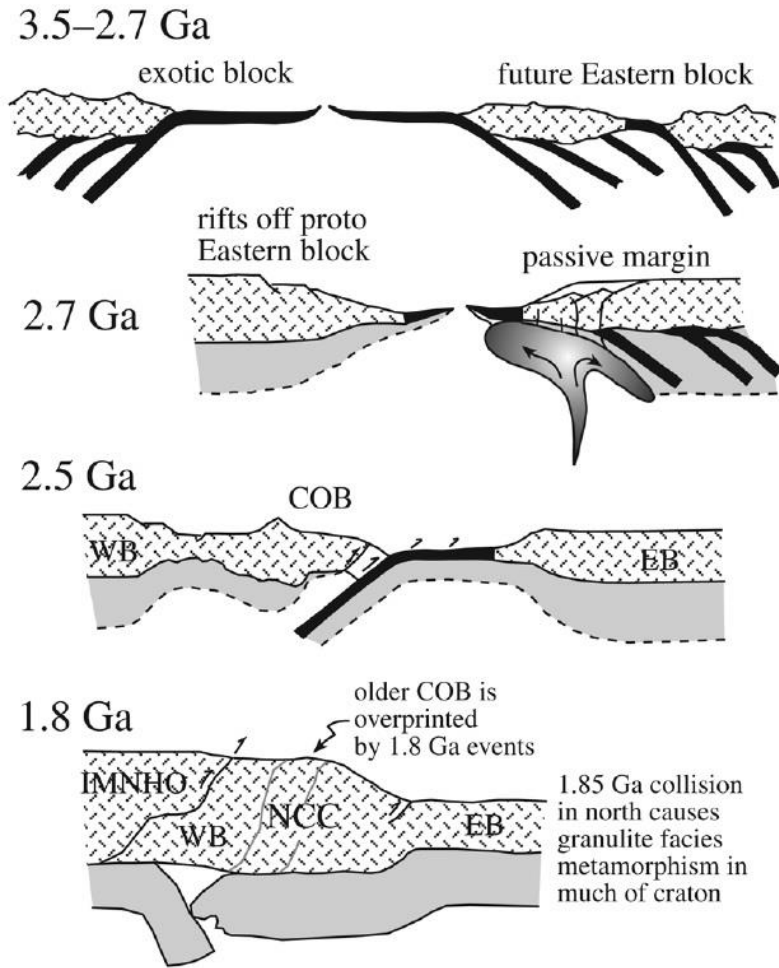
- Growth of the craton by subduction–accretion in arc settings probably involved the underplating of buoyant oceanic slabs (mantle root formation)
- Plume-influenced rifting at 2.7 Gyr broke apart the future Eastern Block and led to the development of a passive margin sequence on the western side of the Eastern block. This margin collided with a convergent margin at 2.5 Gyr, amalgamating the craton.
- At 1.85 Gyr the craton experienced a major collision event along its northern margin, which resulted in partial replacement of the mantle root and the formation of a collisional plateau and foreland basin.
- For much of the Palaeozoic the craton was relatively internally stable, but accommodated cumulative subduction along its northern, southern, and eastern margins.

- Subduction-related dehydration reactions in the slab released fluids that hydrated the mantle, which allowed the root to release a low-density melt phase during Mesozoic tectonism, become denser, and sink into the asthenosphere after being triggered by near-simultaneous collisions along its northern and southern margins.

Wyoming Craton
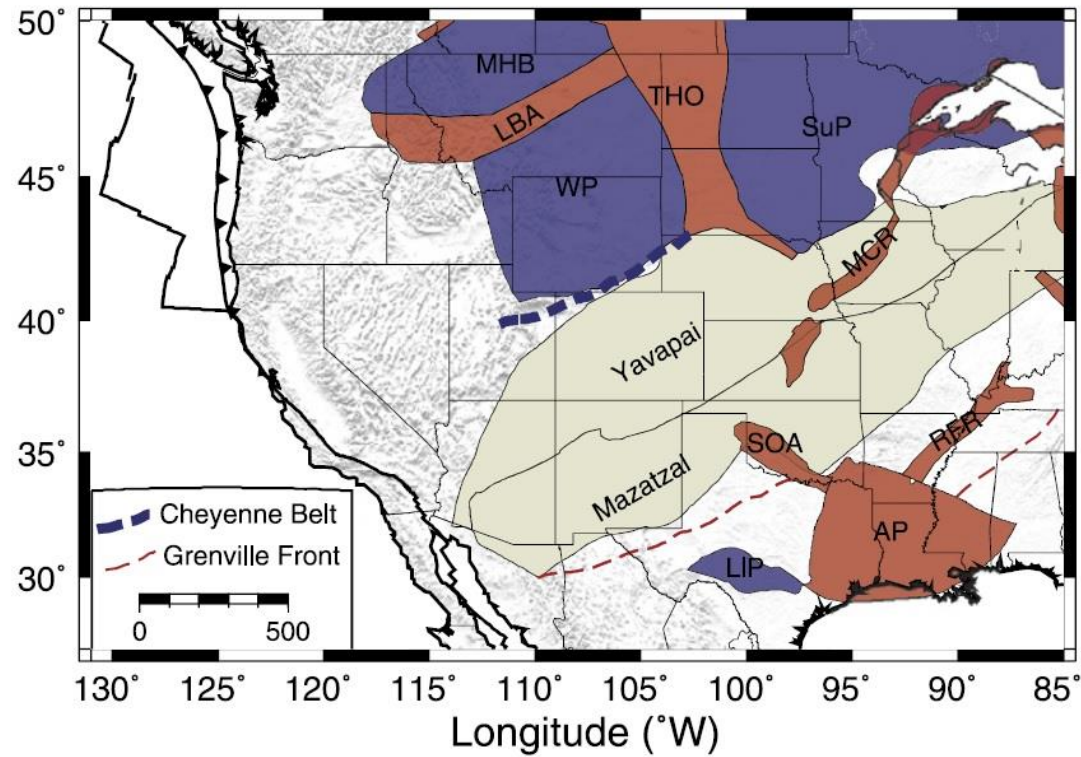
Porritt et al., 2014, EPSL, 402
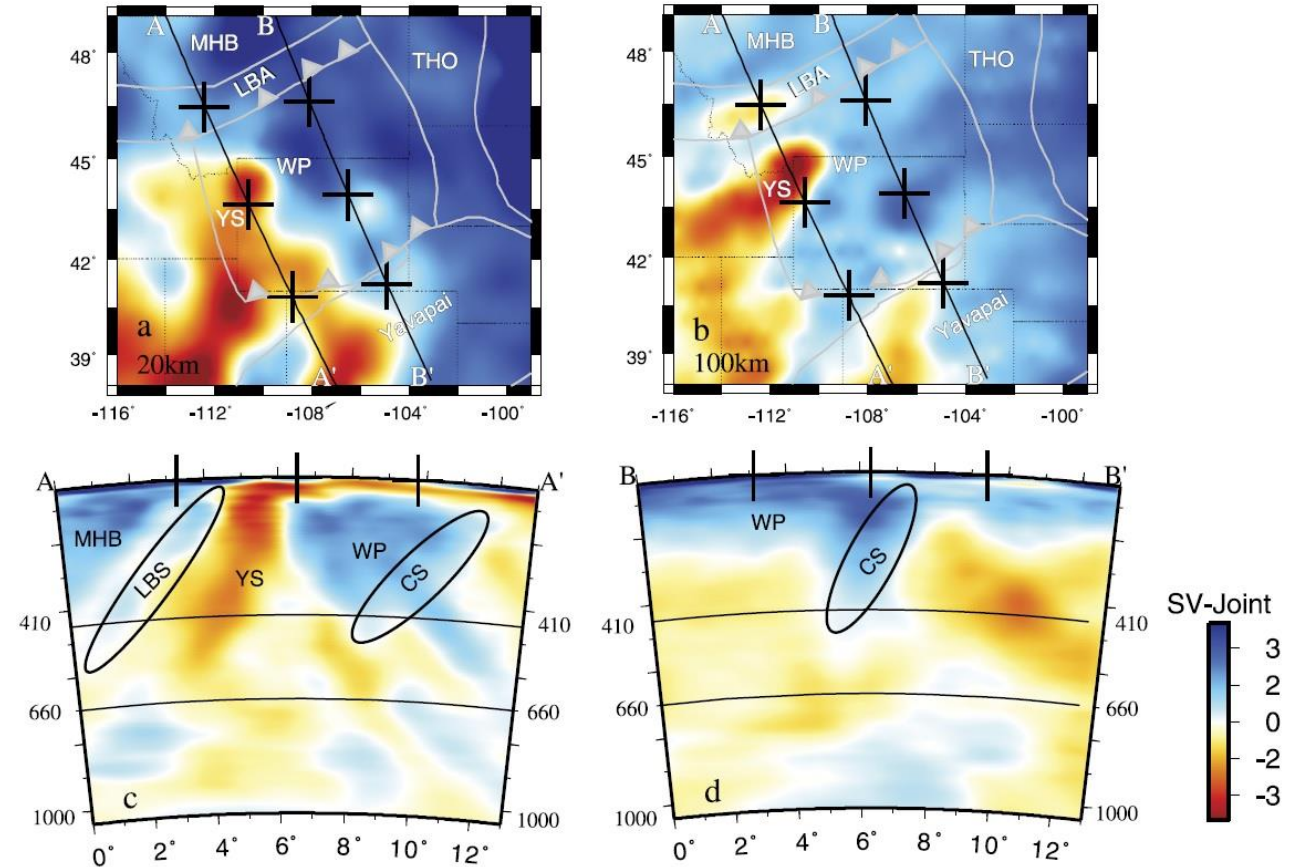
Gray triangles denote overriding plate in last collisional event. MedicineHatBlock (MHB), LittleBeltArc (LBA), LittleBeltSlab (LBS), Yellowstone (YS), Wyoming Province (WP), CheyenneSlab (CS), Trans-Hudson Orogen (THO), LaurentiaCraton (LC), Southern Oklahoma Aulacogen (SOA), Mid-Continent Rift (MCR), Reelfoot Rift (RFR), ArgentinePrecordillera (AP), and Llano Province(LlP).

- Low velocity anomalies are associated with the Little Belt Arc and the Yellowstone Plume.
- The Wyoming Province retains evidence of fossil slabs along its southern (Cheyenne) and northern (LittleBelt) boundaries. The Yellowstone plume is impinging on its western edge.
- The mantle lithosphere near the northern boundary of the Wyoming Craton has been more severely affected by post-Archean events occurring on the borders of the Craton (xenoliths show clear evidence of extensive interaction with incompatible-element-rich melts).

Causes of decratonization
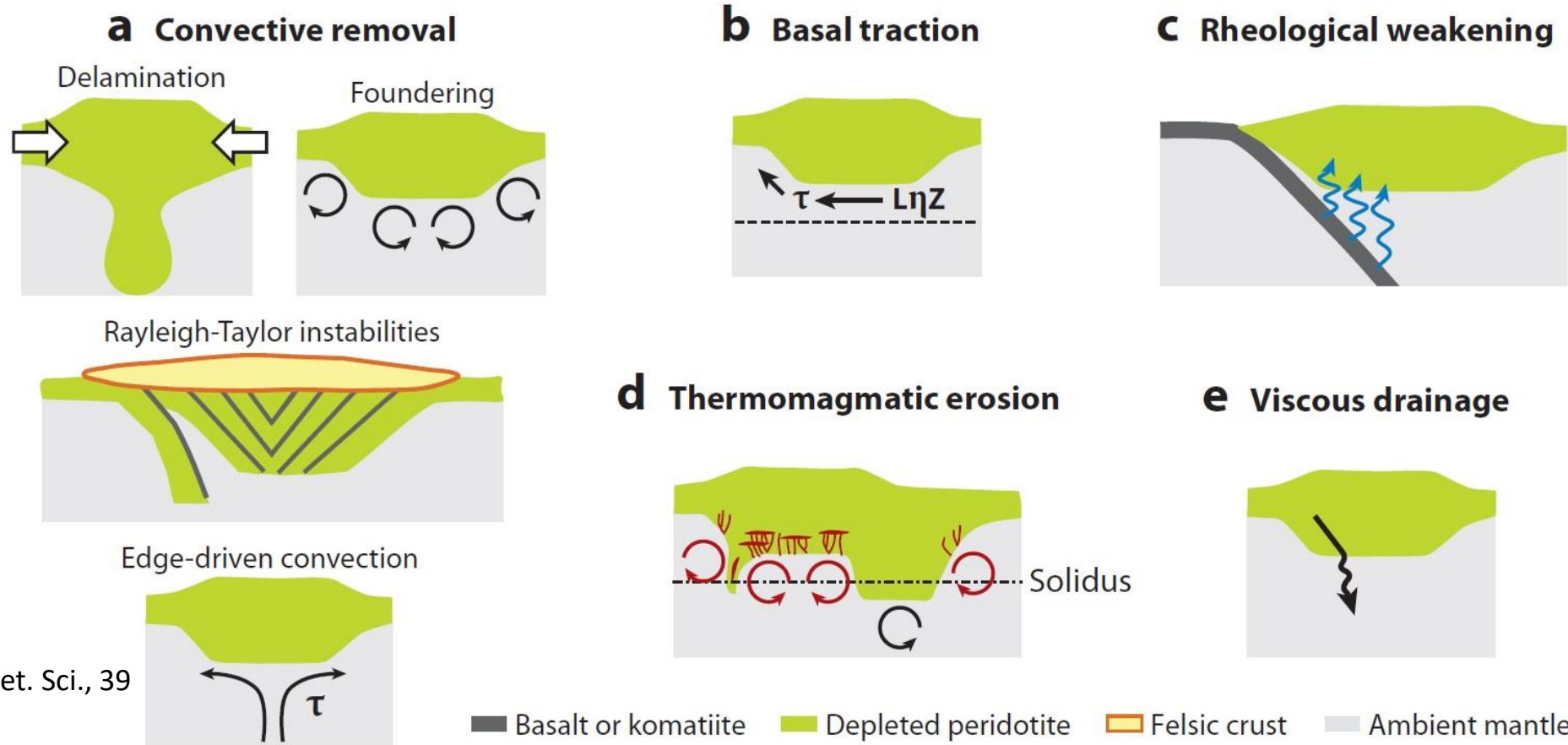
Lee et al., 2011,
Annu. Rev. Earth Planet. Sci., 39

a. Any lithospheric removal driven by thermal or chemical buoyancy forces (e.g., density-driven forces) is referred to as convective removal.
b. Erosion of continental lithosphere can be driven by basal shear stresses imposed by mantle flow in the asthenosphere (cratonic destruction is unlikely, since shear stresses decrease rapidly as craton thickness increases).
c. Weakening the rheology of continental mantle through fluids infiltration can facilitate convective removal.
d. Both plume impingement and small-scale convective instabilities are favorable environments for generating melts and cause a thermomagmatic erosion of the cratonic roots.
e. Inclined layers of garnet pyroxenite could "drain" back into the convecting mantle owing to their high densities and low viscosities compared with peridotite.

Plume and Cratonic Lithosphere
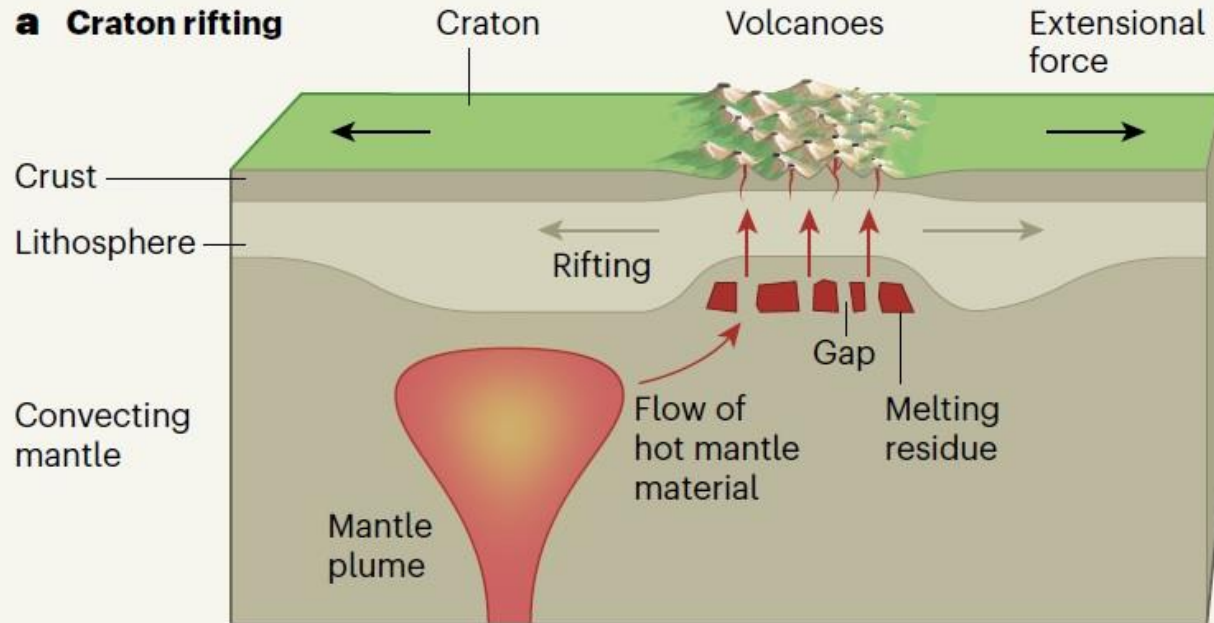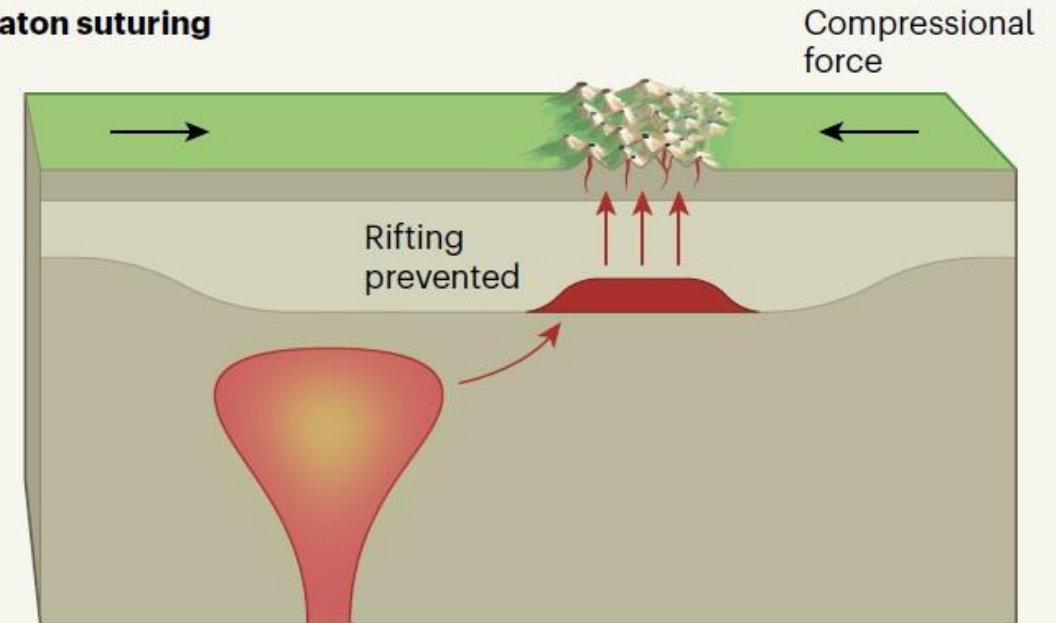
Foley and O'Neill, 2021, Nature, 592

- Mantle melts of plumes can repair and thicken cratonic plates, by sealing them along existing gaps, even if these thinned parts are far away from the main heat source.
- If regional forces related to the large-scale movement of tectonic plates are extensional, the craton can undergo rifting and the residue from the melting of the hot mantle material cannot plug the gaps in the underside of the lithosphere.
- However, if these tectonic forces are compressional, craton rifting is prevented, and the authors show that the melting residue can plug the gaps and thicken the base of the lithosphere.

Middle Lithosphere Discontinuity (MLD)

- **Negative velocity gradients beneath cratons at ~170– 250 km depth are generally interpreted as the LAB, while seismic discontinuities, with a thickness of ~30–40 km, occurring around 80-120 km depth have been interpreted as MLDs.**
- **The MLD boundaries are characterised by both positive and negative seismic velocity anomalies (usually strong *S*-wave velocity drop), often accompanied by azimuthal and radial anisotropy.**

Origin of the MLDs

- Partial melting of mantle material in presence of volatile (e.g., Thybo and Perchuc, 1997, Science, 416).
- Changes in azimuthal (Sodoudi et al., 2013) or radial anisotropy (Rychert and Sherer, 2009, Science, 324), accompanied by seismic velocity reduction (Aulbach et al., 2017), may result from the accumulation of metasomes as layers at or as subvertical veins.
- Boundary between depleted and metasomatized lithosphere: lower lithosphere altered by metasomatic fluids resulting in crystallization of low-velocity minerals (e.g., amphibole: $x\mathrm{Si_8O_{22}(OH)_2}$ or phlogopite: $\mathrm{KMg_3(AlSi_3O_{10})(F,OH)_2}$) (Sodoudi et al., 2013, G3, 14).
- Grain boundary sliding (elastically accomodated) at a temperature of 900°C (Karato, 2012, EPSL, 321-322).

MLD under stable craton

Hopper and Fischer, 2018, G-cubed
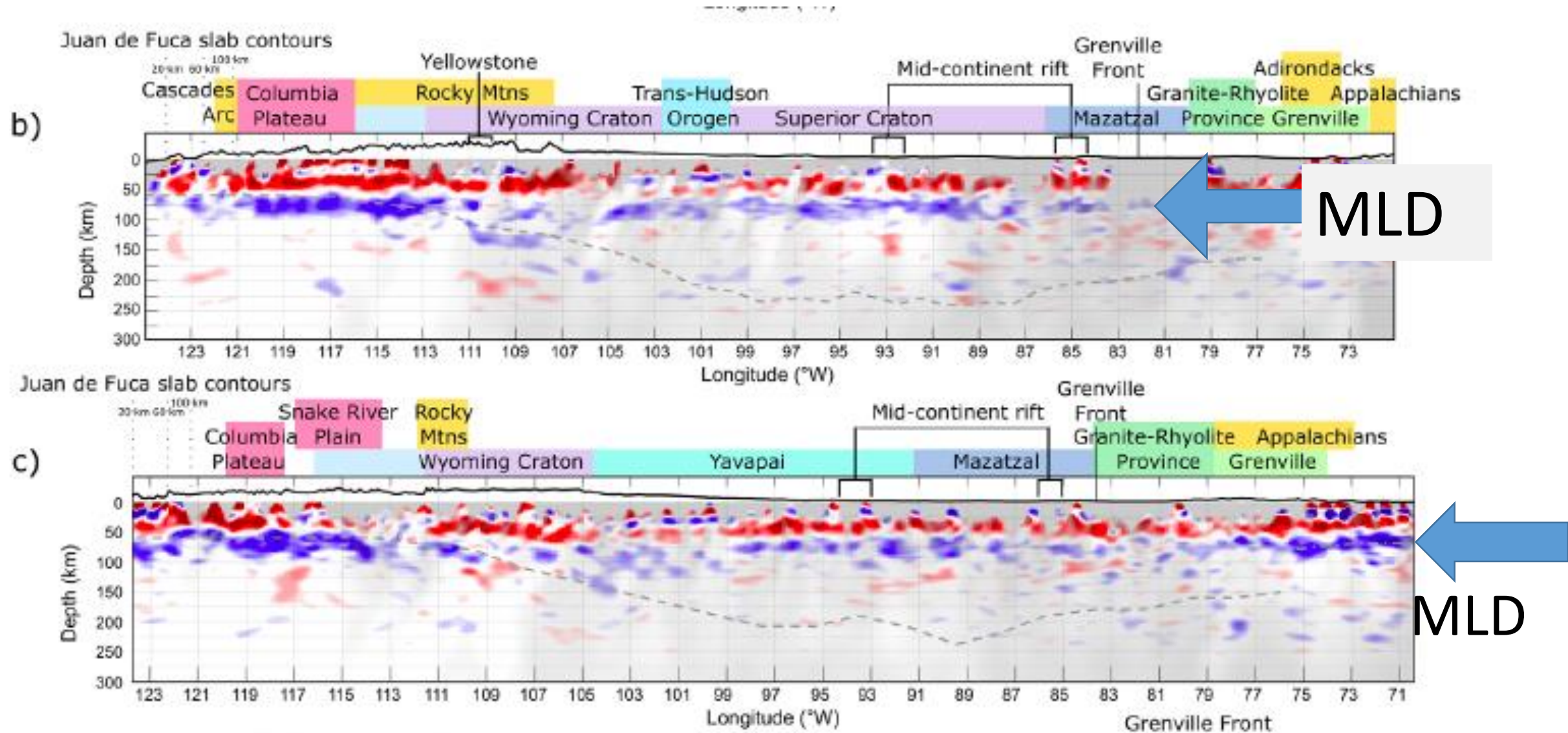
Models for craton thickening and associated development of fabric

Aulbach et al., Lithos, 268–271
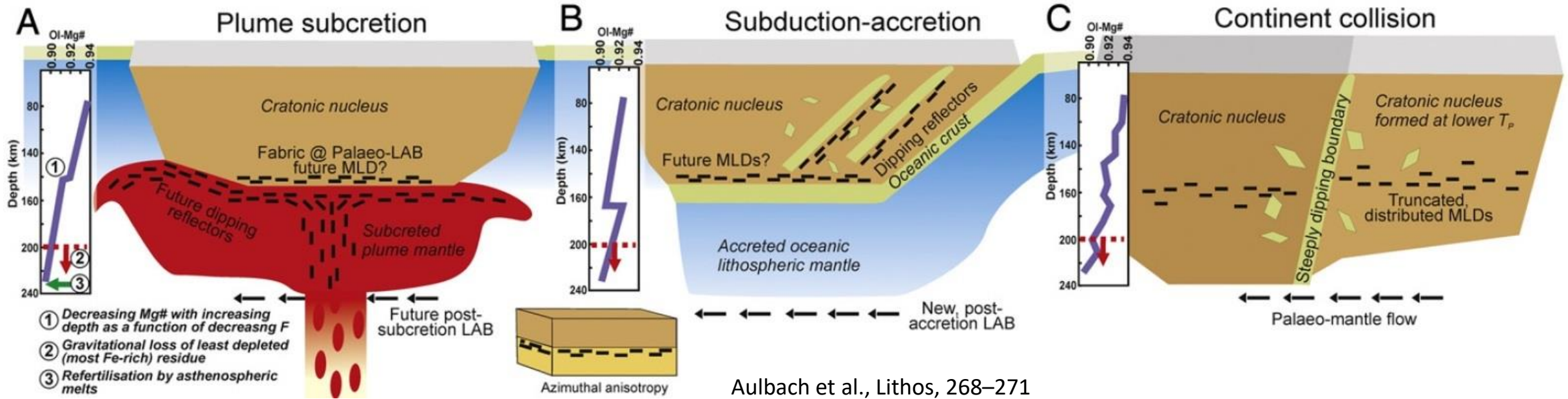
o Vertical lineation in the plume stem gives way to horizontal lineation when the plume impinges upon the LAB: Mg# decreases due to the effects of polybaricmelt extraction, while a discrete step forms when mantle packages formed at different T_P are juxtaposed.

o Imbrication of oceanic slabs leads to dipping lineations while horizontal lineations result from flat subduction: if the two packages formed at similar time by partial melting to low pressure, the Mg# profile of each lithosphere package would be identical.

o Collision of two cratonic nuclei subsequent to ocean closure, with different thicknesses at the time of collision due to formation at different T_P: near the boundary, Mg# with depth may show complexity.

Strong vs. weak or absent cratonic seismic LAB signals

The cratonic LAB is known to produce a much weaker seismic signature than the oceanic LAB, and is often characterized by a small and gradual velocity change with a weak and intermittent seismic signal:

- When present, seismically imaged discontinuities beneath cratons cannot be produced by thermal effects alone and instead require contrasts in composition, fabric, water content or the presence of partial melt or volatiles (e.g., in the cratonic lithosphere melt-related reworked and rejuvenated).

- Where discrete LABs are not detected in the cratonic lithosphere, the boundary is characterized by a velocity gradient and hence more accurately described as a transition zone that is spread out over a large depth interval (e.g., in the intact and undisturbed cratons).
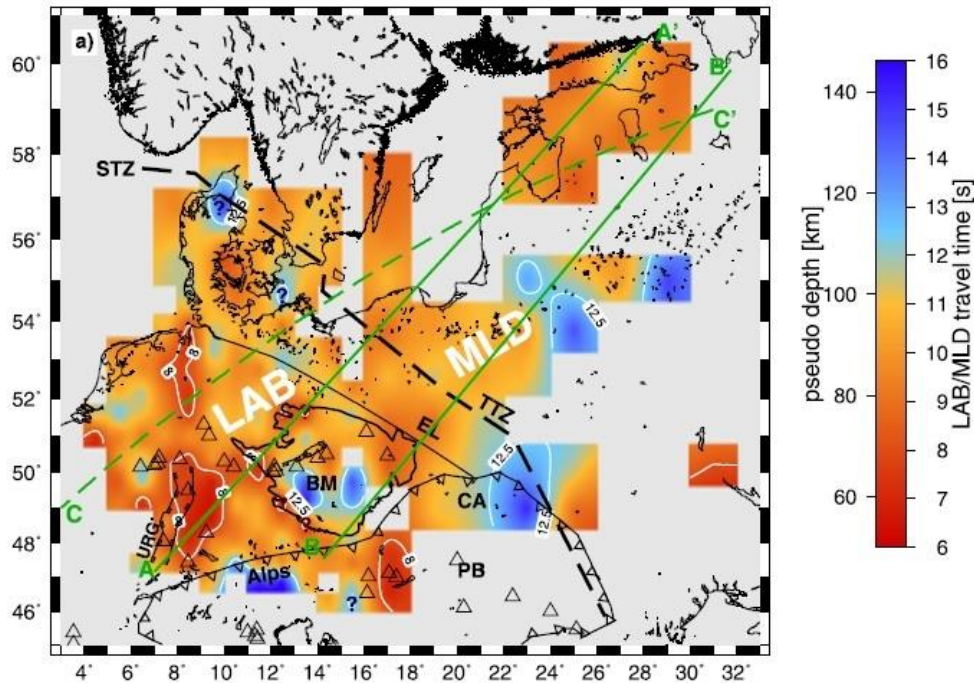
STZ: Sorgenfrei–Tornquist Zone, TTZ: Teisseyre–Tornquist Zone
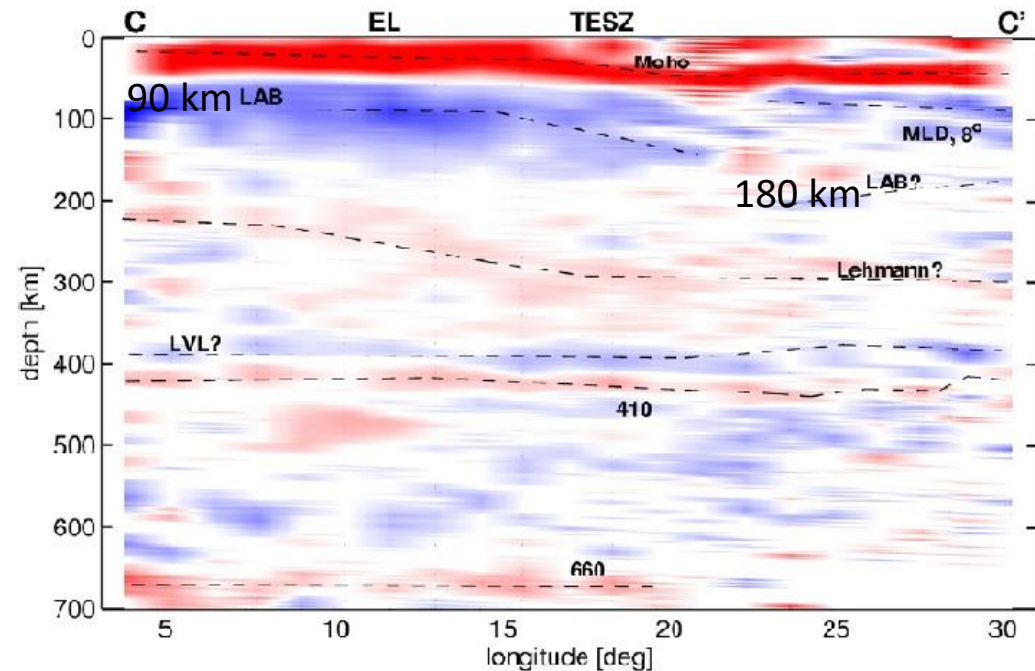
(Knapmeyer-Endrun et al., 2017, EPSL, 458)

LAB deeper, but weaker and less consistent in the EEC than in the Phanerozoic Europe

Is the MLD an artifact?

No Deconvolution
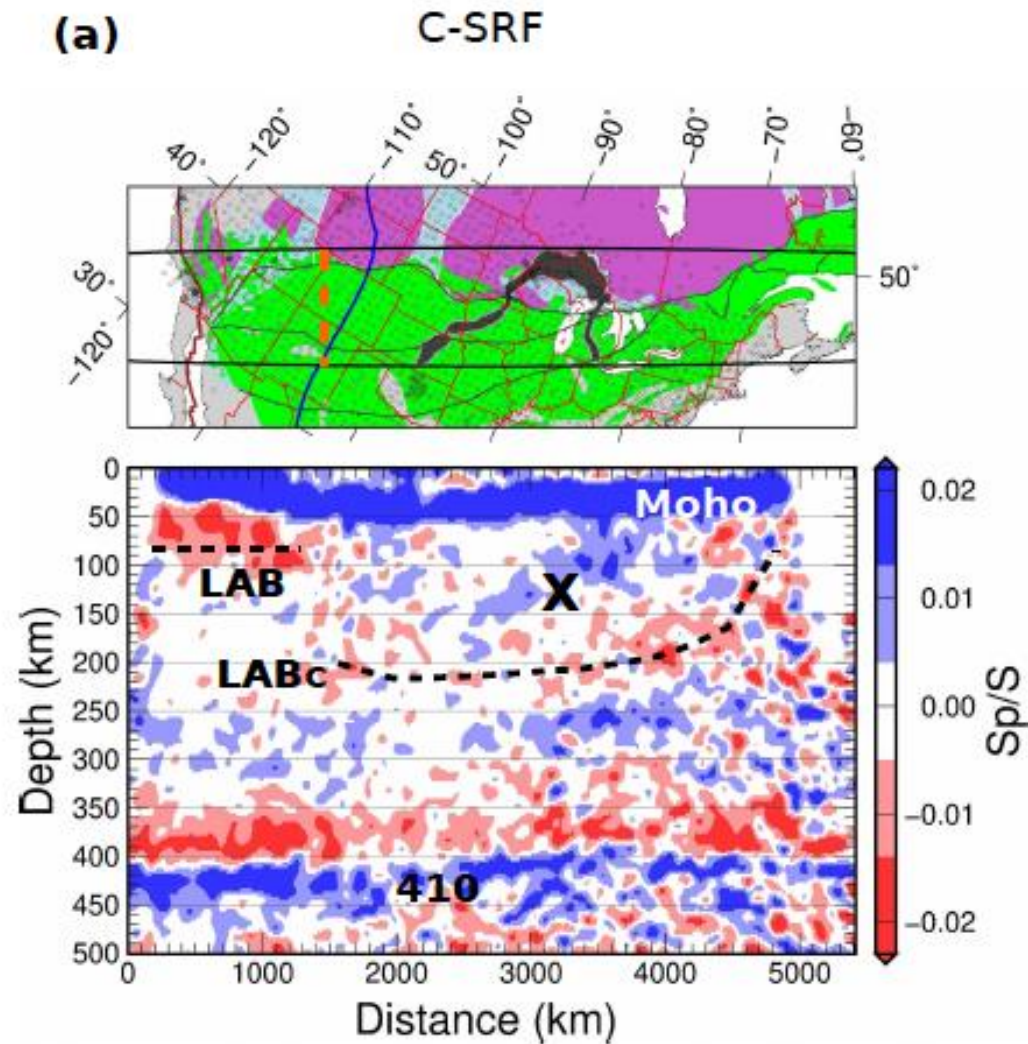
With Deconvolution
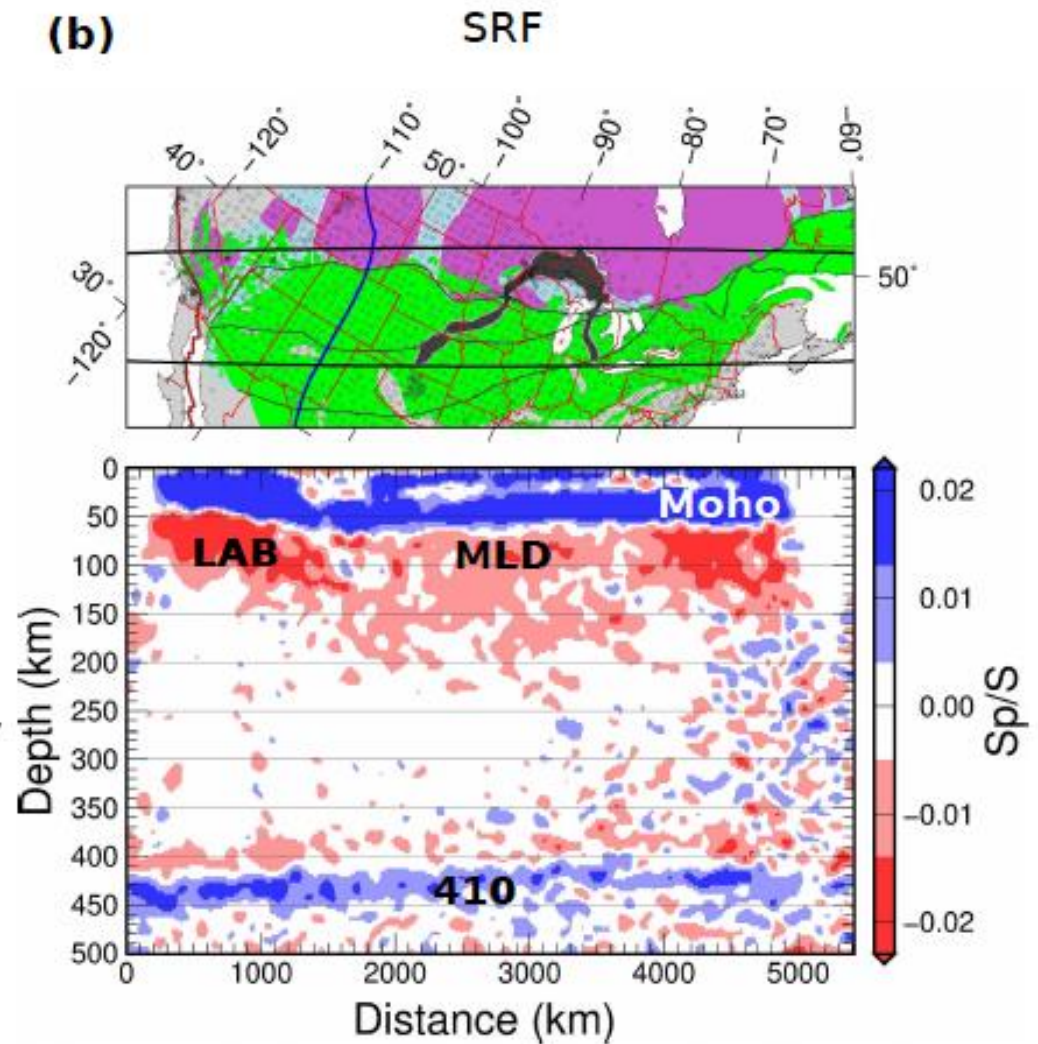
Thermal state of the lithosphere
(why do we want to know it?)

- Knowledge of the present thermal state of the Earth is crucial for models of crustal and mantle evolution, mantle dynamics, and processes of deep interior.

- Physical properties of crustal and mantle rocks are temperature dependant (density, seismic velocity, seismic attenuation, electrical conductivity, viscosity).

Temperature of the Earth is controlled by internal heat:

80% from the radiogenic heat production and 20 % comes from secular cooling of the Earth.

Heat is transferred to the surface of the Earth through three mechanisms: conduction (in the lithosphere), convection (below the lithosphere), and advection (hydrothermal circluation in sediments).

Knowledge of the thermal state of the lithosphere from more than 20000 heat flux measurements at the Earth's surface

Heat

EXAMPLE 1.
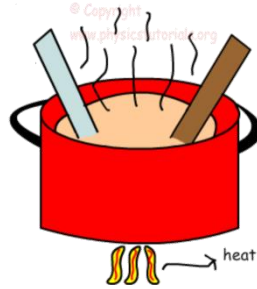
MORE HEAT = HIGHER TEMPERATURE

$$Q = T$$

EXAMPLE 2.
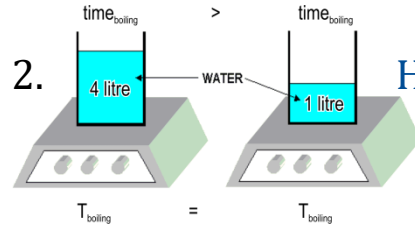
HEAT depends on the MASS, TEMPERATURE NO

$$Q = m\,T$$

EXAMPLE 3.
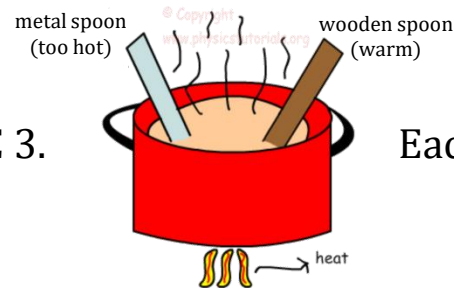
Each material has its own characteristic to absorb HEAT

$$Q = m\,c_p\,T$$

Global Heat Flow Data
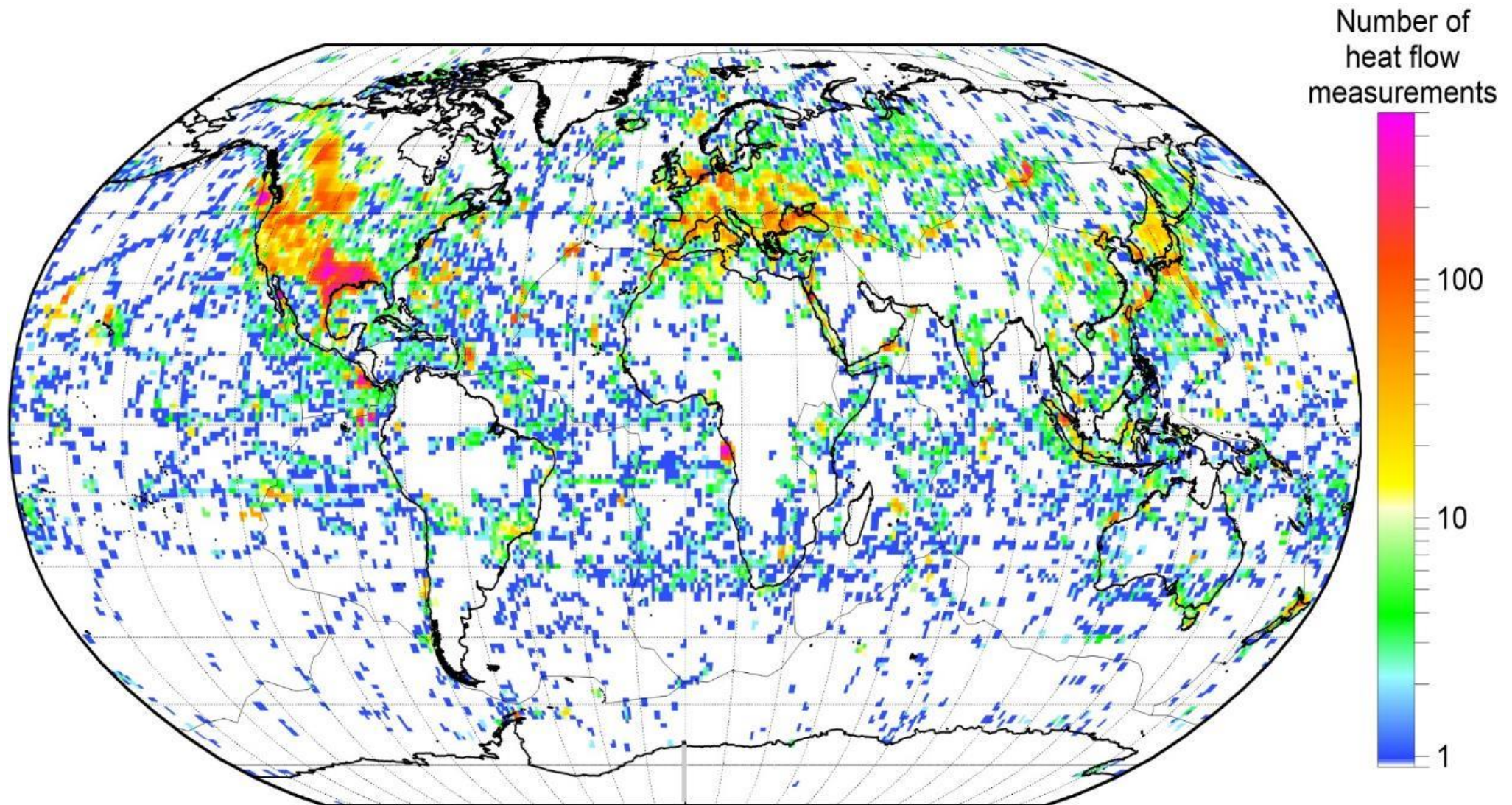
Global Surface Heat Flux

- Oceanic heat flux follows a decreasing trend as a function of age, average: 67 mWm² (only due to conduction), 101 mWm^{-2} (including heat loss form hot fluids).
- Oceanic lithosphere is in a transient thermal state
- Over 96% of heat flow from oceanic lithosphere originates from beneath the crust, poor of ^{238}U, ^{235}U ^{40}K, and ^{232}Th.
- In the continents there is not a clear trend of heat flux with age (due to their longer evolution and complicated structure), average: 65 mWm^{-2}.
- Old continental lithosphere is close to thermal steady state .
- A large percentage of the heat flow is generated in the upper crust (10-20 km), rich of ^{238}U, ^{235}U ^{40}K, and ^{232}Th.
- Mantle thermal anomalies cause surface heat flow perturbation with wavelength of several hundred km.

- **Global average: 87 mWm^{-2}. Most common Q_0 and geothermal gradient values: 20-125mWm^{-2} 10-80°C/km (largest values in the tectonically active regions and lowest where mafic crust is present)**

Final Estimate of Heat Flow (mW m^-2) (Area-weighted Median)

4 - 50	55 - 58	61 - 63	70 - 80	99 - 129
51 - 54	59 - 60	64 - 69	81 - 98	130 - 919
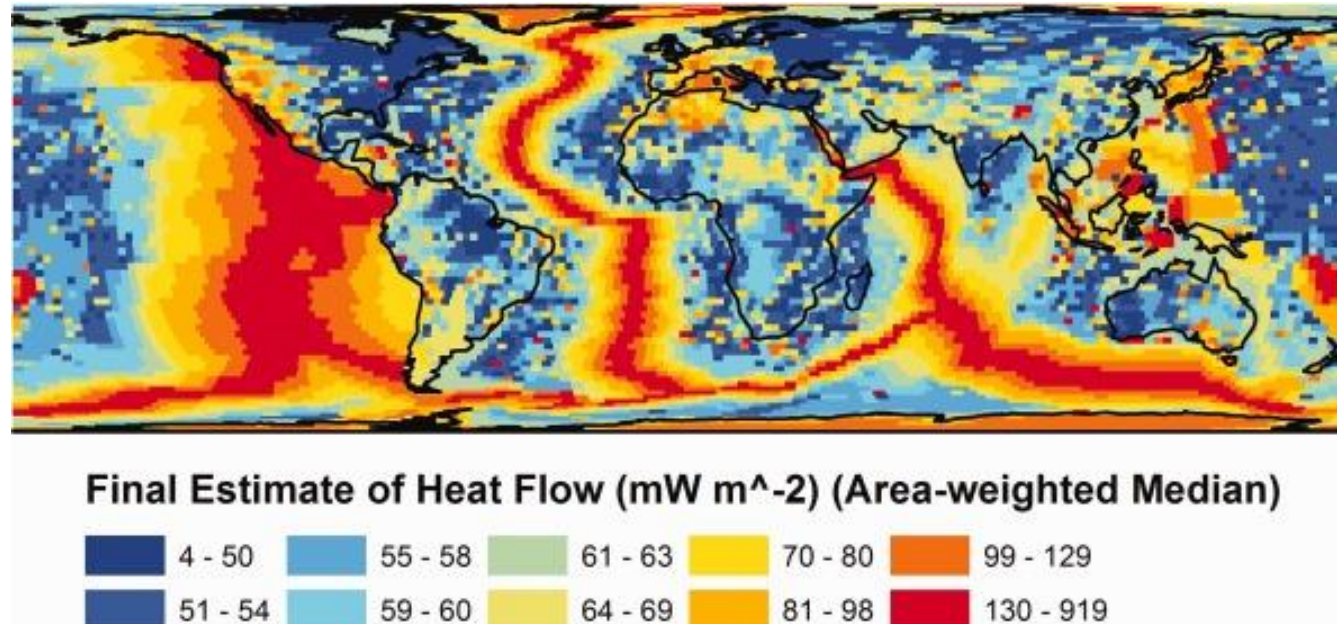
Thermal state of the continental lithosphere
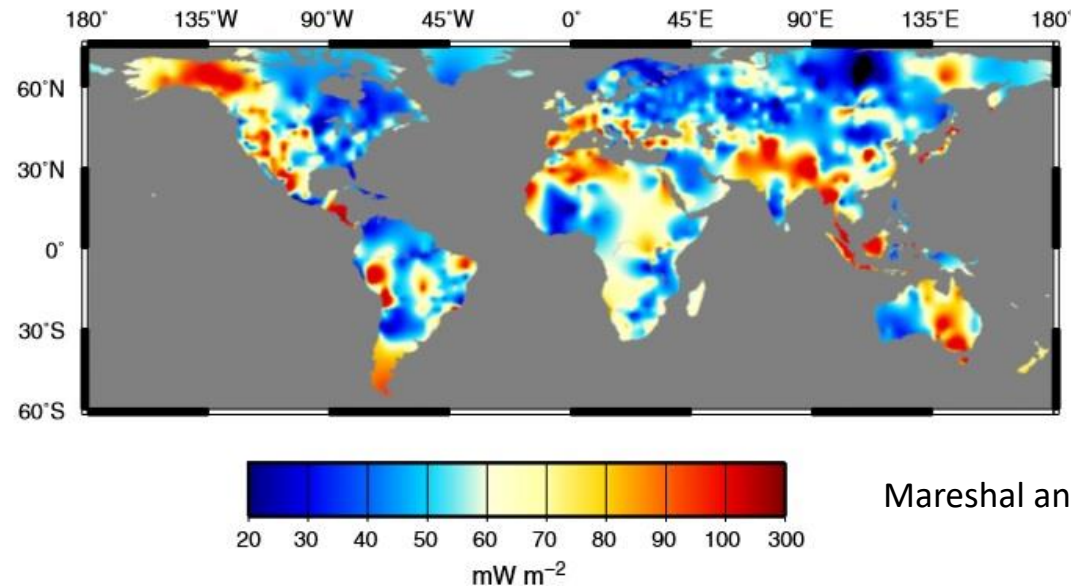
Mareshal and Jaupart, 2013, Tectonophiscis, 609

Heat flow density (HFD) determines the amount of heat per unit of area and per unit of time which is transmitted by heat conduction from the Earth's interior.

Fourier Law states that the rate of flow of heat is proportional to the temperature gradient:

$$\mathbf{q} = -\lambda \, \mathrm{grad}\, T = -\lambda \nabla T.$$

For 1D: $q = -\lambda \dfrac{\partial T}{\partial x}$

- minus sign shows that heat flows from points with high T to points with lower T
- λ or K= thermal conductivity (rocks dependent), for an isotropic and homogeneous layer has only one value

- Most of heat loss derives from heat production (A) due to the decay of ^{238}U, ^{235}U, ^{232}Th, and ^{40}K in ^{206}Pb, ^{207}Pb, ^{208}Pb, and ^{40}Ar or ^{40}Ca, respectively, which contributes 18-38 mWm^{-2} to the observed heat flow:

$$q = -\lambda \dfrac{\partial T}{\partial x} + A$$

- The Archean mantle was 100-300 °C hotter. Heat production was higher because of large amounts of long and short half-life (e.g., ^{36}Cl and ^{26}Al) unstable isotopes.

Thermal Conductivity

Thermal conductivity or the thermal conductivity coefficient (λ) of a material defines its ability to transfer heat

λ (W m^{-1} K^{-1}) of rocks is dependent on T, P, porosity (ϕ), composition, and properties of pore-filling fluids and gases.

Material	Wm^{-1} K^{-1}	Source
Earth's crust	2.0–2.5	Mean value, Kappelmeyer and Hänel (1974)
Rocks	1.2–5.9	Sass et al. (1971)
Sandstone	2.5	Clark (1966)
Shale	1.1–2.1	Clark (1966), Blackwell and Steele (1989)
Limestone	2.5–3	Clark (1966), Robertson (1979)
Water	0.6 at 20 °C	Birch et al. (1942)
Oil	0.15 at 20 °C	Birch et al. (1942)
Ice	2.1	Gretener (1981)
Air	0.025	CRC (1974) Handbook
Methane	0.033	CRC (1974) Handbook

Rock	From published data[a]		After Sharma (2002)
	No. of samples	Average heat conductivity	Average heat conductivity
Sand	1,149	1.79	1.1–2.1
Siltstone	476	1.58	–
Argillite, clay schist	783	1.67	2.09
Clay	660	1.43	0.8–1.5
Marl	217	1.78	–
Limestone	781	2.37	3.44
Chock	21	1.63	
Granite	383	2.68	3.07
Granodiorite	83	2.79	2.63
Porphyrite	137	1.74	–
Diorite	78	2.10	2.5
Andesites, andesite-basalt	81	1.87	2.26
Basalt	98	2.11	1.69
Diabase	67	2.50	2.2
Gabbro	116	2.47	2.57
Schist	181	2.55	–
Gneiss	88	2.41	2.7–3.1
Amphibolite	47	2.39	3.33
Gneiss-granite	35	2.04	–
Quartzite	–	5.00	5.03
Anhydrite	–	–	5.43
Harzburgite	106	2.69	–
Dunites	23	2.77	–
Olivine gabbro	55	2.65	–
Gabbro-norite	36	2.22	–

Heat flux and age: is there any trend?

Archean

Regional variations of the heat flow in some Archean Cratons

Province, Craton	HFD range (mW m^{-2})	References
Superior Province	22–48	Mareschal and Jaupart (2006)
Australian Cratons	34–54	Mareschal and Jaupart (2006)
Baltic Shield	15–39	Mareschal and Jaupart (2006)
Siberian Shields	18–46	Mareschal and Jaupart (2006)
Anabar Shield	15–25	Duchkov (1991)
Ukrainian Shield	30–50	Galushkin et al. (1991)
Karelia, Baltic Shield	35–40	Slagstad et al. (2009)
Dharwar Craton, India	25–51	Roy and Rao (2000)
eastern Dharwar Craton, India	33–73	Kumar et al. (2007a)
Karelian and Belomorian prov., Baltic Shield	20–30	Shwartsman (2001)
Belomorian Belt, Baltic Shield	20–30	Čermák et al. (1993)
Karelia and Kola Peninsula, Baltic Shield	<20–35	Čermák et al. (1993)
Laponian supracrustals	20–30	Čermák et al. (1993)

Paleozoic

Regional mean heat flows in different Paleozoic regions

Region	Average HFD (mW m^{-2})	References
The Appalachians	57	Jaupart and Mareschal (1999)
Mainland United Kingdom	54	Lee et al. (1987)
Dnieper aulacogen, the Ukraine	45	Čermák (1993)
Pripyat Depression, Belorussia	66	Čermák (1993)
Russian Platform	68	Čermák (1993)
Caledonian	~50	Čermák et al. (1993)
Hercynian	~70	Čermák et al. (1993)
Altay-Ergula Belt (China)	60	Hu et al. (2000)
Junggar-Higgan Belt (China)	47	Hu et al. (2000)
The Urals	30	Kukkonen et al. (1997)
Ural Foredeep[a]	29	Kukkonen et al. (1997)
West Ural Folded Zone[a]	28	Kukkonen et al. (1997)
Central Ural Uplift[a]	24	Kukkonen et al. (1997)
Tagil-Magnitogorsk Zone[a]	14	Kukkonen et al. (1997)
East Ural Uplift[a]	18	Kukkonen et al. (1997)
East Ural Depression[a]	27	Kukkonen et al. (1997)
Trans-Ural Uplift[a]	20	Kukkonen et al. (1997)
Tyumen-Kustanay Depression[a]	26	Kukkonen et al. (1997)

[a] Different regions of the Urals

Regional variability of heat flux

	Minimum	Maximum
	(mW m^{-2})	
Superior Province	22	48
Trans-Hudson Orogen	22	50
Australia	34	54
Baltic Shield	15	39
Siberian Shield	18	46

Minimum and maximum values obtained by averaging over 200 km × 200 km windows.
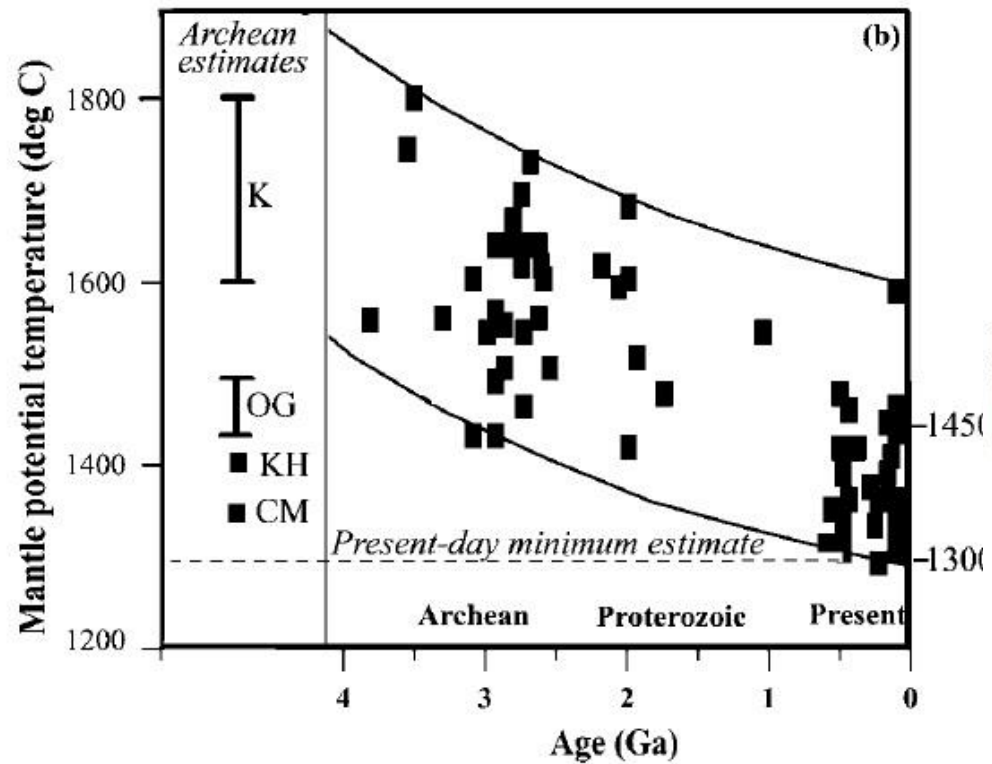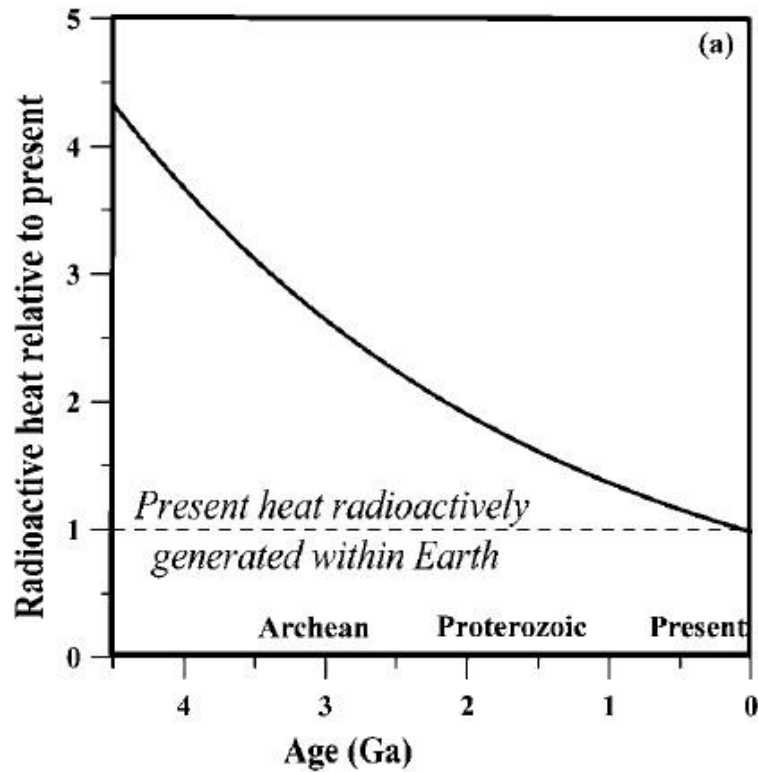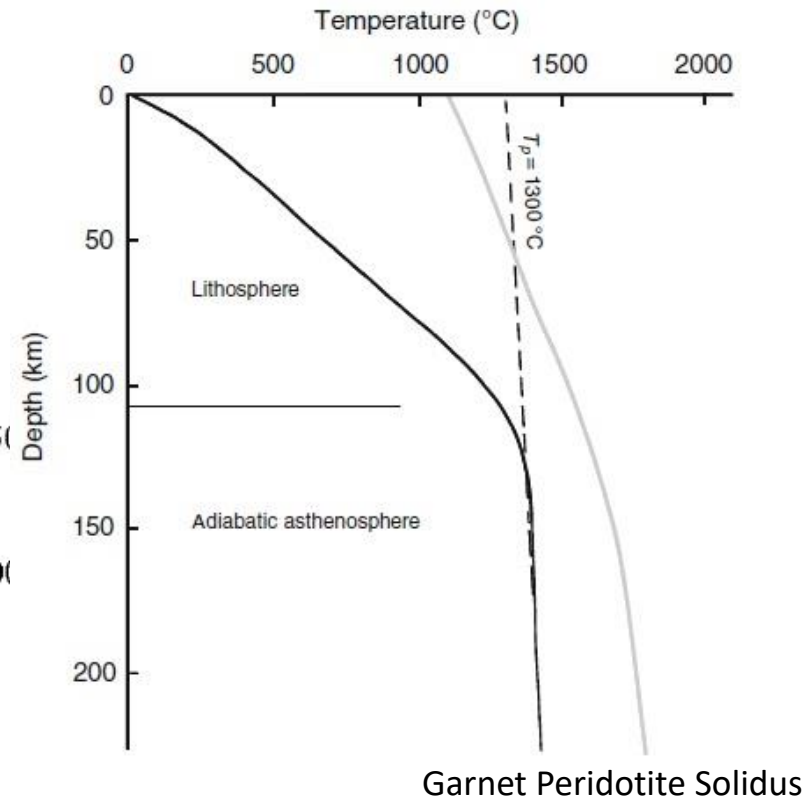
Range of Heat Flux:

Archean: 36–50mWm^{-2}

Proterozoic: 36–94mWm^{-2}

Paleozoic: 30–57 mWm^{-2}

Thermal history of the Earth

K=Komatiite
KH=Hydrous Komatiites
OG=Ophiolites and Greenstone belts
CM=Mantle convection models

Radiogenic Heat Generation

$$A = \rho \sum P A_s c$$
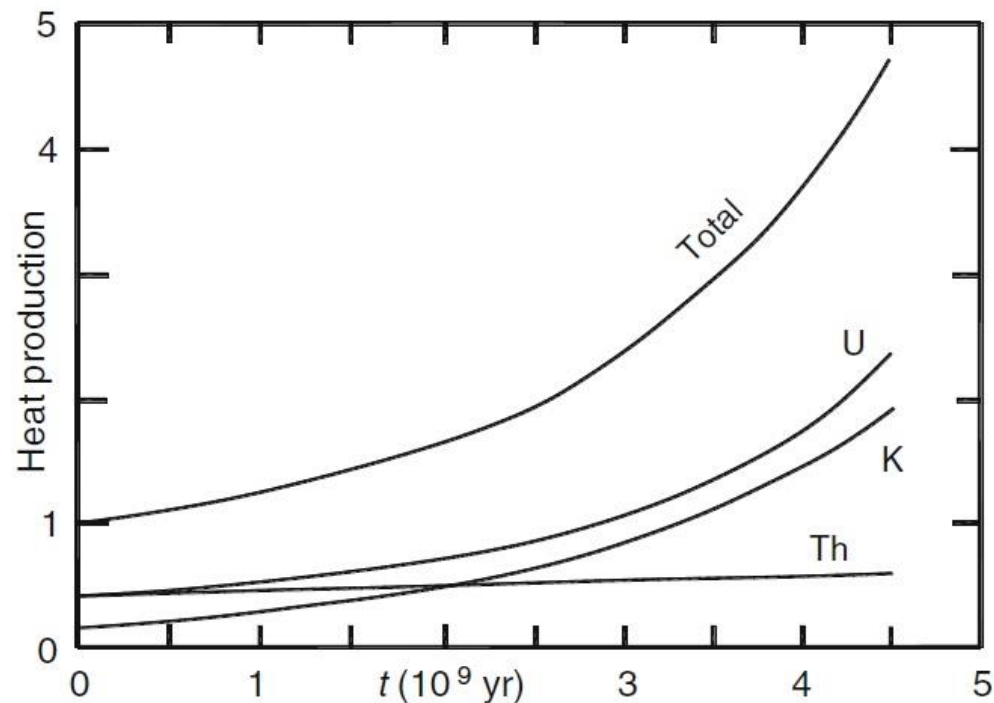
ρ is the rock density, P the abundance and A_s the rate of heat generation per *kg* of isotope and *c* the concentration.

$$c_t = c \, \exp(t \ln2/\tau)$$

$$A = \rho \begin{bmatrix} 0.993\, c_U \, A_{U^{238}} \exp(t\ln2/\tau_{U^{238}}) + 0.0071\, c_U \, A_{U^{235}} \exp(t\ln2/\tau_{U^{235}}) \\ + c_{Th}\, A_{Th^{232}} \exp(t\ln2/\tau_{Th^{232}}) + 0.00012\, c_K \, A_{K^{40}} \exp(\ln2/\tau_{K^{40}}) \end{bmatrix}$$

c_t = concentration of an isotope at time *t*

$\tau = \ln2/\lambda$ = half life with λ decay costant

$^{238}U \longrightarrow {}^{206}Pb$

$^{235}U \longrightarrow {}^{207}Pb$

$^{232}Th \longrightarrow {}^{208}Pb$

$^{40}K \nearrow {}^{40}Ca \ (89\%)$
$\phantom{^{40}K} \searrow {}^{40}Ar \ (11\%)$
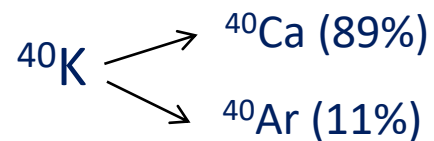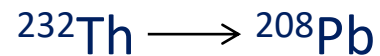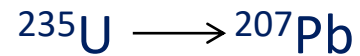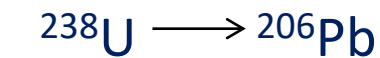
t is in 10^9 years

Radiogenic Heat Generation in Depth

$$A(z) = A_o \exp\left(-\frac{z}{D}\right) \qquad q_0 = q_a + A_oD$$ **The linear relationship supposes an exponential variation of A**

A_0 (in $\mu W\ m^{-3}$) = radiogenic heat at the surface and D (km) = thickness of layer enriched by heat producing elements (5-15 km), q_0 = heat flowing out from the Earth' surface, and q_a is the component of heat flow from the mantle.

If the thickness of _D_-layer is much smaller than the scale of horizontal fluctuation in radioactivity, the effect of lateral heat production variation on _Q_ is negligible.

_A_ = 2.5 μW/m³ through a depth of 10 km produce a surface heat flux of 25 mWm⁻² (about half of typical continetnal heat fluxes)

For magmatic and metamorphic rocks A=2.5–3.5 μW m⁻³

Measurements in boreholes have shown that _A_ does not systematically decrease with depth, since tectonics can modify the distribution

Compositional model of the Variscan crust as inferred from the $v_P(z)$ structure and the corresponding radiogenic heat A deduced from petrographical data (after Verdoya et al. 1998b)

Depth range (km)	Lithotype	Percentage of rock type	A ($\mu W\ m^{-3}$)
Upper crust			
0–12	Granite-granodiorite	100	3.0
12–18	Granitic gneiss	55	
	Granite-granodiorite	20	1.6
	Tonalitic gneiss	25	
Lower crust			
18–22	Amphibolite	60	0.4
	Mafic granulite	40	
22–30	Mafic garnet granulite	65	0.3
	Amphibolite	35	
30–32	Mafic garnet granulite	100	0.2
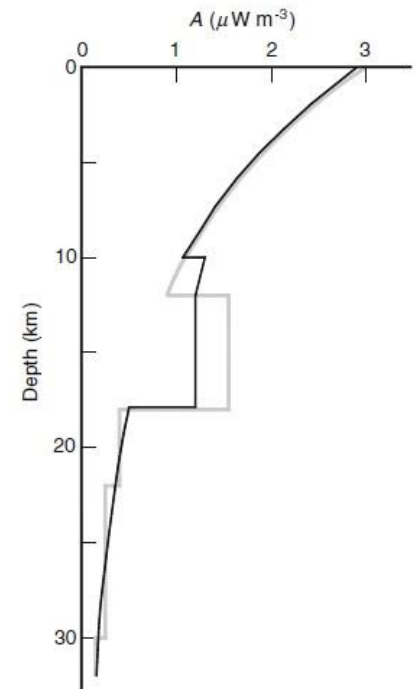
For the lower crust, xenolith lead to a global average of 0.28 mWm⁻³

Radiogenic Heat Generation of igneous rocks

(a) plutonic

(b) volcanic

Heat Production — μW m⁻³ : 0.01 0.1 1 10 100
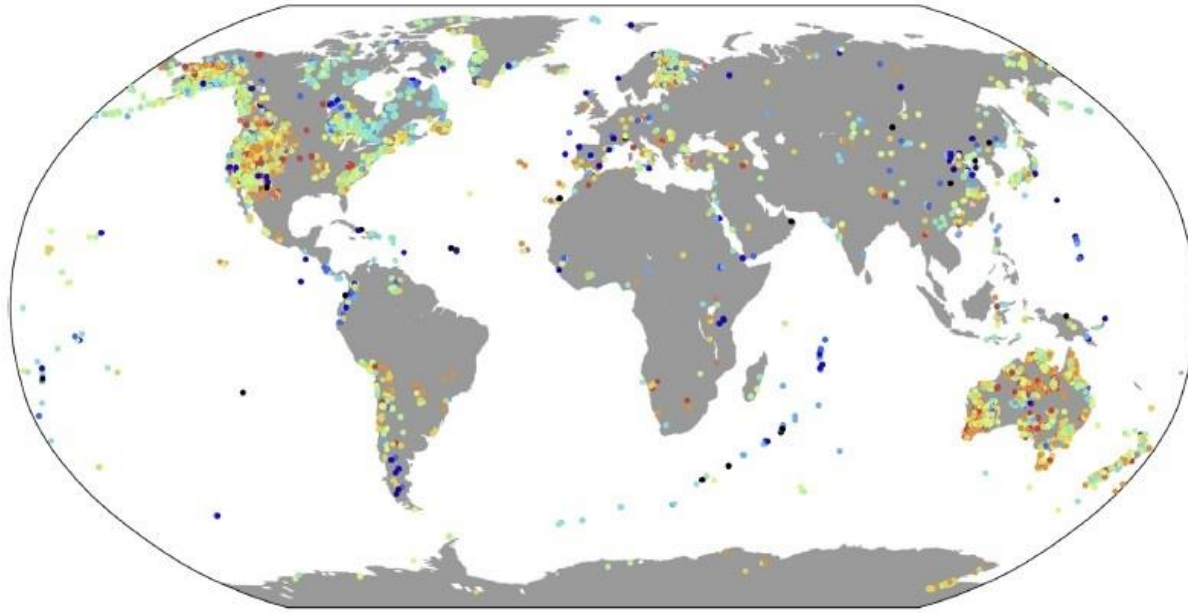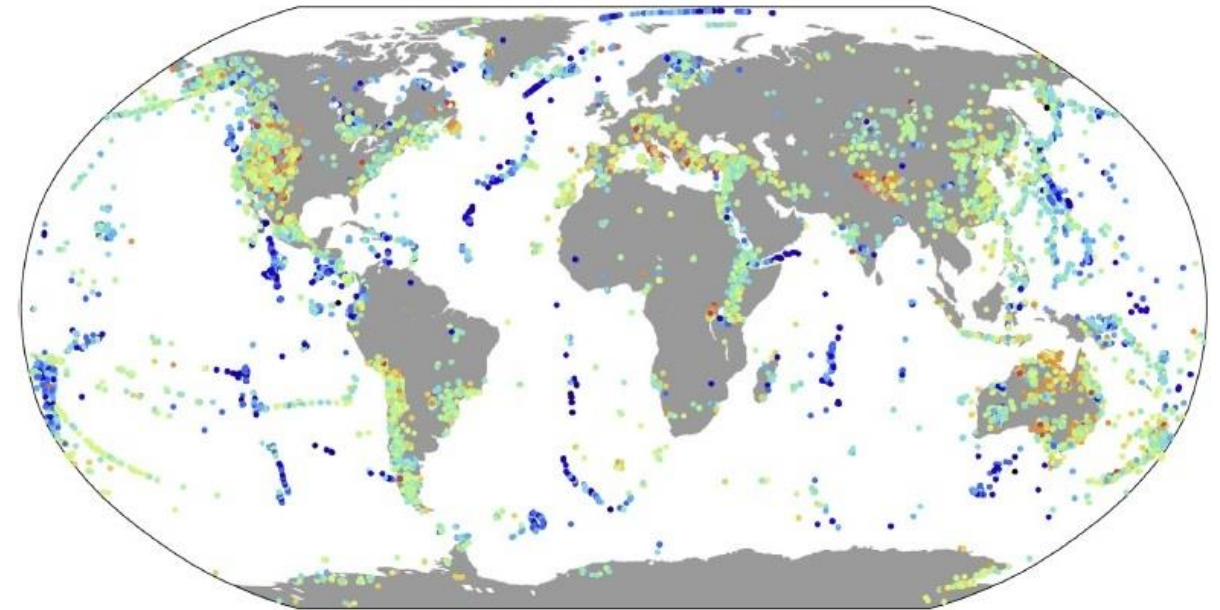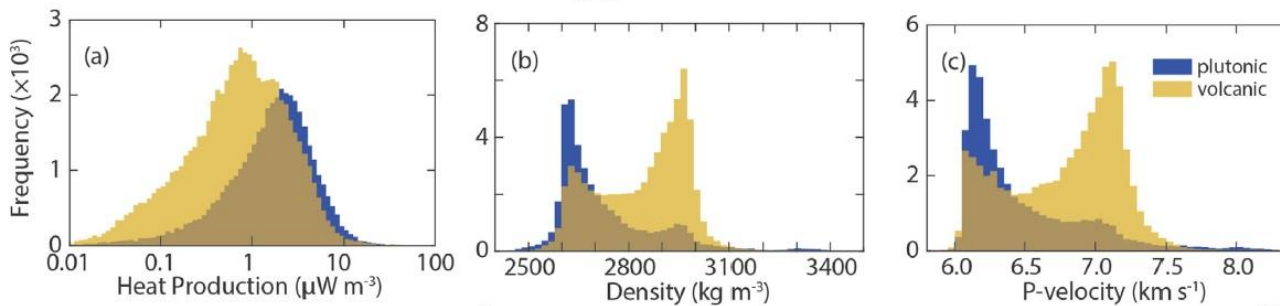
Hasterok and Webb, 2017, Geoscience Frontiers, 8

Heat production estimates range from a maximum of 14,000 mWm³ to a minimum of 0.001 mWm³, but the vast majority of the data fall between 0.01 and 30 mWm³.

(a) Global — N: 17788, Median 2.8, Mean 3.7

(b) Australia — N: 6529, Median 3.6, Mean 4.6

(c) North America — N: 8492, Median 2.5, Mean 3.2
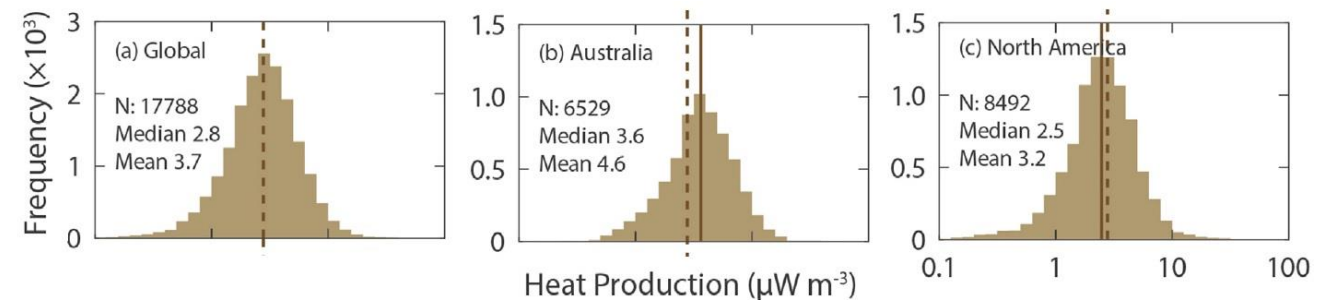
Radiogenic Heat Generation, density, and *P*-wave velocity: dependency on SIO$_2$ (first order compositional variations)
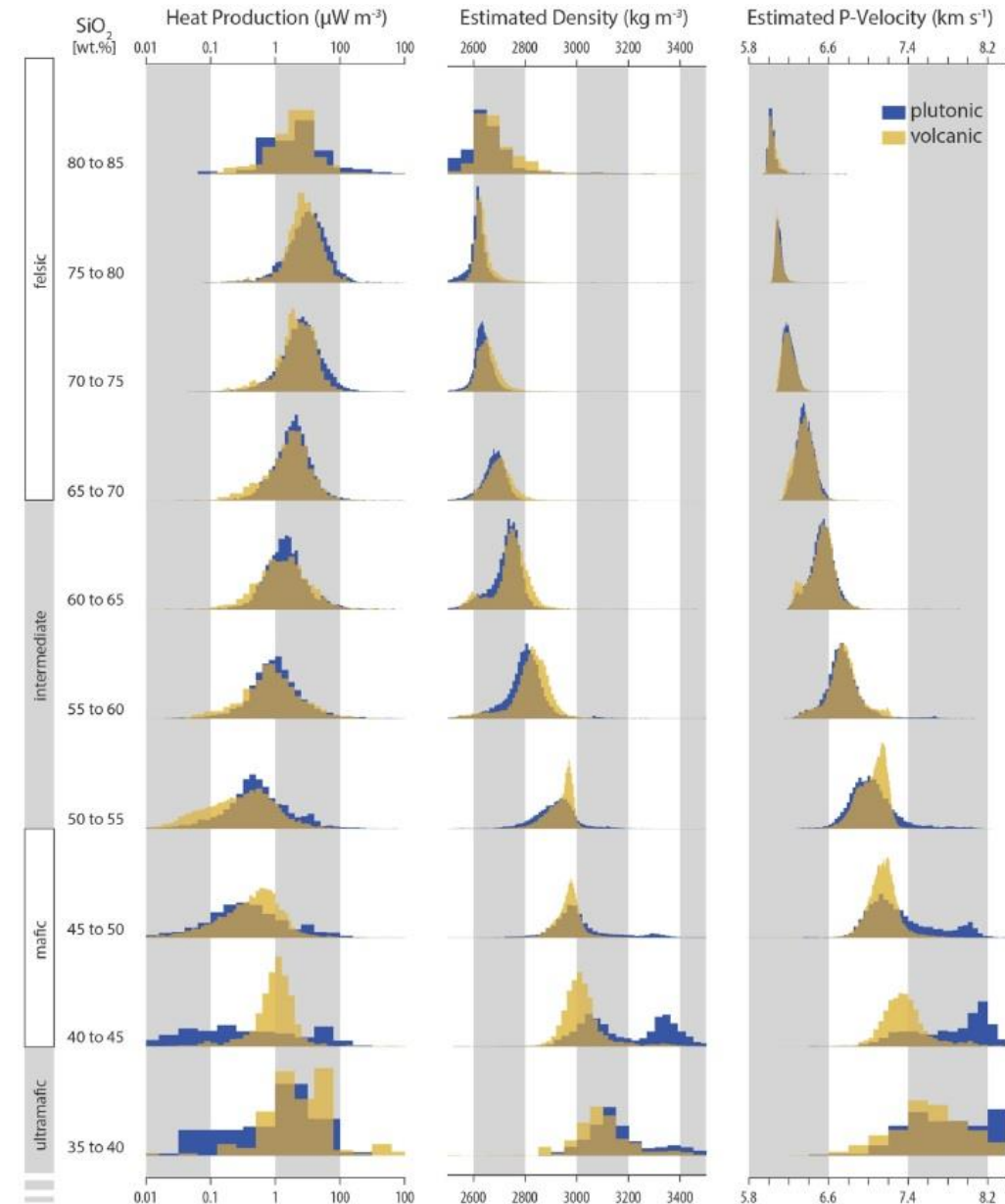
- Density and seismic velocity generally increase as composition ranges from felsic to mafic, while heat production decreases from felsic to mafic compositions.
- Density and seismic velocity distributions show a more complex behaviour for SIO$_2$ <65 wt.%, while heat production distribution for SIO$_2$ <55 wt.%, due to the presence of other oxides in the rocks.

Hasterok and Webb, 2017, Geoscience Frontiers, 8

Radiogenic Heat Generation and Surface Heat flow

Radiogenic heat production and surface heat flow values from a range of geological provinces. Data from Roy et al. (1968).

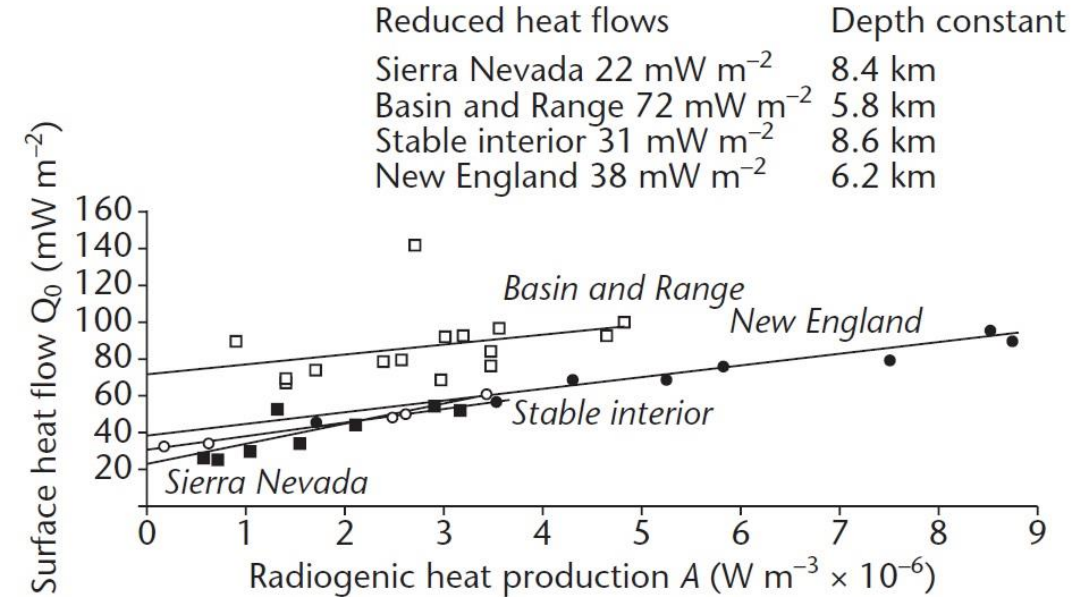| Locality	A Radiogenic heat production 10^{-13} cal cm^{-3} s^{-1} (μW m^{-3})	Q$_0$ Surface heat flow 10^{-6} cal cm^{-2} s^{-1} (mW m^{-2})	Locality	A Radiogenic heat production 10^{-13} cal cm^{-3} s^{-1} (μW m^{-3})	Q$_0$ Surface heat flow 10^{-6} cal cm^{-2} s^{-1} (mW m^{-2})
New England			19	6.4 (2.7)	1.06 (44.4)
1	20.7 (8.7)	2.27 (95.0)	20	4.7 (2.0)	0.83 (34.7)
2	21.2 (8.8)	2.15 (90.0)	21	3.2 (1.3)	0.73 (30.5)
3	17.6 (7.4)	1.89 (79.1)	22	1.8 (0.75)	0.62 (25.9)
4	12.9 (5.4)	1.80 (75.3)	23	2.2 (0.92)	0.60 (25.1)
5	11.6 (4.9)	1.63 (68.2)			
6	9.6 (4.0)	1.63 (68.2)	Basin and Range province		
7	7.8 (3.3)	1.34 (56.1)	24	10.7 (4.5)	2.40 (100.4)
8	3.8 (1.6)	1.08 (45.2)	25	6.0 (2.5)	3.40 (142.3)
			26	7.9 (3.3)	2.30 (96.2)
Central Stable region			27	10.3 (4.3)	2.22 (92.9)
9	7.6 (3.2)	1.46 (61.1)	28	7.1 (3.0)	2.20 (92.0)
10	5.8 (2.4)	1.22 (51.0)	29	6.7 (2.8)	2.20 (92.0)
11	5.5 (2.3)	1.17 (49.0)	30	2.0 (0.84)	2.14 (89.6)
12	1.4 (0.59)	0.82 (34.3)	31	7.7 (3.2)	2.00 (83.7)
13	<0.4 (0.17)	0.81 (33.9)	32	5.7 (2.4)	1.90 (79.5)
14	<0.4 (0.17)	0.79 (33.1)	33	5.3 (2.2)	1.88 (78.7)
15	<0.4 (0.17)	0.81 (33.9)	34	7.7 (3.2)	1.82 (76.1)
			35	3.8 (1.6)	1.78 (74.5)
Sierra Nevada			36	3.1 (1.3)	1.65 (69.0)
16	8.8 (3.7)	1.30 (54.4)	37	6.6 (2.8)	1.64 (68.6)
17	4.0 (1.7)	1.25 (52.3)	38	3.1 (1.3)	1.60 (66.9)
18	9.6 (4.0)	1.25 (52.3)			

$$q_0 = q_a + A_0 D$$

Reduced heat flows	Depth constant
Sierra Nevada 22 mW m^{-2}	8.4 km
Basin and Range 72 mW m^{-2}	5.8 km
Stable interior 31 mW m^{-2}	8.6 km
New England 38 mW m^{-2}	6.2 km

Surface heat flow Q_0 (mW m^{-2}) vs Radiogenic heat production A (W m^{-3} $\times 10^{-6}$)

Basin and Range — New England — Stable interior — Sierra Nevada

- Surface heat flow reflect the amont of radiogenic heat production in the shallow crust (e.g., New England), as well as the contribution of deeper sources, such as a shallow hot upper mantle (Basin and Range)

Conductive Heat Transfer
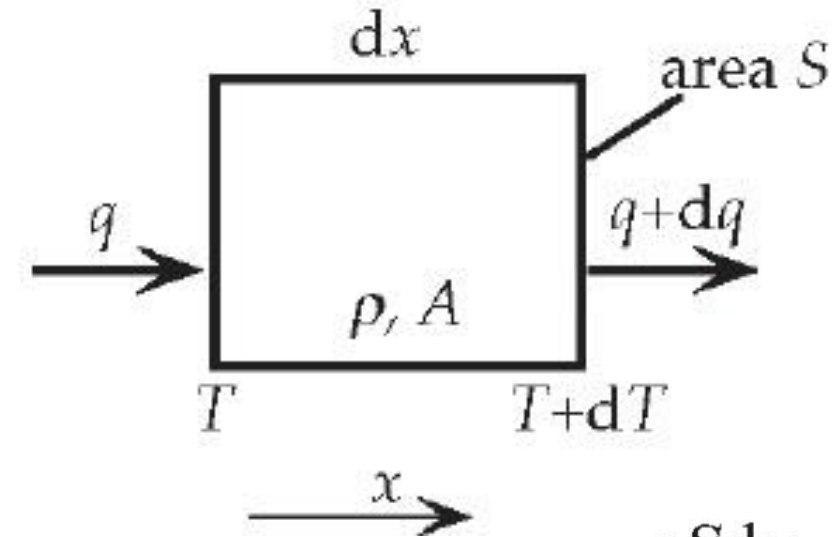
The change in heat content of the block during a time interval will be equal to the heat conducted in minus the heat conducted out plus the heat generated internally (A).

$$dH = \rho S dx \cdot C_P \cdot dT$$

$$\rho S dx \cdot C_P \cdot dT = qS\,dt - (q + dq)S\,dt + A \cdot Sdx \cdot dt$$

$$\rho C_P \frac{\partial T}{\partial t} = -\frac{\partial q}{\partial x} + A$$

H = heat content, ρ = density, *S* = area of the end surfaces of the block (*ρSdx* = mass of the block), and C_p = specific heat at constant pressure, which measures the capacity of a material to hold heat, and for mantle minerals it has a value of the order of 1000 J/kg K.

$$q = -\lambda \frac{\partial T}{\partial x}$$

λ=K

$$\partial T / \partial t = 0$$

Poisson Equation

$$\frac{\partial T}{\partial t} = \kappa \frac{\partial^2 T}{\partial x^2} + a$$

κ=K/ρC_p and   a=A/ρC_p

$$\frac{\partial^2 T}{\partial z^2} = -\frac{A}{K}$$

Change of the vertical geothermal gradient with depth

κ = **thermal diffusivity** (physical property that controls the rate at which heat dissipates through a material)

Temperature variations with depth
(steady state conditions)

If $A=0$ $\qquad$ $T_0' = -q_0/K \approx 20\,^\circ\text{C/km}$

For a constant gradient, at 60 km depth the temperature would be 1200 °C (it would approach the melting point)

$$\frac{\partial^2 T}{\partial y^2} = -\frac{A}{K}$$ First integration gives $\qquad$ $\frac{\partial T}{\partial y} = -\frac{A}{K}y + c_1$ $\qquad$ $T=T_0$ at y=0, then: $\partial T/\partial y = Q_0/K$ at $y = 0$

Second integration $\qquad$ $T = -\frac{A}{2K}y^2 + \frac{Q_0}{K}y + c_2$ $\qquad$ since $T=T_0$ at y=0, $c_2 = T_0$ $\qquad$ $T = T_0 + \frac{Q_0}{K}y - \frac{A}{2K}y^2$

Heat Generation changes exponentially with depth If q_0 varies linearly with q_a:
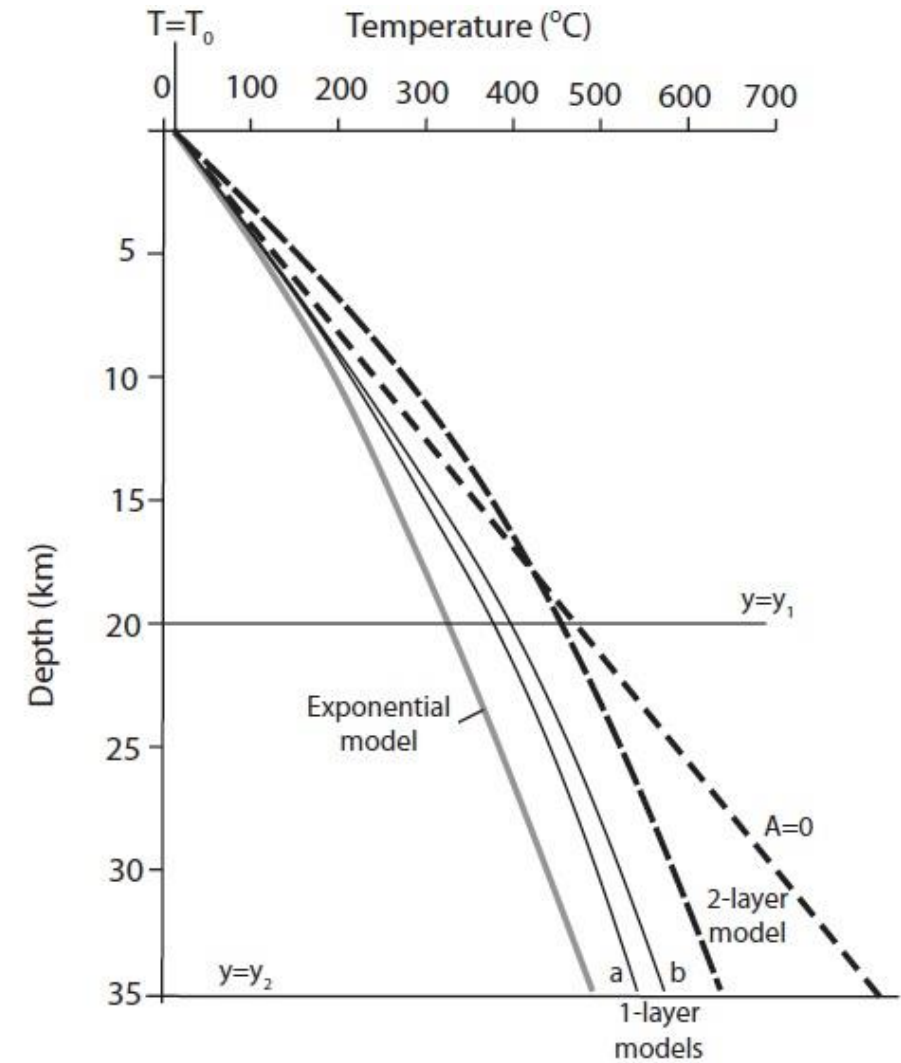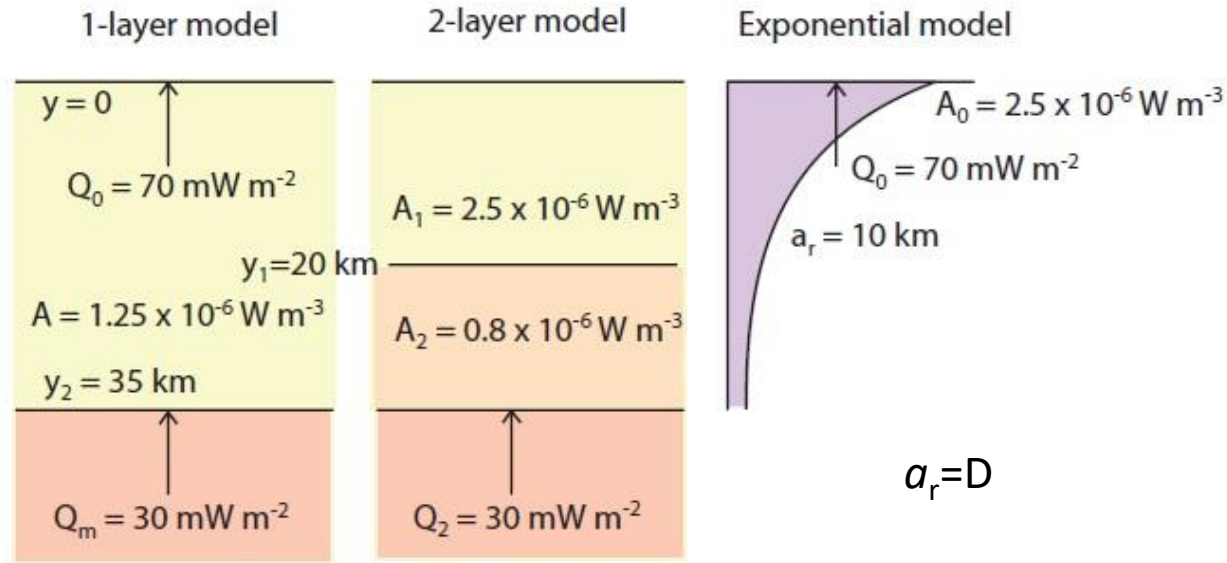
$$q_0 = q_a + A_0 D \qquad A(z) = A_0 \exp\left(-\frac{z}{D}\right) \qquad q_a = \text{mantle heat flow}$$

$$\partial T/\partial t = 0$$

$$\frac{\partial^2 T}{\partial z^2} = -\frac{A}{K} \qquad\qquad T = T_0 + \frac{D^2 A_0}{k}\left[1 - \exp\left(-\frac{z}{D}\right)\right] + \frac{q_a}{k}z$$

If A_0 is unknown we can substitute DA_0 with $Q_0 - Q_a$, since $q_0 = q_a + A_0 D$

Temperature variations with radiogenic heat production

1-layer model

$y = 0$

$Q_0 = 70 \text{ mW m}^{-2}$

$y_1 = 20 \text{ km}$

$A = 1.25 \times 10^{-6} \text{ W m}^{-3}$

$y_2 = 35 \text{ km}$

$Q_m = 30 \text{ mW m}^{-2}$

2-layer model

$A_1 = 2.5 \times 10^{-6} \text{ W m}^{-3}$

$A_2 = 0.8 \times 10^{-6} \text{ W m}^{-3}$

$Q_2 = 30 \text{ mW m}^{-2}$

Exponential model

$A_0 = 2.5 \times 10^{-6} \text{ W m}^{-3}$

$Q_0 = 70 \text{ mW m}^{-2}$

$a_r = 10 \text{ km}$

$a_r = D$

$T = T_0$ Temperature (°C)

Depth (km)

$y = y_1$

Exponential model

$A = 0$

2-layer model
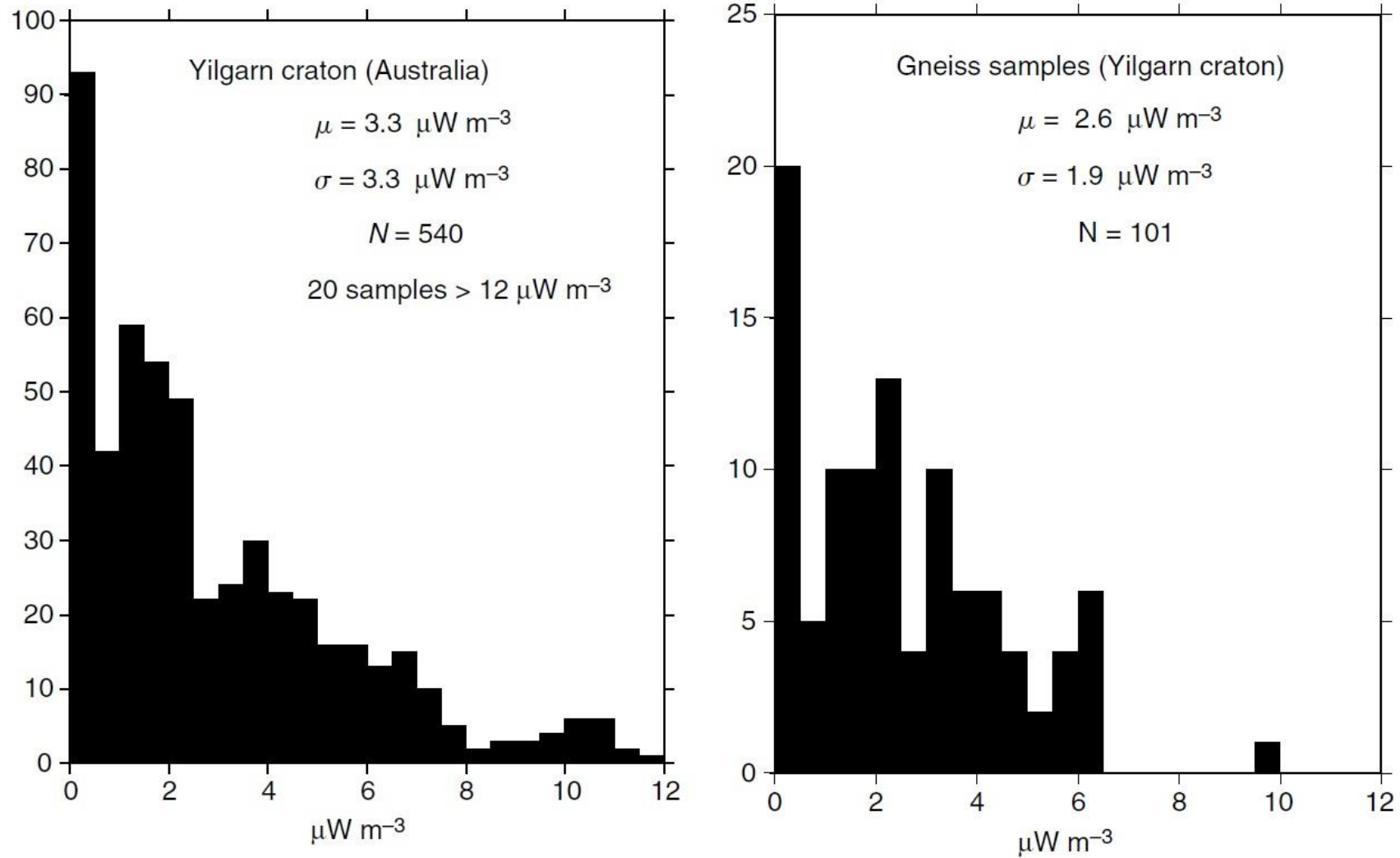
$y = y_2$ a b

1-layer models

Relationship between local heat flow and heat production values ?
## Test : Trans Hudson Orogen
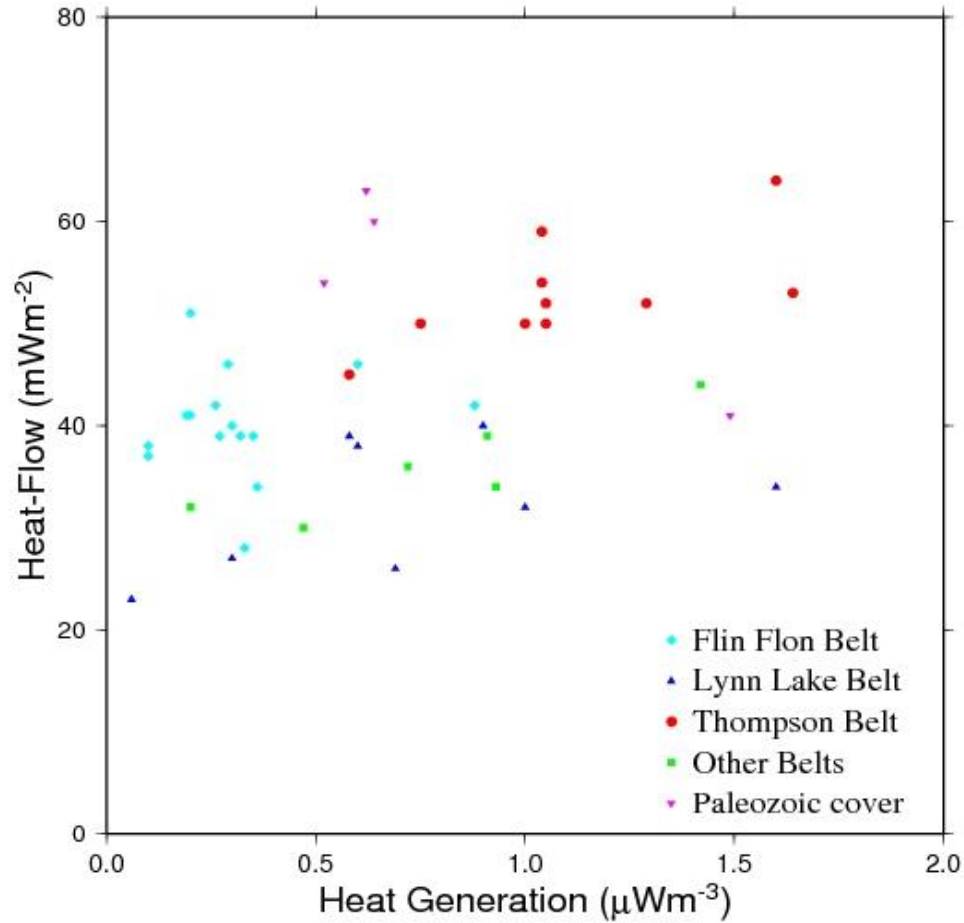
- No clear heat flow – heat production relationship for the entire THO nor for its individual belts.

- No meaningful relationship for any province of the Canadian Shield.

Radiogenic Heat Generation lateral variability

Yilgarn craton (Australia)

$\mu = 3.3 \ \mu W \ m^{-3}$

$\sigma = 3.3 \ \mu W \ m^{-3}$

$N = 540$

20 samples $> 12 \ \mu W \ m^{-3}$

$\mu W \ m^{-3}$

Gneiss samples (Yilgarn craton)

$\mu = 2.6 \ \mu W \ m^{-3}$

$\sigma = 1.9 \ \mu W \ m^{-3}$

$N = 101$

$\mu W \ m^{-3}$

- Heat Generation may vary by a factor of 5 over horizontal distances of few tens of meters, due to rocks heterogeneity, fluid migration, and phase changes.

Scale for a representative heat production model
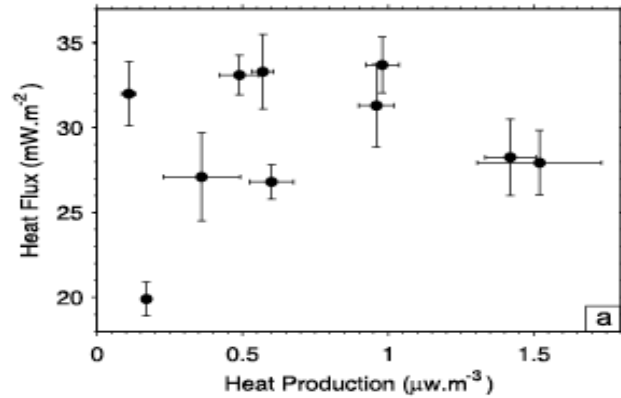

Individual measurements

- **On a large scale there is a relationship between heat flux and heat production when they are averaged on a province.**
- **Variations in surface heat flux between geological province occur on a short distance (< 50 km, due to variations of surface heat flow in the crust)**
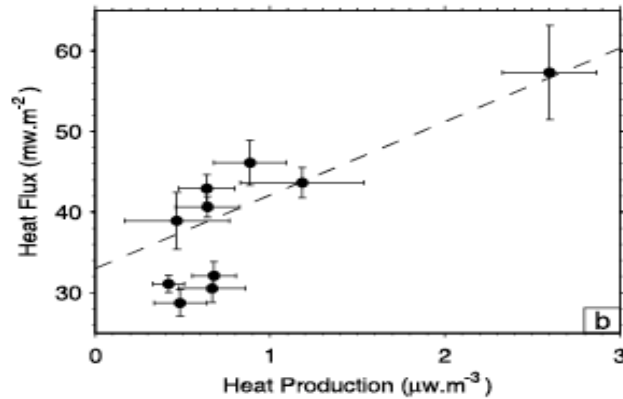
$\approx$ 200x200 km windows

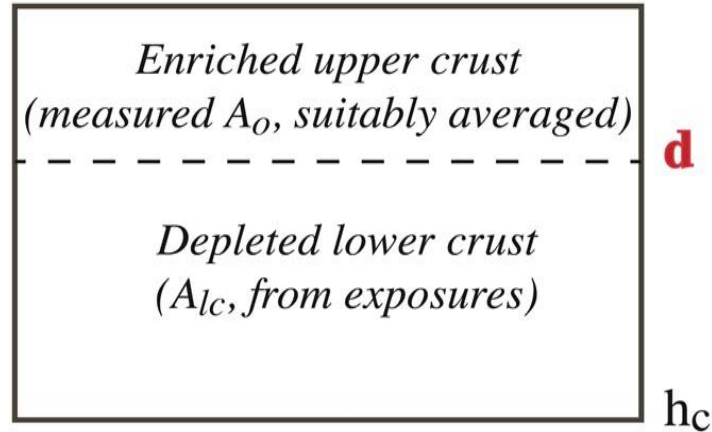**On a large scale, three key control variables on lithospheric temperatures are correlated:**
- **average surface heat flux,**
- **average crustal heat production,**
- **vertical variation of heat production.**
- **Variations in the basal heat flux are small (3 mWm^2).**
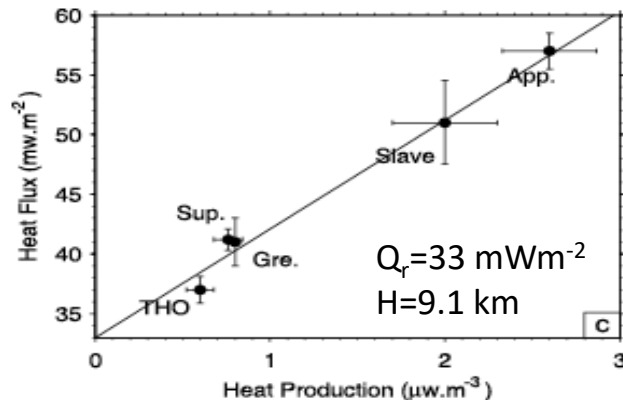
$\approx$ 500x500 km windows

Estimating the degree of enrichment in the upper crust (Differentiation Index)

Measured Q_O (suitably averaged)

| |
|---|
| *Enriched upper crust* (measured A_O, suitably averaged) |
| - - - - - - - - - - - - - - - - **d** |
| *Depleted lower crust* (A_{lc}, from exposures) |

h_c

Q_m (estimated)

$$q_0 = q_a + A_o D$$

$q_a = Q_m \quad A_0 = A_c \quad D = z_m$

$$D_i = \frac{A_s}{A_c} = \frac{A_s z_m}{Q_0 - Q_m}$$

A_s = average surface heat production
A_c = average crustal heat production
$A_c = (Q_0 - Q_m) / Z_m$
z_m = Moho depth

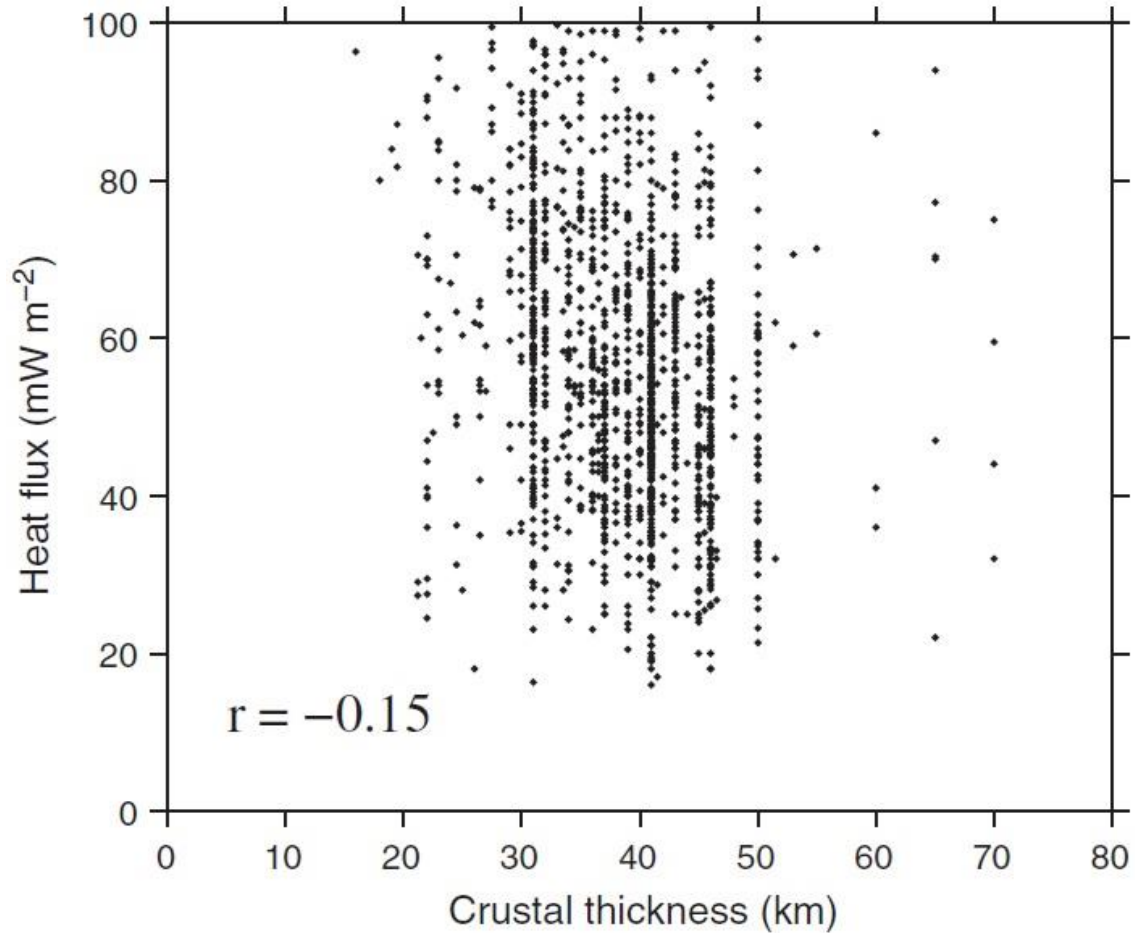- Usually $D_i > 1$ (e.g., D_i ~3 for Phanerozoic Appalachian and D_i ~ 1 for Proterozoic Greenville).

- *D_i=0.4* at Kola peninsula (Baltic Shield), since Proterozoic rocks were tectonically transported over Archean basement (more radiogenic).

- Moho temperature increases with increasing A_c and decreases with increasing D_i.
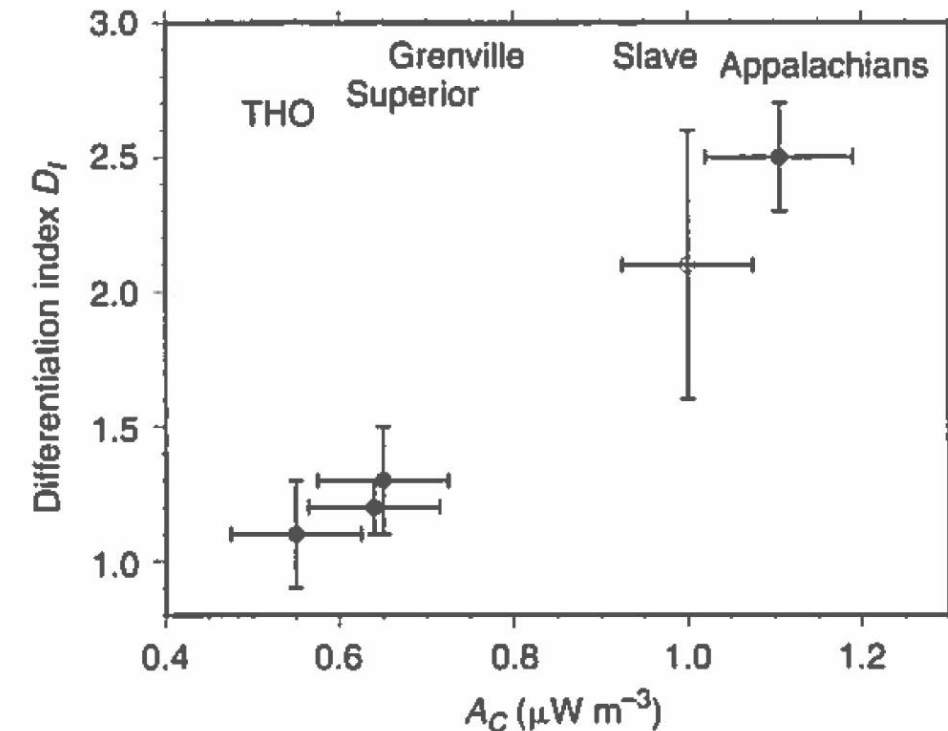
Heat Flux and Crustal Thickness

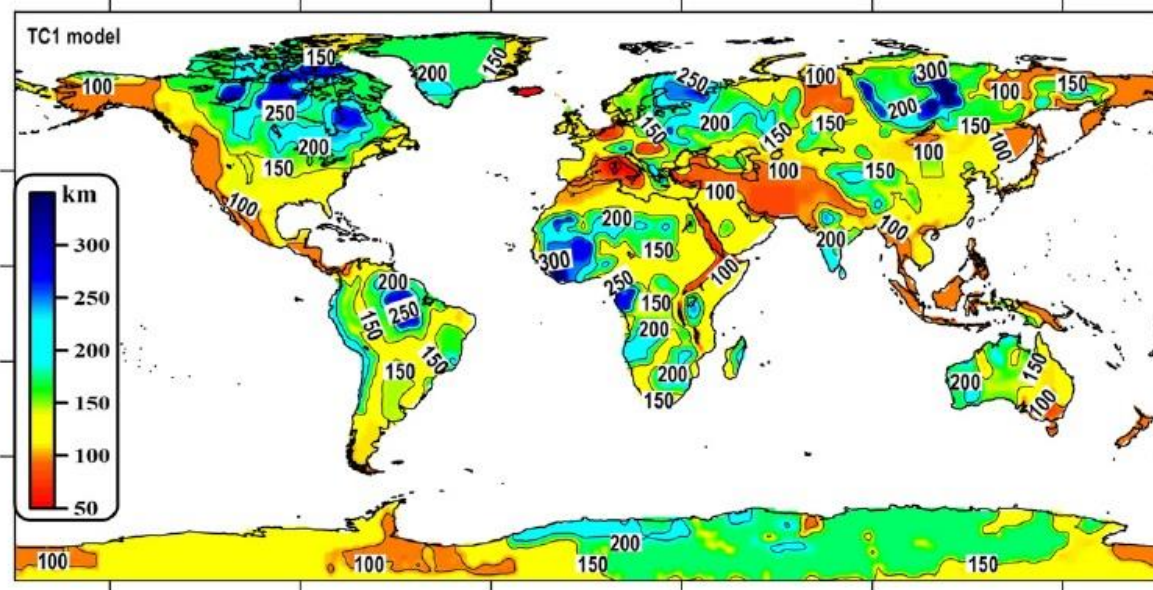## Moho Temperatures and Radiogenic Generation Distribution
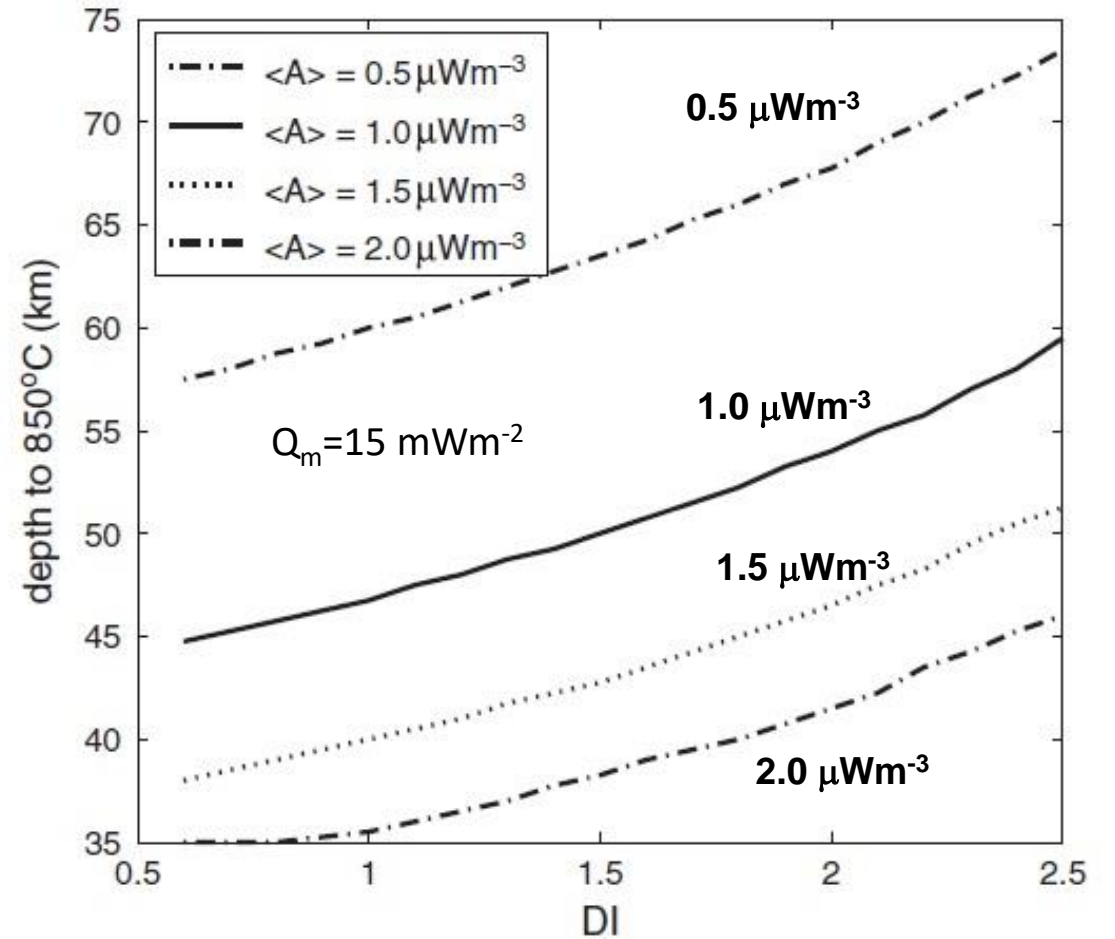
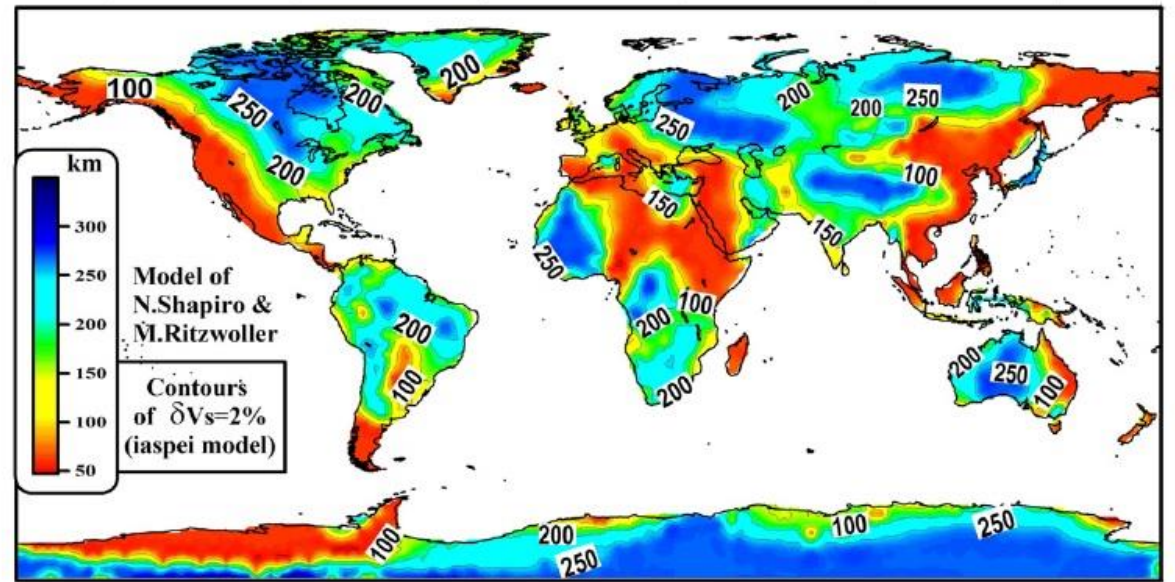Mareschal and Jaupart, 2013, Tectonophysics, 609

No correlation between surface heat flux and Moho depth, since the crust is differentiated

Thermal Lithosphere (heat flow data, electromagnetic, and xenolith data) and Seismic Lithosphere

**Thermal Lithospheric Thickness**

Lithospheric Thickness from surface-wave seismic tomography

Artemieva, 2009, Lithos, 109

- **Thermal Lithospheric Thickness:** determined by the intersection of a lithospheric geotherm with a mantle adiabat T_m~ 1350°C or at T~ $0.8T_m$ (~ 1100°C), at the top of the transitional layer from high to low viscosity. It is usually 40-50 km shallower than the seismological boundary detected from seismic tomography (based of the convective boundary).
- **Seismic Lithospheric Thickness**: the lithospheric base is defined here as the depth where Vs velocity in the upper mantle is 2.0±0.5% higher.

Depth of the lithosphere: from conduction to convection
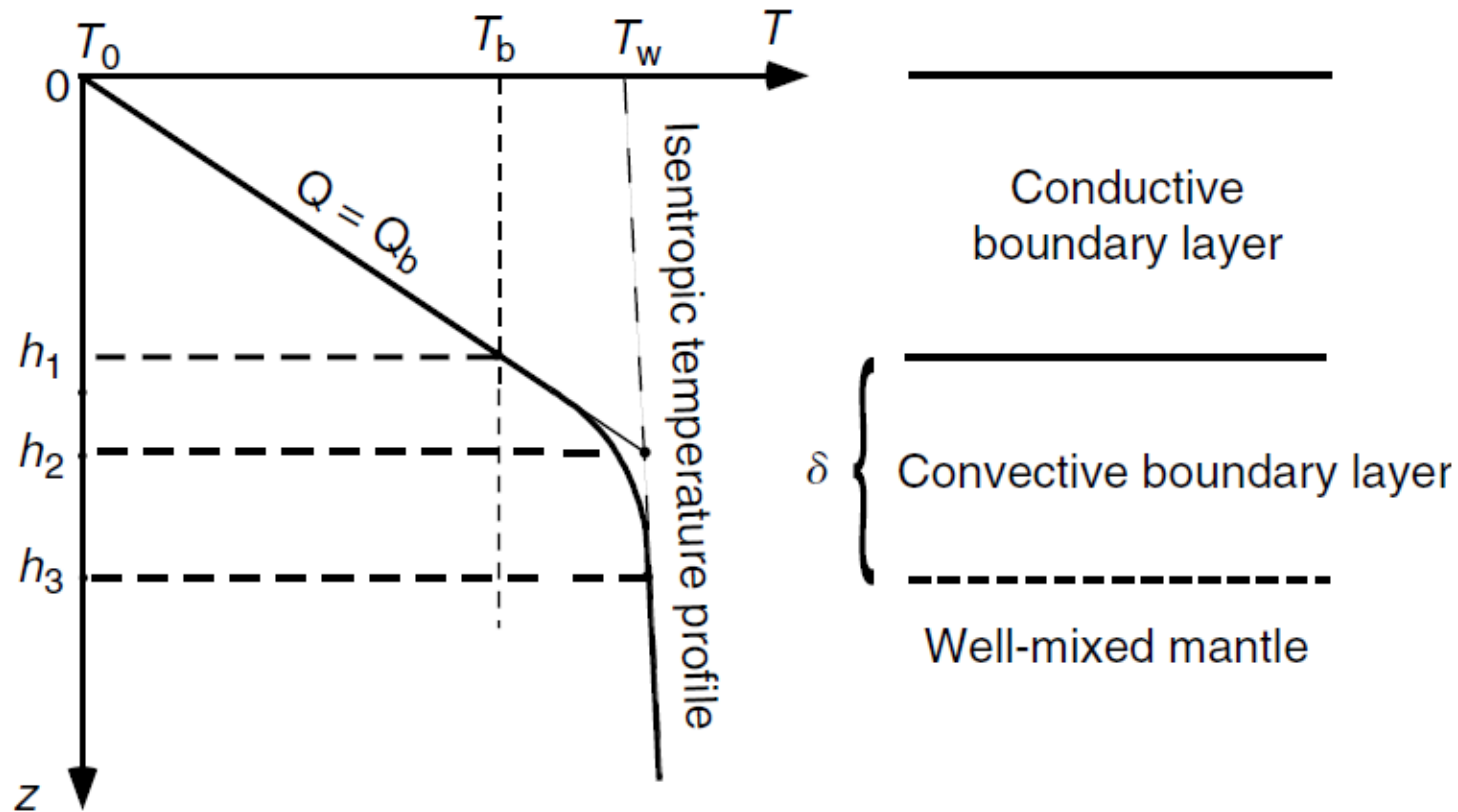
h_1= lower boundary of the conductive part (bottom of the thermal lithosphere).
h_2= intersection between the downward extrapolation of the conductive geotherm and the temperature profile for the convective mantle.
h_3= lower limit of the thermal boundary layer (transition between lithospheric regime and fully convective mantle regime).
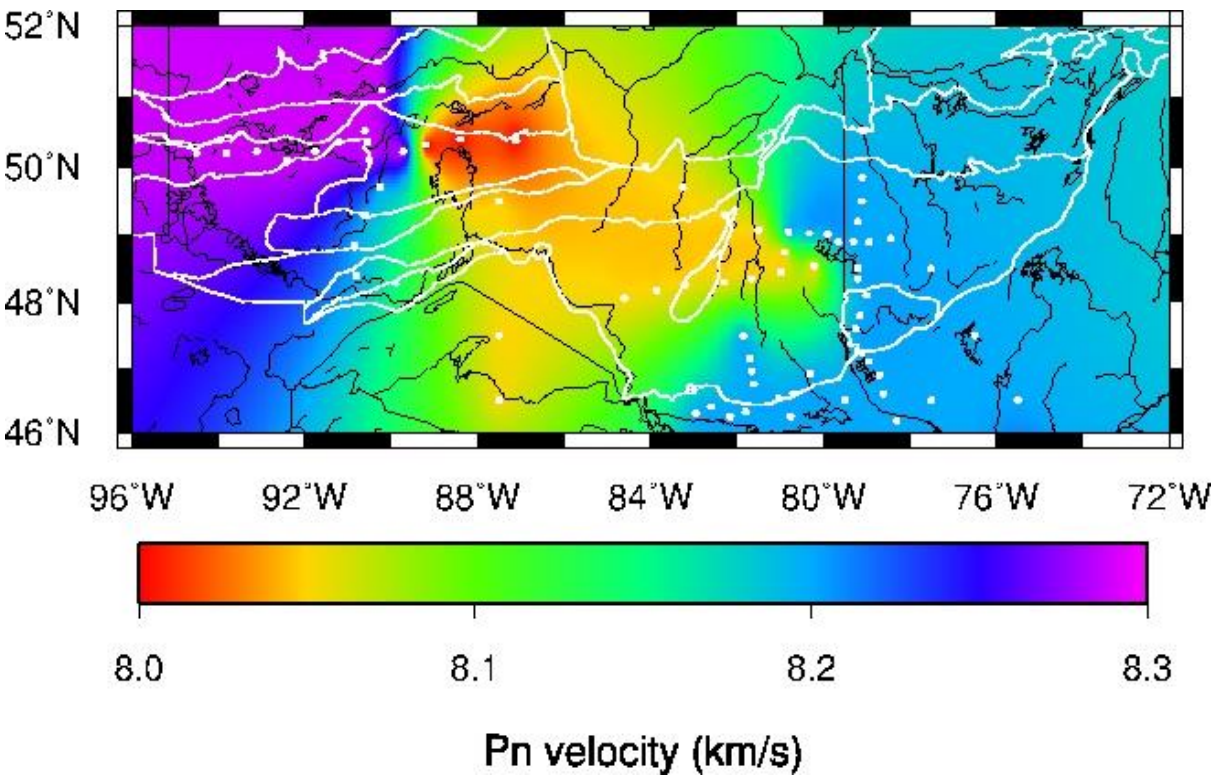T_0=temperature at the surface
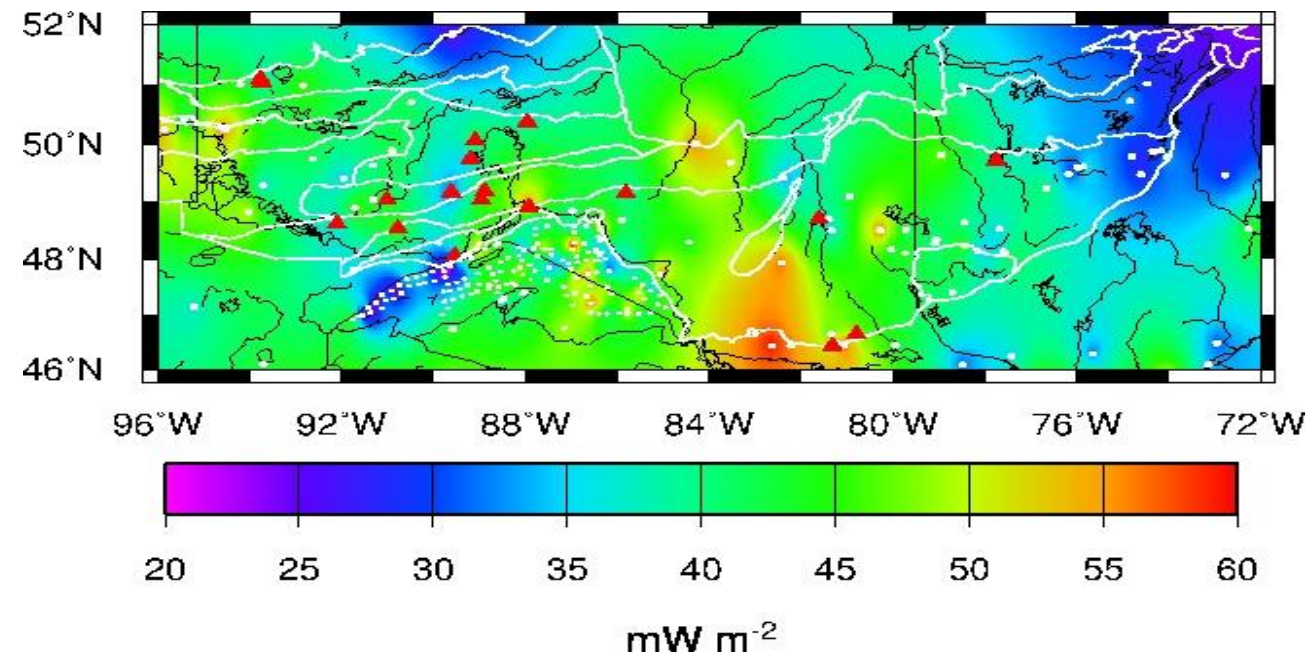T_b=temperature at the base of the lithosphere
T_w=temperature of well-mixed convective interior
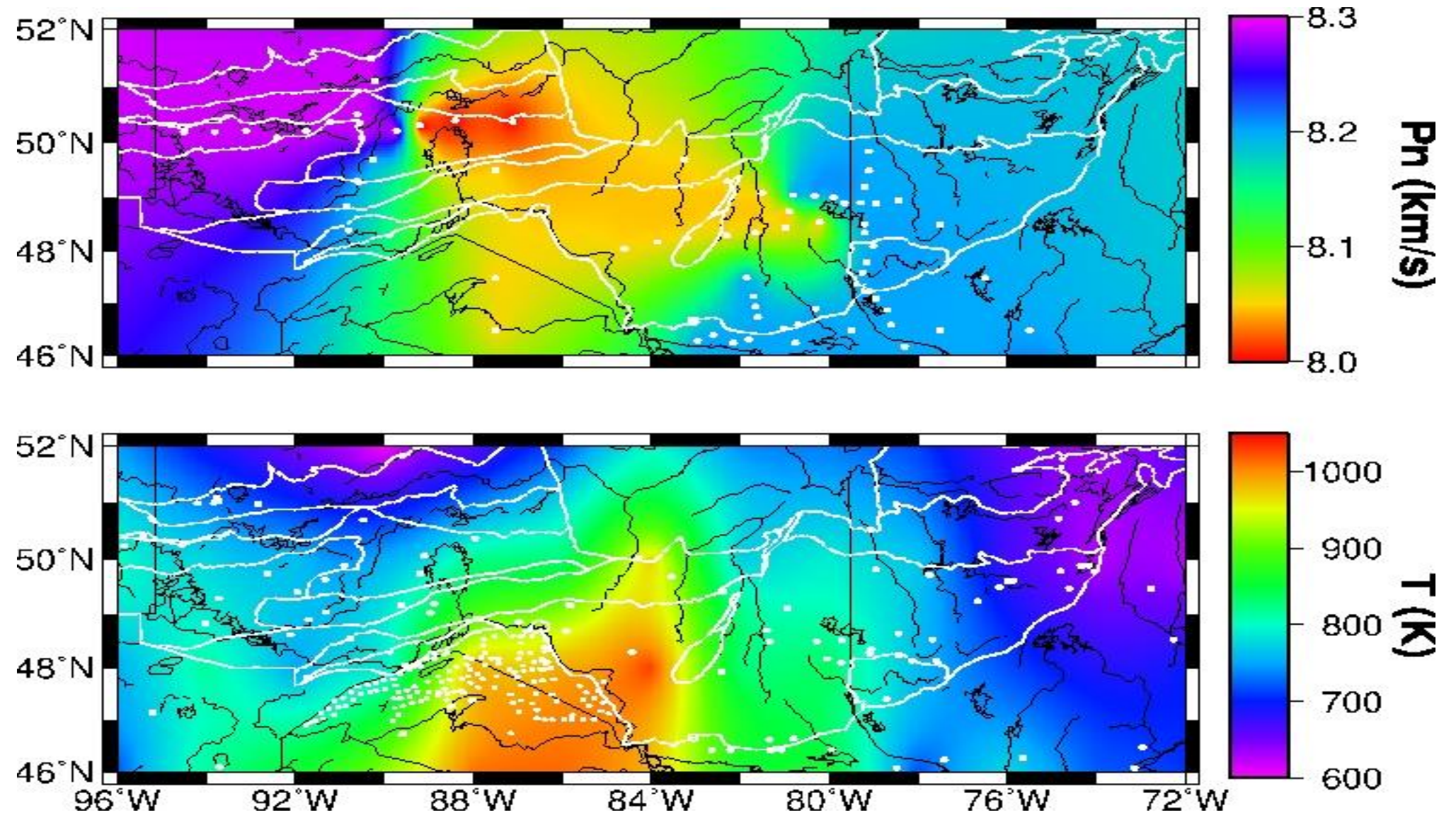
Seismic velocity and temperature

Pn velocity

Heat Flow

Seismic velocity and temperature

P-wave velocity as a function of temperature and composition
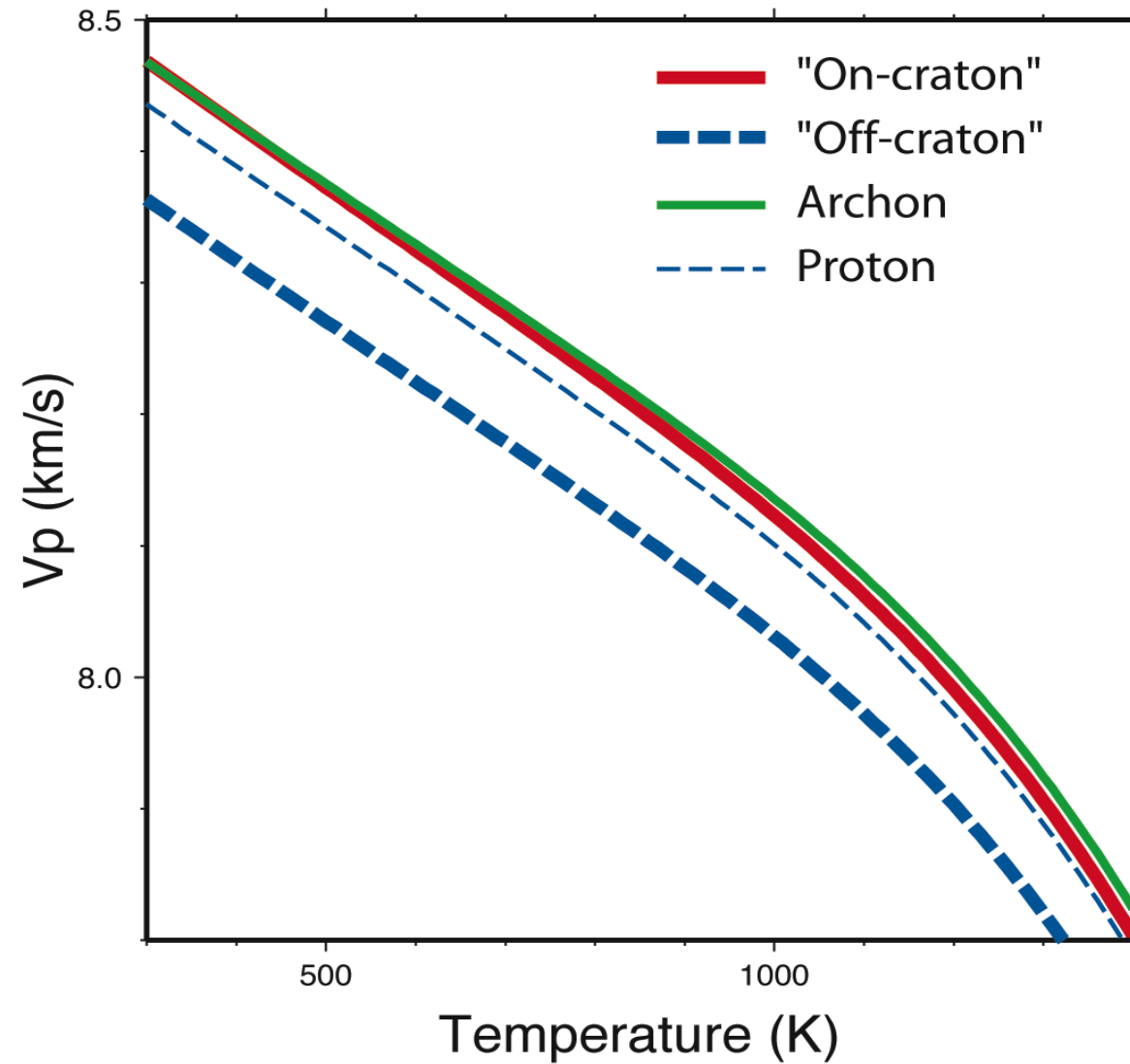
Temperature variations in depth constrained by xenoliths

Lee et al., 2011, Annu. Rev. Earth Planet. Sci

Artemieva, 2009, Lithos, 109
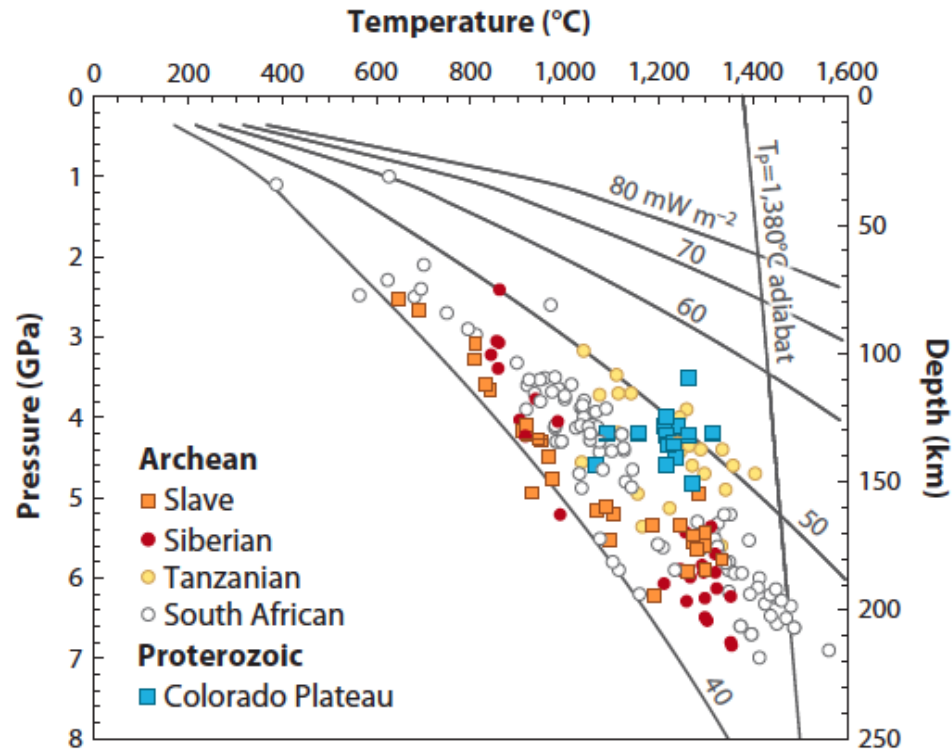
Issues for thermobarometry:

Pressures more uncertain than temperatures

Some xenoliths were sheared just prior to quenching and do not represent conductive steady-state

Some xenoliths may have been transported upward along adiabat
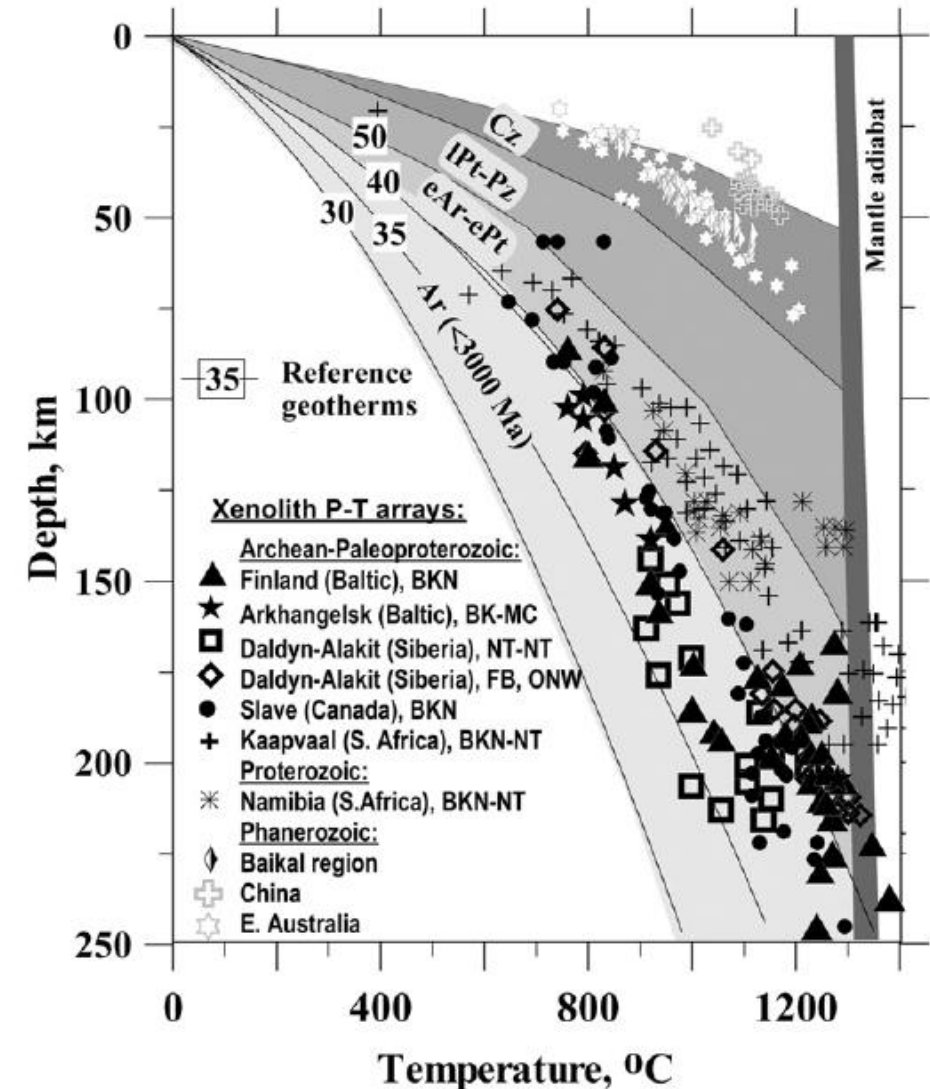
No Steady-state conditions

Heat flow > 90 mWm² imply melting in the crust or a weak lithospheric mantle
(other heat transport mechanisms are effective in tectonic active areas)

<u>Crustal thickness variations imply changes of crustal heat production and deformation</u> (change of temperature distribution)

- Erosion or crustal extension initially cause steeper geotherms and enhanced heat flux and later the reduced crustal thickness and possible injection of basaltic melts (depleted in radioelements) leads to a lower heat flux than initial.
- Crustal thickening causes the geothermal gradient and the heat flux to decrease at first and then to increase due to higher crustal heat production (e.g., Tibet and Alps).
- Heat flux may record shallow processes such as the cooling of recently emplaced plutons. The anomalously high heat flux in the Basin and Range Province (about 110 mWm²) and the high elevation (about 1750 m) is consistent with an extension of 100% and presence of shallow magma intrusions.

- *crustal thinning causes subsidence and reduces heat flux*

- *crustal thickening causes uplift and increases heat flux*

vertical movements

vertical movements
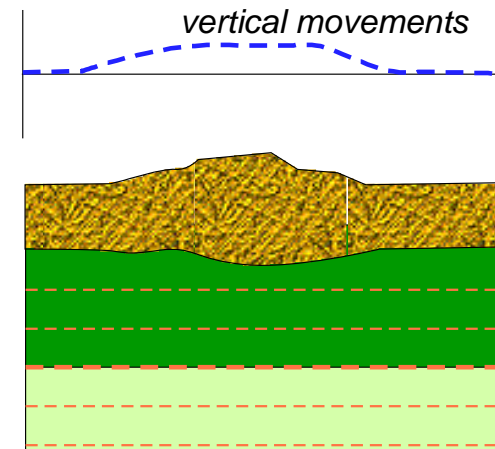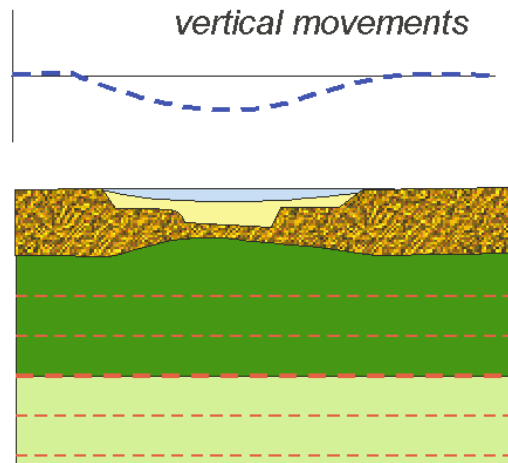
Crustal temperatures return to equilibrium with local heat sources in less than 100 My.
Mantle lithosphere re-equilibrate much slower. For thick lithosphere, such transients may last as long as 500 My

References

Main Readings:

Books:
- Artemieva, 2011, Seismic Structure of the lithosphere (Chapter 3), The lithosphere an interdisciplinary approach.
- Jaupart and Mareshal, 2009, Heat Flow and Thermal Structure of the Lithosphere, Treatise of Geophysics, Volume 6, Crust and Lithosphere Dynamics.
- Kearey, Klepeis, and Vine, 2015, Precambrian tectonics and the supercontinent cycle (Chapter 11), Global Tectonics.
- Stuwe, 2007, Energetics: Heat and Temperature (Chapter 3), Geodynamics of the Lithosphere, Springer.

Articles:

- Jones et al., 2010, Europe from the bottom up: A statistical examination of the central and northern European lithosphere–asthenosphere boundary from comparing seismological and electromagnetic observations, Lithos, 120, 14-29.
- Kusky et al., 2018, Tectonic evolution of the North China Block: from orogen to craton to orogen, Geological Society, London, Special Publications, 280, 1–34.
- Lee et al., 2011, Building and Destroying Continental Mantle, Annu. Rev. Earth Planet. Sci., 39.
- Silver et al., 2004, Seismic anisotropy, mantle fabric, and the magmatic evolution of Precambrian southern Africa, S. Afr. J. Geol., 107, 45-58.

References

Further Readings:

- Artemieva, 2009, The continental lithosphere: Reconciling thermal, seismic, and petrologic data, Lithos, 109, 23–46.
- Artemieva and Mooney, 2001, Thermal thickness and evolution of Precambrian lithosphere: A global study, J. Geophys. Res. 106B, 16387-16414.
- Aulbach et al., 2017, Origins of cratonic mantle discontinuities: A view from petrology, geochemistry and thermodynamic models, Lithos, 268–271.
- Celli et al., 2020, African cratonic lithosphere carved bymantle plumes, Nature Communications, 11:92.
- Cooper et al., 2017, The structural evolution of the deep continental lithosphere, Tectonophysics 695, 100–121.
- Foley and O'Neill, 2021, Continents soldered from below, Nature, 592.
- Gerya, 2014, Precambrian geodynamics: Concepts and models, Gondwana Research, 25, 442–463.
- Gorczyk et al., 2018, Plume-lithosphere interaction at craton margins throughout Earth history. Tectonophysics, 746, 678–694
- Griffin et al., 2003, The origin and evolution of Archean lithospheric mantle, Precambrian Research, 127, 19–41.
- Hasterok and Webb, 2017, On the radiogenic heat production of igneous rocks, GeoscienceFrontiers, 8, 919-940.
- James et al., 2001, Tectospheric structure beneath southern Africa, GRL, 28, 13, 2485-2488.
- James et al., 2004, Xenolith constraints on seismic velocities in the upper mantle beneath southern Africa, G3, 5.
- Jordan, 1988, Structure and formation of the continental tectosphere. Journal of Petrol, Special Lithosphere Issue, 11-37.
- Knapmeyer-Endrun et al., 2017, Upper mantle structure across the Trans-European Suture Zone imaged by S-receiver functions, EPSL, 458, 429–441.
- Lee, 2003, Compositional variation of density and seismic velocities in natural peridotites at STP conditions: Implications for seismic imaging of compositional heterogeneities in the upper mantle, JGR,108, B9, 2441.
- Mareschal and Jaupart, 2013, Radiogenic heat production, thermal regime and evolution of continental crust, Tectonophysics, 609, 524–534.
- Obrebski et al., 2012, Shear wave tomography of China using joint inversion of body and surface wave constraints, JGR, 117, B01311.
- Porritt et al., 2014, Seismic imaging east of the Rocky Mountains with USArray, EPSL, 402, 16-25.
- Scaheffer and Lebedev, 2013, Imaging the North American continent using waveform inversion ofglobal and USArray data, Geophys. J. Int., 194, 417–449.
- Simmons et al., 2009, Joint seismic, geodynamic and mineral physical constraints on three-dimensional mantle heterogeneity: Implications for the relative importance of thermal versus compositional heterogeneity, Geophys. J. Int., 177, 1284–1304.
- Wang et al., 2018. Making Archean cratonic roots by lateral compression: A two-stage thickening and stabilization model. Tectonophysics, 746, 562–571.
- Yuan et al., 2011, Lithospheric layering in the North American craton, Geophys. J. Int., 184, 1237–1260.
- Youssof et al., 2013, Moho depth and crustal composition in Southern Africa, Tectonophysics, 609, 267–287.